SISSA – International School for Advanced Studies

Ph.D. course in Statistical Physics

Ideal quantum glass transitions: many-body localization without quenched disorder?

Thesis submitted for the degree of *Doctor Philosophiae*

27 November 2015

Advisors:
Markus Müller
Alessandro Silva

Candidate:
Mauro Schiulaz

Academic Year 2014/2015

Abstract

In this work the role of disorder, interaction and temperature in the physics of quantum non-ergodic systems is discussed. I first review what is meant by thermalization in closed quantum systems, and how ergodicity is violated in the presence of strong disorder, due to the phenomenon of Anderson localization. I explain why localization can be stable against the addition of weak dephasing interactions, and how this leads to the very rich phenomenology associated with many-body localization. I also briefly compare localized systems with their closest classical analogue, which are glasses, and discuss their similarities and differences, the most striking being that in quantum systems genuine non ergodicity can be proven in some cases, while in classical systems it is a matter of debate whether thermalization eventually takes place at very long times.

Up to now, many-body localization has been studies in the region of strong disorder and weak interaction. I show that strongly interacting systems display phenomena very similar to localization, even in the absence of disorder. In such systems, dynamics starting from a random inhomogeneous initial condition are non-perturbatively slow, and relaxation takes place only in exponentially long times. While in the thermodynamic limit ergodicity is ultimately restored due to rare events, from the practical point of view such systems look as localized on their initial condition, and this behavior can be studied experimentally. Since their behavior shares similarities with both many-body localized and classical glassy systems, these models are termed "quantum glasses".

Apart from the interplay between disorder and interaction, another important issue concerns the role of temperature for the physics of localization. In non-interacting systems, an energy threshold separating delocalized and localized states exist, termed "mobility edge". It is commonly believed that a mobility edge should exist in interacting systems, too. I argue that this scenario is inconsistent because inclusions of the ergodic phase in the supposedly localized phase can serve as mobile baths that induce global delocalization. I conclude that true non-ergodicity can be present only if the whole spectrum is localized. Therefore, the putative transition as a function of temperature is reduced to a sharp crossover. I numerically show that the previously reported mobility edges can not be distinguished from finite size effects. Finally, the relevance of my results for realistic experimental situations is discussed.

List of my publications

- W. de Roeck, F. Huveneers, M. Müller and M. Schiulaz, *Absence of many-body mobility edges*, arXiv:1506.01505.
- M. Schiulaz, A. Silva and M. Müller, *Dynamics in many-body localized quantum systems without disorder*, Phys. Rev. B **91**, 184202 (2015).
- M. Schiulaz and M. Müller, *Ideal quantum glass transitions: many-body localization without quenched disorder*, in *15th International Conference on Transport in Interacting Disordered Systems*, edited by M. Palassini, AIP Conf. Proc. No. **1610**, (AIP, New York, 2014), p. 11.

Acknowledgements

I first want to give my deepest thanks to my Ph.D. supervisors, Markus Müller and Alessandro Silva, for everything I have learned from them, and for the effort they put in teaching and helping me. I next want to thank all the people with which I have worked in the past, or with whom I am collaborating now: so thank to Wojciech de Roeck, Francois Huveneers, Vipin Varma and Thuong Nguyen. I also want to thank Valentina Ros, Francesca Pietracaprina, Antonello Scardicchio, John Goold, Sebastiano Pilati and Alessio Lerose for the invaluable discussions with them.

I obviously thank the Statistical Physics Group at SISSA for taking and supporting me as a student, and ICTP for its prolonged hospitality. I also acknowledge the hospitality from the University of Basel and PSI Villigen, where part of this work was carried out.

I want to thank all professors, students and post-doctoral researchers, both at SISSA and ICTP, for the time I spent with them, what I have learned and the fun we had together. My Ph.D. has been a wonderful experience, both from the scientific and personal point of view.

Finally, I have to thank my family, my friends and all the people that supported me in these years. I would never have been able to arrive to this point without you.

Contents

Chapter 1

Introduction

The ergodic hypothesis is the pillar upon which statistical physics is built: it states that a generic many-body system, starting from any initial condition, explores the whole phase space compatible with the constraint of energy conservation, and eventually of the other conservation laws of the system. [1] If we wait for a long enough time, all information about the initial condition is erased (apart from the total energy), and the expectation values of observables relax to equilibrium values. As a consequence, temporal averages of macroscopic observables can be replaced by averages over a suitable statistical ensemble, and therefore can be computed without having to solve the equations of motion. This picture is not significantly modified by the presence of a few global conservation laws, apart from energy, like total momentum or number of particles: one simply has to choose the proper ensemble, in order to take into account these extra constraints. Ergodicity holds in the large majority of known physical systems, and statistical mechanics is nowadays believed to be one of the fundamental tools at our disposal to study physical phenomena.

In spite of this generality, there are some cases in which ergodicity is known to break down. The first one are exactly solvable systems: in this case, the ergodic hypothesis fails due to the presence of an extensive set of integrals of motion, that severely constrain the dynamics. At present, many exactly solvable systems are known, especially in one dimensional systems, [2, 3] and they constitute a very active topic of research. They are highly fine-tuned, though: a generic weak local perturbation breaks their integrability, and reinstates thermal behavior in the long time limit. Additionally, it is believed that these systems relax to a non thermal stationary state, which is described by the so called *"Generalized Gibbs Ensemble"* (GGE), and can still be treated with the (properly adjusted) tools of statistical mechanics [4, 5, 6], even though some recent results have raised doubts about this fact. [7, 8]

There are other kinds of systems in which relaxation to equilibrium is absent, and memory of the initial condition is retained for very long (possibly infinite) times. This is the case of classical structural glasses. These are models where no disorder is present, but whose dynamics become extremely slow as temperature is decreased (for a review, see [9, 10] and references therein). These

systems do not have an infinite set of conserved quantities, and are not integrable. Their key properties are frustration and strongly constrained dynamics. Frustration means that their Hamiltonian include terms which can not be minimized simultaneously. This induces very complicated energy landscapes, with many different minima separated by high energy barriers. To explore the full set of available configurations, the system needs to overcome those barriers through thermal jumps. Consequently, as temperature is decreased, relaxation times become very large, and relaxation is not seen, neither numerically nor experimentally. Still, it is not known whether relaxation times can become truly infinite at temperature $T \neq 0$, or if they are simply too large to be measured: therefore, it is still a matter of debate whether their non-ergodicity is genuine, or if it is simply a consequence of our incapacity to run long enough simulations and experiments.

Genuine breakdown of the ergodic hypothesis can however be proven rigorously in quantum mechanical systems. After the seminal work by Anderson [11], it is known that in the presence of strong disorder non-interacting quantum particles get localized in a finite volume due to quantum interference among different paths, as long as the dephasing effects of interactions and the presence of phonons are neglected. This phenomenon, termed "*Anderson localization*", leads to the complete absence of diffusion and dc transport, and has been observed experimentally (see [12] for a complete review). In $d \geq 3$, if the disorder strength is smaller than a critical value, the spectrum splits in two parts: at the band edges, localization survives due to the small density of states available for scattering, and localization persists. In the middle of the band, instead, the single particle hopping overcomes the disorder, and conducting delocalized eigenstates appear. The energy threshold separating these two kinds of states is called "mobility edge". [13] On the other hand, in $d = 1, 2$, the whole spectrum is localized for any non-vanishing disorder strength, due to the interference among all paths which allow a particle to return to its initial position. [14] Obviously, ergodicity is strictly defined only for many-body systems, but even in the non-interacting case it is expected that, starting from a generic initial many particle configuration, local observables will evolve towards thermal values. This does not happen if localized states are present in the spectrum: particles which are prepared in a state with finite overlap with a localized eigenstate do not diffuse through the system, but remain bounded to a finite region of space, even if their energy is high enough to (classically) allow them to overcome all the potential barriers.

This picture holds for non-vibrating lattices only: in real solids, it is known that transport is restored by the presence of phonons. Due to inelastic electron-phonon scattering processes, at finite temperature electrons are able to hop from one localized state to another, and weak conduction is always possible [15]. For a long time it has been a matter of debate whether transport could be restored by electron-electron interaction too: the reason is that the electron-electron coupling is much larger than the electron-phonon one, and therefore this effect is expected to be dominant. In the case of electronic systems, this indeed happens, since Coulomb interaction allows hopping of energy at large distance, and hybridizes far-away single particle states, whose energy is very close to one another. [16, 17] However, localization is indeed robust in lattice models with weak local

interactions, which can be realized e.g. using neutral cold atomic gases in optical lattices [18, 19]: this can be argued from the fact that particles live in a rugged and quantized energy landscape, which strongly suppresses inelastic scattering [20, 21, 22, 23, 24]. In this kind of systems, diffusion and transport are absent even in presence of interactions, not necessarily weak. This phenomenon has been termed *"Many-body localization"* (MBL), and has been subject to a large number of studies in the past years.

At the moment, a general definition for the MBL phase of quantum matter is lacking. There are many peculiar features with are associated with it, even though they do not necessarily imply one another, and therefore do not always appear together [25, 26]. Still, its most fundamental property seems to be the presence of an extensive set of quasi-local integrals of motions (LIOM), which makes MBL systems pictorially similar to integrable ones [27, 28, 29]. There are however two important differences between the two classes of systems: the first one is that MBL is much more robust, in the sense that it is retained if weak enough local perturbations are added the the Hamiltonian. The second one is that the integrals of motion of MBL Hamiltonians are quasi-local, in the sense that their support is non-exponentially small only on a finite region of space, whereas for integrable models they are defined over the whole volume, due to translation invariance. The existence of LIOMs allows one to argue for many other peculiar features of MBL, like the absence of transport at arbitrarily long distances, or the absence of thermalization starting from generic initial conditions [30]. Therefore, the MBL is not a thermodynamic transition, but rather a dynamical one, between a regime in which ergodicity is present and one in which it is absent.

1.1 Main issues addressed in this thesis

1.1.1 Many-body localization in the absence of quenched disorder

In most examples of MBL previously studied, quenched disorder is of paramount importance, since it assures that local rearrangements of particles require a significant cost in energy, which suppresses hybridizations in perturbation theory. However, it is known from the physics of classical glasses that disorder is not essential to obtain non ergodicity: their putative absence of ergodicity is not due to the presence of a disorder potential. Indeed, their Hamiltonians are translation invariant. The question naturally arises, whether thermalization may be absent in quantum non-integrable systems without disorder, too.

Some pioneering work on this topic was already present in the literature, before the start of this thesis work. It was known that putatively non-ergodic classical model can keep their glassiness, once dressed with weak enough quantum fluctuations [31, 32, 33, 34]. Their absence of relaxation is still due to classical mechanisms, though: therefore, they are qualitatively different from MBL models, since the latter are made non ergodic by quantum effects only. Localization due to genuine quantum interference effects was postulated in the context of diffusion of impurities

in He lattices [35], and in magnetic systems with couplings not restricted to nearest neighbors only [36]. However, in these works only qualitative arguments in favor of the presence of localization are given. In particular, they do not analyze the possible mechanisms that can restore delocalization, and therefore they fail to provide a plausible phase diagram for the models they are studying.

In this work, I present some models where phenomena very similar to MBL are present, and study them in detail. Those are systems in which interactions are very strong with respect to their hopping amplitudes, but no disorder is present in the Hamiltonian. At the perturbative level in the hopping, one indeed finds that ergodicity should be strictly absent. [37] However, the picture changes dramatically once non-perturbative effects are taken into account. The reason is that, for very large systems, rare regions which are internally ergodic appear as large deviations of the energy density. These regions can act as mobile baths for the rest of the system, and therefore reinstate thermalization. [39, 40] This effect is relevant only in the thermodynamic limit, though: for system sizes accessible to experiments and numerical investigations, the predictions of perturbation theory are correct, and these systems look for all practical purposes MBL. [38] As a consequence, it is still interesting and relevant for experiments to study how apparent non-ergodicity manifests in such models, in finite systems.

At the perturbative level, these systems localize on their own configurational disorder: once prepared in a random inhomogeneous initial configuration, interactions among the different constituents forbid most local relaxation processes, and therefore memory of the initial density profile is retained for long times. In the presence of periodic boundary conditions (PBC), translation invariance will obviously be restored by time evolution, but the time scales required for homogenization increase exponentially with system size. Due to the non-perturbative effects mentioned above, this divergence is not expected to persist in the thermodynamic limit, but the relaxation times may be extremely long, despite being eventually finite.

Perturbation theory predicts a quite peculiar phase diagram for such models, in the sense that the role of temperature is reversed as compared to models where disorder dominates. In standard MBL, temperature has an analogous role as in single particle localization, in the sense that it increases the phase space available for scattering, and therefore the tendency towards delocalization. Indeed, perturbative arguments suggest that a many-body mobility edge exist, separating ergodic states at high energy density from localized states at the bottom of the spectrum [22, 23], even though in this case too non-perturbative effects may reduce the putative transition to a crossover [41], as I shall discuss in this thesis. In interaction-driven localization, the situation is very different: the higher the temperature, the stronger the configurational disorder, and therefore the tendency towards localization. Vice-versa, at low temperature spatial correlations imply that the number of local resonances proliferate, and therefore the lower part of the spectrum is expected to delocalize at any finite hopping strength. This is the reason why this phenomenon, despite appearing in very simple models (e.g., one dimensional Bose-Hubbard models at strong interaction [42, 43, 39, 40]) was not previously noticed: low energy excitations above the ground state can

never get localized in absence of disorder. Once again, it is important to be aware that no sharp transition is expected in the thermodynamic limit.

1.1.2 Absence of many-body mobility edges in the thermodynamic limit

The concept of mobility edges appeared for the first time in the context of single-particle localization, where its existence is well established. On the other hand, the nature of the putative finite temperature transition in interacting systems is much less clear. As stated above, such a transition is predicted by perturbative arguments in the interaction strength [22, 23], according to which there should be a sharp energy threshold separating ergodic conducting states from non-ergodic insulating ones. These studies focus on the behavior of typical regions, though, and fail to take into account the behavior of rare, anomalous ergodic regions: indeed, once such regions are included in the description of the MBL phase, one finds that they rule out the existence of mobility edges, exactly as happens in translation invariant systems [41]. Despite this close analogy, there is a fundamental difference between disorder- and interaction-driven MBL: in the presence of disorder, for small hopping amplitude the whole spectrum is non-ergodic. In this regime, no rare ergodic regions can be formed, and MBL is expected to be present, even in the thermodynamic limit. On the contrary, perturbation theory predicts that translation invariant systems are ergodic at low temperature for any finite hopping amplitude, therefore they do not possess a genuine non-ergodic phase in the thermodynamic limit. According to this argument, no transition is expected as a function of temperature, but rather a crossover from plain ergodic states at high T to a sort of Griffiths phase behavior at low temperature: the former is characterized by transport due to rare regions, which act as carriers of particles and energy. In a sense, this can be seen as an extension of the famous Mott argument to the many-body case: while in non interacting case Mott proved that localized and delocalized states can not exist at the same energy density, in the presence of interactions coexistence of ergodic and non-ergodic states is not possible even at very different energies. Moreover, this argument rules out the possibility of MBL in the continuum: in the absence of a lattice, the energy density is unbounded, and perturbatively one always expects a mobility edge to be present for any disorder strength. The rare-region argument can then be applied to rule out the presence of a truly non-ergodic phase.

This argument may look inconsistent with the fact that mobility edges have been reported numerically [44, 45, 46, 47]. However, as in the disorder free case, it applies only to very large system sizes, and therefore it is not contradicted by these studies. I have checked this via a careful numerical analysis Additionally, numerical investigations in large systems have failed to detect the presence of mobility edges [48, 49], even though others do report their existence.

1.2 Structure of this thesis

The remainder of this thesis is organized as follows: in Chapter 2, a pedagogical overview of the physics of localization is provided, aimed to provide the reader with all the instruments necessary to understand the following Chapters. First, to set up the conceptual framework, I discuss what thermalization means in closed quantum systems. Next, I review how ergodicity breaks down in the presence of strong disorder, and why localization is robust against weak local interactions. These arguments are presented because the perturbative description used to describe translation invariant systems is based on the same procedure. I shall discuss the main analogies and difference between localization in the single-particle and many-body cases, too, and introduce the various properties which define the MBL phase, at current knowledge. Finally, the pioneering work about localization in absence of disorder by Kagan et al. [35, 36] is presented, and a comparison with the physics of classical glasses is made.

In Chapter 3, the physics of translation invariant MBL is discussed. After introducing the general properties that such "ideal quantum glasses" are expected to show, I shall analyze a concrete and experimentally reproducible model where such features appear. I shall show why perturbation theory in the hopping predicts this non-ergodic phase to exist, and what peculiar properties it is expected to have, at least as long as finite sizes are involved.

In Chap. 4 the behavior of MBL systems in the thermodynamic limit is discussed, both with and without disorder. I provide a careful mathematical argument, that shows the instability of localization against the presence of bubbles of energy density very different from the typical one. For systems with disorder in the Hamiltonian, this implies that only an infinite temperature transition is possible, between a fully localized and a fully ergodic spectrum. For translation invariant systems, transport is present at all finite hopping strengths, even though with non-perturbatively small conductivity (a phenomenon referred as *"asymptotic localization"* in [43]). Still, for experimentally and numerically realizable systems, mobility edges and localization are present for all practical purposes, due to the rarity of bubbles.

In Chap. 5 the main results of this thesis are summarized, and future perspectives are discussed.

Chapter 2

Breakdown of ergodicity in disordered systems

In this Chapter, an introduction on various mechanisms that can lead to a breakdown of the ergodic hypothesis is provided. Its aim is to provide the reader with the conceptual framework, which is necessary to understand my work. It is not aimed to show the technical details of the works that will be discussed: it will rather present the conceptual tools, which are used in the following Chapters. This Chapter is organized as follows: in Sec. 2.1, thermalization in closed quantum systems is discussed. I shall review in which sense a closed system can be expected to thermalize, and what the presence of thermalization implies for the structure of many-body eigenstates. In Sec. 2.2, the seminal work by Anderson [11] is presented, which explains how transport and diffusion can be absent in non-interacting quantum systems. Once the physics of single particle localization is clear, one should add interactions to the system, and discuss the physics of MBL: this is done in Sec. 2.3. Finally, in Sec. 2.4 I briefly introduce the physics of classical glasses, and compare it with the one of quantum MBL systems, which can be seen as quantum glassy systems.

2.1 Thermalization in closed quantum systems

I consider a closed quantum many-body system, described by a Hamiltonian H. For simplicity, I assume that, at time $\tau = 0$, the system is prepared in a pure state $|\psi_0\rangle$. This assumption may be relaxed, allowing for the initial condition to be a statistical ensemble ρ, without qualitatively changing the description. I work in the Schrödinger picture, in which states evolve and operators are fixed in time. [50] Since the system is not in contact with any thermal bath, the time evolution is given by the Schrödinger equation

$$i\frac{d}{d\tau}\left|\psi\left(\tau\right)\right\rangle = H\left|\psi\left(\tau\right)\right\rangle, \tag{2.1.1}$$

where $\hbar = 1$ is set. The formal solution of the equation is given by

$$|\psi(\tau)\rangle = e^{-iH\tau} |\psi_0\rangle . \tag{2.1.2}$$

The expectation value of any observable O at time τ is then

$$O(\tau) = \langle\psi(\tau)| O |\psi(\tau)\rangle . \tag{2.1.3}$$

I am interested in discussing in which sense a closed quantum system can undergo thermalization processes (for a more complete discussion, see the review [26] and references therein). Strictly speaking, real thermalization is not possible in the absence of a thermal bath: while a system in thermal equilibrium is characterized by a small set of macroscopic parameters (like temperature, volume and density), unitary evolution preserves the memory of all microscopic details of the initial condition at all times, due to reversibility. This apparent contradiction can be solved realizing that, while information cannot be erased in Schrödinger evolution, after a certain time it becomes impossible to experimentally recover it: this is due to the fact that entanglement between all system components is built, and information is hidden in non-local correlations. In order to recover this information, one would need to measure operators which simultaneously act over the whole system, but such a measure is obviously not feasible. This process is called *"decoherence"* of the individual degrees of freedom. From the experimental point of view, only operators which act on a finite number of degrees of freedom, either in real or momentum space, can be measured. If the total number of degrees of freedom is much larger than the one over which measurements are performed, the outcomes are expected to be indistinguishable from thermal averages: in this sense, the system acts as its own bath, and thermalizes any small enough subsystem.

To discuss thermalization somewhat more precisely, I consider for simplicity a system, in which energy is the only conserved quantity. This assumption can be relaxed, allowing the conservation of a few other quantities, such as e.g. particle number or total momentum, with no further complication. The full system is arbitrarily partitioned in two spatial regions, a "small" subsystem A and a large subsystem B, as shown in Fig. 2.1.1. I will sometimes refer to B as the *"environment"*. The full Hilbert space $\mathcal{H}$ can then be written as a direct product between the two subspaces $\mathcal{H}_{A,B}$, describing subsystems A, B, respectively:

$$\mathcal{H} = \mathcal{H}_A \otimes \mathcal{H}_B. \tag{2.1.4}$$

I work in the thermodynamic limit, sending the volume V_B to infinity, but keeping V_A fixed. Chosen the initial state $|\psi_0\rangle$, I define the inverse (quasi-)temperature β as the solution of the following equation:

$$\langle\psi_0| H |\psi_0\rangle = \frac{1}{Z(\beta)} \mathrm{Tr}\left[H e^{-\beta H}\right], \tag{2.1.5}$$

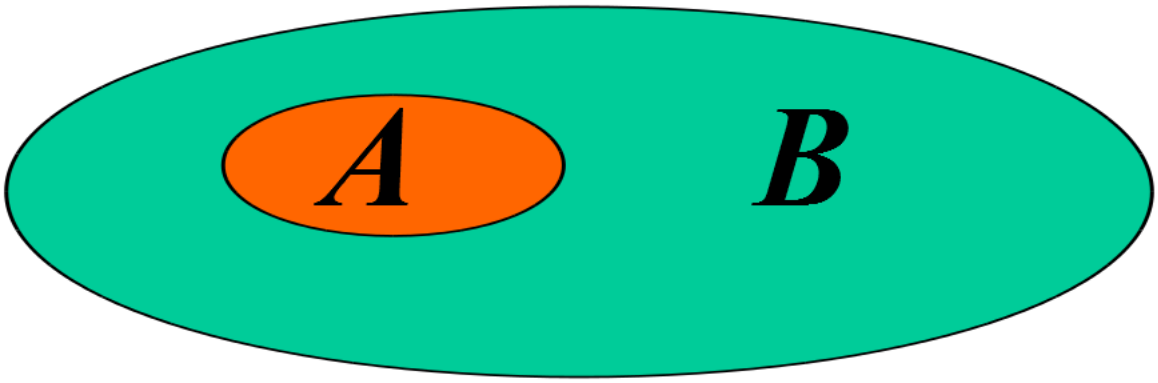

Figure 2.1.1: Partition of a closed quantum system into a "small" subsystem A and a "large environment" B. For generic models, mean values of observables acting on A are described by a thermal distribution in the long time limit, due to decoherence induced by the interaction with degrees of freedom belonging to B. This is not the case in many-body localized systems.

where

$$Z(\beta) \equiv \mathrm{Tr}\left[e^{-\beta H}\right] \tag{2.1.6}$$

is the partition function. The meaning of Eq. (2.1.5) is the following: if the system were put in contact with a thermal bath, the inverse temperature of that bath should be set to β, in order for the average energy to be $\langle\psi_0| H |\psi_0\rangle$. It can be checked that in general Eq. (2.1.5) admits a unique solution.

I am interested in measuring only observables which are defined on A. Therefore, it is not necessary to know the time evolution of the full system $A + B$: indeed, one can trace out all degrees of freedom living in B, and study the *"reduced density matrix"*

$$\rho_A(\tau) \equiv \mathrm{Tr}_B\left[|\psi(\tau)\rangle\langle\psi(\tau)|\right], \tag{2.1.7}$$

where Tr_B means that we take a trace over $\mathcal{H}_B$ only. If the system equilibrates, then in the long time limit expectation values of any local observable should be predicted by the Gibbs ensemble:

$$\rho_G(\beta) \equiv \frac{1}{Z(\beta)} e^{-\beta H}, \tag{2.1.8}$$

where $Z(\beta)$ is defined by Eq. (2.1.6). When looking at A only, one just needs to trace out the subspace $\mathcal{H}_B$ once again:

$$\rho_G^{(A)}(\beta) \equiv \mathrm{Tr}_B\left[\rho_G(\beta)\right]. \tag{2.1.9}$$

I am now ready to give a definition for thermalization. Sub-system A is said to thermalize if

$$\lim_{T\to\infty}\lim_{V_B\to\infty}\frac{1}{T}\int_0^T d\tau \rho_A(\tau) = \rho_G^{(A)}(\beta), \tag{2.1.10}$$

i.e. if the long time average of the reduced density matrix reproduces the Gibbs ensemble, at the appropriate temperature. [51, 52, 53, 54] It is important that both the long time and large system limit are taken: for finite times, energy can diffuse only to finite distances, degrees of freedom in A are not able to interact with all degrees of freedom in B, and therefore there can be no full equilibration. Conversely, for finite sizes one always sees quantum revivals, since the dynamics are quasi-periodic.

The common expectation is that, taken a generic Hamiltonian H, the system thermalizes starting from any initial state $|\psi_0\rangle$. This is a very strong statement, which is in general impossible to prove. It seems quite reasonable, though: if H is able to connect all degrees of freedom, one expects all memory of the initial condition to disappear due to dephasing processes, in which different components of the system exchange energy among them. Here, by *"dephasing"*, I mean the decrease of the amplitude of the off-diagonal matrix elements of $\rho_A(\tau)$ in the basis of the many-body eigenstates, due to interaction with degrees of freedom living in B. A Hamiltonian which behaves in this way is called *"ergodic"*. The large majority of physical Hamiltonians are indeed believed to be ergodic.

2.1.1 The eigenstate thermalization hypothesis

If I assume that indeed the system thermalizes starting from any initial state, this must hold also if it is prepared in an exact many-body eigenstate $|n\rangle$ of the Hamiltonian. In this case, time evolution is trivial: $|\psi(\tau)\rangle = e^{-iE_n\tau}|\psi_0\rangle$, where E_n is the corresponding eigen-energy. Obviously, mean values of observables do not evolve: $O(\tau) = O(0)$ for any Hermitian operator O. Thermalization of all states thus implies that *all eigenstates are thermal,* in the sense that expectation values of observables on them are indistinguishable from thermal values. This statement is known as *"eigenstate thermalization hypothesis"* (ETH) [51, 52, 53, 54], and corresponds to an extreme limit of the microcanonical ensemble, in which one single eigenstate is fully representative of the properties of the system at its energy. Since the eigenstates of the Hamiltonian are the fundamental tool to describe dynamics, it is worth to discuss some of the implications of this hypothesis.

I assume for simplicity that no exact degeneracies are present in the spectrum, and label the energies E_n in increasing order. A first consequence of ETH is that, given any local operator O, its diagonal matrix elements on the basis of energy eigenstates $O_{nn} \equiv \langle n|O|n\rangle$ are a smooth function of n: to be more precise, it can be checked that the difference$|O_{n+1n+1} - O_{nn}|$is exponentially small in system size, whenever ETH holds. [55] To justify this statement, let us take an initial state $|\psi_0\rangle$, with mean energy $E \equiv \langle\psi_0|H|\psi_0\rangle$. The time evolved expectation value $O(\tau)$ is

$$O(\tau) = \sum_{n,m} e^{-i(E_n - E_m)\tau} \langle\psi_0|m\rangle \langle n|\psi_0\rangle O_{mn}. \tag{2.1.11}$$

Let us now take the time average:

$$\langle O\rangle(T) \equiv \frac{1}{T}\int_0^T d\tau O(\tau) = \sum_{n,m} \frac{e^{-i(E_n-E_m)T}}{-i(E_n-E_m)T} \langle\psi_0|m\rangle\langle n|\psi_0\rangle O_{mn}. \tag{2.1.12}$$

Now the limit $T\to\infty$ can be taken: all terms with $m\neq n$ in the right-hand side of Eq. (2.1.12) vanish, and only the diagonal terms remain:

$$\langle O\rangle(\infty) = \sum_n |\langle n|\psi_0\rangle|^2 O_{nn}. \tag{2.1.13}$$

The statistical ensemble defined by the weights $|\langle n|\psi_0\rangle|^2$ is sometimes called the *"diagonal ensemble"*. Since thermalization is assumed to occur, the diagonal ensemble has to be equivalent to a thermal ensemble; additionally, since I am working in the thermodynamic limit, thermal averages have in turn to be equivalent to microcanonical ones [1],

$$\bar{O}(E) \equiv \frac{1}{\mathcal{N}_\Delta}\sum_{n:|E_n-E|<\Delta} O_{nn}. \tag{2.1.14}$$

In the above, Δ is the width of a narrow energy window centered at E, while $\mathcal{N}_\Delta$ is the number of states within such window. Thermalization implies that

$$\langle O\rangle(\infty) = \bar{O}(E). \tag{2.1.15}$$

The left hand side of this equation formally depends on the initial state $|\psi_0\rangle$, whereas the right hand side does not: this means that the left hand side must be independent of the initial state too. Since the coefficients $|\langle n|\psi_0\rangle|^2$ are given, this can happen only if the matrix elements O_{nn} are roughly constant within the window $|E_n-E|<\Delta$. In some sense, it can be said that *"all eigenstates close enough in energy look the same"* when only local quantities only are considered. For finite sizes, however, rare anomalous eigenstates are present, which do not obey this rule and therefore ETH, and that prevent thermalization of initial states which have a non-negligible overlap with them [56].

Another important prediction of ETH is the behavior of the entanglement entropy S_{AB} between regions A and B:

$$S_{AB} \equiv -\mathrm{Tr}\left[\rho_A \ln \rho_A\right]. \tag{2.1.16}$$

As is well known, the entanglement entropy is non-negative, and it vanishes if and only if $|\Psi_{AB}\rangle = |\phi_A\rangle\otimes|\chi_B\rangle$, i.e., if the state of a global system is the product of a state of $\mathcal{H}_A$ and one of $\mathcal{H}_B$. Consequently, it is taken as a quantitative measure of the entanglement between regions A and B: the larger S_{AB}, the more correlated the two regions. For eigenstates corresponding to temperature

$T \neq 0$, ETH predicts that the entanglement entropy must coincide with the thermodynamic entropy: therefore, it must obey a *"volume law"* scaling, i.e. $S_A \propto V_A$.

Finally, using ETH it is possible to analyze the statistical properties of eigenvalues and eigenvectors. This is due to the fact that, at high energies, the thermodynamic properties of a system are independent on the microscopic details of the model, like the geometry of the lattice or the precise form of the interaction. Only the symmetries of the problem are important to compute such quantities. Consequently, if eigenstates are thermal, their statistics can only depend on symmetries as well. It is then convenient to take the simplest possible models with the relevant symmetries, use them to make analytical predictions, and extend those via ETH to more realistic and complicated systems. It turns out that the easiest models to treat are Gaussian random matrices. In particular, the Gaussian Orthogonal Ensemble (GOE) describes particles with even spin and no magnetic field; the Gaussian Unitary Ensemble (GUE) describes particles in a magnetic field and the Gaussian Symplectic Ensemble (GSE) corresponds to particles with odd spin and spin-orbit interaction. [57]

While ETH and thermalization apply to a large number of quantum systems, there are models which do not thermalize under unitary evolution. One such exception are exactly integrable models: these models have the peculiarity of admitting an extensive set of local integrals of motion, where local means that they act on a finite number of degrees of freedom only. Therefore, it is commonly believed that they relax to a non-thermal steady state described by the "Generalized Gibbs Ensemble" (GGE), which is constructed by imposing the conservation of all integrals of motion [4, 5, 6], even though some recent results have risen doubts about this hypothesis [7, 8]. These models are very fine-tuned, however, and are in general unstable against weak perturbations, which restore ergodicity.

A more robust exception are many-body localized systems: these systems fail to thermalize in any sense, and ETH does not apply to them. In the following I will now introduce localization at the single particle level, which is useful to introduce the tools for the study of MBL. The remainder of this thesis is dedicated to the discussion of this class of systems, and their remarkable properties.

2.2 Single-particle localization

It is known from Einstein's seminal paper [58] that the motion of classical particles in a random environment is governed by a diffusion equation:

$$\frac{\partial \rho}{\partial \tau}\left(\vec{r},\tau\right) = D\nabla^2 \rho\left(\vec{r},\tau\right), \tag{2.2.1}$$

where ρ is the density of particles, and D is the diffusion constant. This equation holds for any kind of random walk without heavy-tailed distributions of step lengths, provided that there is no memory in the dynamics, i.e., that the process is Markovian. Among its many applications, the

diffusion equation has been used to study semiclassically the transport properties of metals, in the presence of impurities. The result is the Einstein-Sutherland relation for the conductivity σ [59]:

$$\sigma = e^2 D \nu, \tag{2.2.2}$$

where ν is the density of states per unit energy and unit volume. From this semiclassical theory, one expects that, as the concentration of impurities increases, the diffusion constant and hence the conductivity decrease, without ever vanishing completely. This picture is correct for a small concentration of impurities (and hence at low disorder strength) in spatial dimension $d > 2$, but it has been proven wrong by Anderson in the presence of strong disorder [11]: in that regime, the system is dominated by quantum effects, which destroy diffusion completely, and render the conductivity exactly zero. This phenomenon is known as Anderson localization.

The essential properties of single-particle localization can be illustrated by the tight-binding model of a spinless fermionic particle living on a d-dimensional regular lattice, with a random on-site potential. This is the well-known Anderson model [11], and its Hamiltonian reads

$$H = -t \sum_{\langle i,j \rangle} \left(c_i^\dagger c_j + c_j^\dagger c_i \right) + W \sum_i \varepsilon_i n_i. \tag{2.2.3}$$

In the above, the sum appearing in the first term runs over all pairs of nearest neighbors, the operator $c_i^\dagger$ creates a fermion on site i, $n_i \equiv c_i^\dagger c_i$ and $\varepsilon_i \in \left[-\frac{1}{2}, \frac{1}{2}\right]$ are independent random variables with uniform distribution. The parameter W tunes the disorder strength.

To qualitatively understand the physics of the model, it is useful to consider the dynamics of a single particle, initially located at site 0. Let us first look at the trivial case $t = 0$: in this case, the initial state is an eigenstate of the total Hamiltonian, so no evolution takes place. In particular, the particle is unable to diffuse. Now a small but finite $t \ll W$ is turned on: in this regime, perturbation theory in t can be applied to compute the eigenvalues and eigenvectors of the total Hamiltonian, starting from the *"atomic limit"*, i.e. from the basis of the eigenstates of site occupation numbers. The coefficient of the admixture between state $c_0^\dagger |0\rangle$, $|0\rangle$ being the vacuum state, and state $c_i^\dagger |0\rangle$, i being a nearest neighboring site, is given by

$$\frac{t}{\varepsilon_0 - \varepsilon_i}. \tag{2.2.4}$$

This object is called a *"locator"*. To compute the admixture coefficient with a generic site j, one has to sum over all possible paths which start from 0 and end to j, multiplying at each step k with the appropriate locator $t/\varepsilon_0 - \varepsilon_k$. This kind of procedure is called "*locator expansion*", and is shown pictorially on the left of Fig. 2.2.1. Since, typically, energy differences among neighboring sites $|\varepsilon_i - \varepsilon_j|$ are of order $O(W)$, they are large with respect to the hopping amplitude t, and one naively expects perturbation theory to be typically well behaved. One then finds typical eigenstates to be

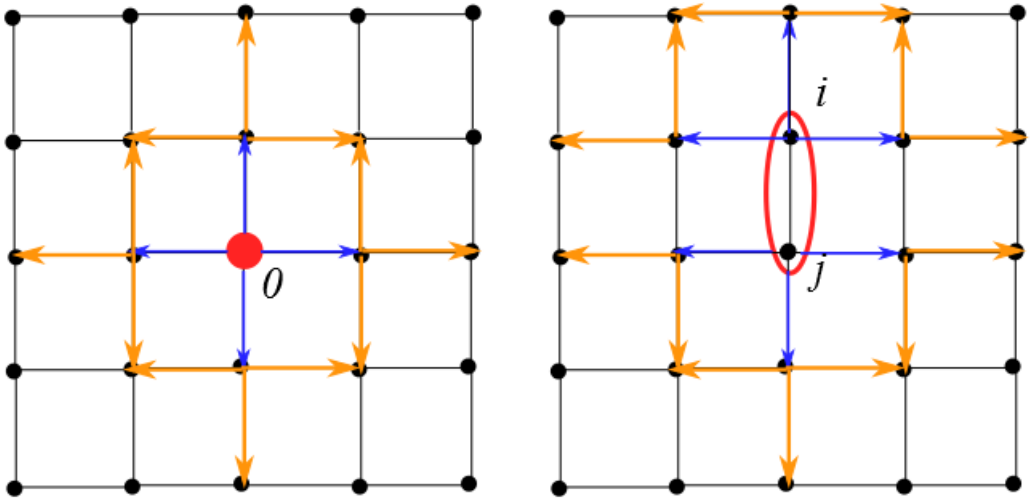

Figure 2.2.1: *Left:* Pictorial representation of the locator expansion, in absence of local resonances: a particle, originally located on site 0, acquires an amplitude of magnitude $\sim O\left(t/W\right)$ on nearest neighboring sites (blue arrows). Its amplitude on next-to-nearest neighboring sites is of order $\sim O\left(\left(t/W\right)^2\right)$ (orange arrows), and so on. The amplitude of the wavefunction decreases exponentially in the distance from the localization center 0, and the particle is localized. *Right:* effect of a local resonance. If two neighboring sites i, j have a small energy difference $|\varepsilon_i - \varepsilon_j| \ll t$, two hybridized states form, in which the particle is equally shared among the two sites. One has then to restart the locator expansion from such states.

centered at a certain site i, and to decay exponentially with distance from it:

$$\psi_i\left(r\right) \propto e^{-\frac{|r-r_i|}{\xi}}, \tag{2.2.5}$$

where $\xi \sim 1/\ln\left(\frac{W}{t}\right)$ is called "*localization length*". The picture that emerges from this naive argument is that the system remains insulating and non-diffusive even at finite t, in spite of the fact that the Hamiltonian (2.2.3) in principle allows a particle to hop through the whole system: particles are not able to diffuse, but are confined in a spatial region of radius of the order of the localization length.

This picture, despite being qualitatively correct, is oversimplified, since it neglects *resonances*, i.e. pairs of sites i, j with unperturbed energies very close to one another:

$$|\varepsilon_i - \varepsilon_j|_{\text{res}} \ll t\left(\frac{t}{W}\right)^{n-1}, \tag{2.2.6}$$

n being the number of sites the particles needs to hop through to move from site i to j. When such a pair of sites is met, one has to resort to degenerate perturbation theory, which predicts that two hybridized states form:

$$|\psi_\pm\rangle \approx \frac{c_i^\dagger \pm c_j^\dagger}{\sqrt{2}}|0\rangle + O\left(\frac{t}{W}\right). \tag{2.2.7}$$

In this kind of eigenstates, a particle can no longer be seen as localized on either site i or j, being instead equally shared among the two sites. This is depicted on the left of Fig. 2.2.1. These resonances do not qualitatively change the picture given above, as long as they are rare enough and well separated from one another. However, resonances become more common as the hopping t is increased: as their density increases, particles become able to explore larger parts of the system hopping between different resonances, and the localization length increases accordingly. Then, in three or more dimensions, at a certain critical value t_c resonances percolate through the whole system, the localization length diverges, and diffusion of particles at arbitrarily long distances becomes possible: the system undergoes a phase transition from a non-ergodic insulator to an ergodic metal. This picture is not correct in $d = 1, 2$, however: as I discuss in Subsec. 2.2.2, in low dimension there is no transition, and particles are localized at any finite disorder strength, despite the percolation of resonances. [60] In the continuum the localization length gets arbitrarily large, however, as energy is increased: in particular one finds a power law divergence for $\xi(E)$ as E tends to infinity for $d = 1$, while for $d = 2$ the divergence is exponential. [14]

In this description, only resonances among nearest-neighboring particles are considered: one may worry that localization could be destroyed by the presence of resonances between sites at large distance $r \gg 1$. In finite dimension, this is not the case, however: the reason is that the effective hopping between sites is exponentially small in the number n of times one needs to apply the hopping term, in order to connect the two sites, as shown in Eq. (2.2.6). So the probability of finding a resonance decreases exponentially in the distance: on the other hand, the number of sites at distance n scales as n^{d-1}, where d is the spatial dimension. Therefore, the typical number of resonances one finds at distance n rapidly tends to zero, and direct hybridizations among distant sites can safely be neglected.

Since the Anderson Hamiltonian (2.2.3) is quadratic, it can be rewritten in terms of its single-particle eigenstates through a basis rotation:

$$H = \sum_{\alpha=1}^{V} E_\alpha n_\alpha, \tag{2.2.8}$$

where n_α is the occupation number of eigenstate $|\alpha\rangle$, and E_α is the energy of that state. The many-particle eigenstates are then obviously products of single-particle ones, and can be labeled through the occupation numbers n_α, which form an extensive set of integrals of motion. In this sense, the Anderson model is *"integrable"*, even though this integrability is a trivial consequence of the fact that the model is non-interacting. These conserved quantities are quasi-local, in the sense that their commutator with local observables acting on sites far away from the localization center R_α decays exponentially in the distance. The importance of this fact becomes clear as interactions are introduced: for weak interaction, one can do perturbation theory starting from the Hamiltonian above, and prove that for local interactions the full Hamiltonian can be written

in terms of some dressed occupation numbers $\tilde{n}_\alpha$, which are still conserved by the dynamics [29]. From this characterization, one can explain most of the peculiar features of many-body localized systems, like the absence of transport, diffusion and thermalization, an area-law entanglement entropy for highly excited states, or the logarithmically slow growth of entanglement starting from initial classical states.

2.2.1 Phase diagram of the Anderson model

Up to now, the Anderson model has been discussed treating all eigenstates as equivalent. I now wish to explain the effect of energy on the localization properties of the system. In the presence of a lattice, for $d > 2$ there is a transition point t_c at which eigenstates close to the middle of the energy band delocalize. Since the entropy is maximal in the middle of the band, this corresponds to the transition point for typical eigenstates. This does not imply that all eigenstates delocalize at that value, though. Indeed, at the band edge the density of states is much smaller, and therefore localization is more robust, since the typical energy differences among consecutive states gets larger. One therefore expects that, for $t > t_c$, localized and ergodic states may coexist in the spectrum.

At the same time, as argued by Mott [13], coexistence of localized and delocalized states at the same energy is not possible in the thermodynamic limit. The reason is that such a coexistence cannot be robust against perturbations: as soon as some weak perturbation is added to the Hamiltonian, the localized state gets coupled to the continuum of delocalized modes, which acts as a bath and thermalizes it. To be concrete, let us consider the Hamiltonian (2.2.3), and let us suppose that there is a localized eigenstate $|\psi_{\rm loc}\rangle$ at the same energy as a set of delocalized states $|\phi_n\rangle$. Let us now modify the Hamiltonian by slightly changing the hopping amplitude: $t \to t + \delta t$, with $\delta t/t \ll 1$, and work perturbatively in δt. The strategy is to estimate the matrix elements between $|\psi_{\rm loc}\rangle$ and the states $|\phi_n\rangle$ at first order in perturbation theory, and show that they can get arbitrarily large when system size is increased. This implies that, for large enough systems, $|\psi_{\rm loc}\rangle$ hybridizes with at least some delocalized states, for any arbitrarily small δt, and therefore becomes delocalized too.

Since states with the same unperturbed energy density are considered, one needs to resort to degenerate perturbation theory. The first step is to estimate the matrix element of the hopping

$$\delta t \times H_{\rm hop} \equiv \delta t \sum_{\langle i,j \rangle} \left(c_i^\dagger c_j + c_j^\dagger c_i \right) \tag{2.2.9}$$

between $|\psi_{\rm loc}\rangle$ and $|\phi_n\rangle$. $|\psi_{\rm loc}\rangle$ have amplitude of $O(1)$ over a finite spatial region, and is exponentially small on the rest of the system; on the other hand, ϕ_n is expected to have amplitude of

$O\left(\frac{1}{\sqrt{V}}\right)$ everywhere in the system, V being the volume. One thus expects the scaling

$$\langle\phi_n|\, H_{\rm hop}\, |\psi_{\rm loc}\rangle \approx O\left(\frac{1}{\sqrt{V}}\right). \tag{2.2.10}$$

Let us now check the energy difference between the two states: since the $|\phi_n\rangle$ are ergodic, one expects that for many of them

$$E_{\rm loc} - E_n \approx O\left(\frac{1}{V}\right), \tag{2.2.11}$$

since $1/V$ is the typical level spacing of the delocalized modes. This means that the coefficient of admixture at first order in δt scales as

$$\delta t \frac{\langle\phi_n|\, H_{\rm hop}\, |\psi_{\rm loc}\rangle}{E_{\rm loc} - E_n} \approx \delta t \times O\left(\sqrt{V}\right). \tag{2.2.12}$$

So, for $V \gg \frac{1}{\delta t^2}$, the localized state is not robust against the perturbation, but hybridizes with the ergodic states and becomes ergodic too.

On the basis of this argument, Mott concluded that, for $t > t_c$, there must be an energy threshold E_c separating low-energy localized states and high-energy delocalized ones. Such a threshold is called a *"mobility edge"*. Since the model under discussion is defined on a lattice, i.e. a single finite energy band is considered, an analogous mobility edge $E_{c'}$ appears in the high end part of the spectrum, too. Coming from large t, one expects the mobility edges to start from the band edges at $t \to \infty$, and to move towards the band center as long as t is decreased. Then, at $t = t_c$, they merge together, and the whole spectrum becomes localized. The resulting phase diagram is shown in Fig. 2.2.2, as a function of hopping and energy density. In the continuum, since the band-width is infinite, there is no localization of the full spectrum at any finite t, but rather a divergence of $E_c(t)$ for $t \to 0$.

When a mobility edge is present, the conduction properties of the system depend on the position of the Fermi energy E_F. For $E_{c'} > E_F > E_c$, the system behaves as a metal, the conductivity σ is finite at all temperatures and can be estimated from the Einstein-Sutherland relation. For $E_F < E_c$ states at the Fermi level are localized, and the situation is very different: at $T = 0$, the system is an insulator, with $\sigma = 0$. If the system is prepared in a thermal state with finite T, however, the conductivity is always finite, due to thermal activation above the mobility edge. This can be done by weakly coupling the system to a thermal bath, letting it equilibrate, and then removing the coupling. Therefore, in the insulating phase the conductivity should scale as an Arrhenius law,

$$\sigma(T) \propto e^{-\beta(E_c - E_F)}. \tag{2.2.13}$$

For a non-vibrating lattice, thermal activation is the only process which leads to conduction for $E_F < E_c$, but this is never observed in reality. Indeed, in realistic systems conduction happens also

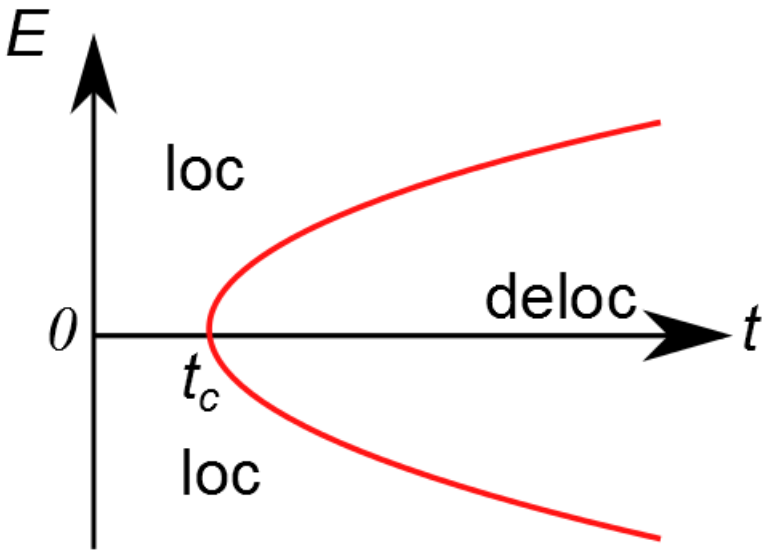

Figure 2.2.2: Phase diagram of the Anderson model on a lattice, as a function of energy E and hopping t, at fixed disorder strength W, in spatial dimension $d \geq 3$. For $t < t_c$, all states are localized. At t_c, two mobility edges appear, separating delocalized states in the middle of the band from localized states at the band edges.

due to phonon assisted hopping between localized states, which dominate by far the conductivity. [15]

2.2.2 Scaling theory of localization: absence of a transition in $d = 1, 2$

Up to now, I have discussed the Anderson model in three dimension, and argued for the presence of a delocalization transition in energy density, for $t > t_c$, using perturbation theory. The situation is dramatically different in low dimensional systems, though: in that case, no transition is present, and any finite disorder localizes the whole spectrum. This result is obtained in [60] using scaling arguments. One starts from the Einstein-Sutherland relation (2.2.2) for the electric conductivity σ, and then computes the electric conductance G of a sample of linear size L as

$$G = \sigma L^{d-2} = \frac{e^2}{h} g(L), \tag{2.2.14}$$

where

$$g(L) \equiv \frac{hD(L)/L^2}{1/\nu L^d} \tag{2.2.15}$$

is the dimensionless *Thouless conductance*. It is the ratio of two quantities: the *Thouless energy* $E_T(L) \equiv hD(L)/L^2$ and the mean *level spacing* $\delta(L) \equiv 1/\nu L^d$, which is the inverse of the density of states multiplied by the volume of the sample. At the classical level, $D(L) = D$ is a constant, and

the dependence of Thouless conductance on system size is trivial. This is not necessarily true in the presence of quantum interference, however.

This quantity has a simple physical interpretation: let us partition our sample in boxes of linear size L. For each of these boxes, $\delta(L)$ is the mean level spacing for the internal states of the box, whereas $E_T(L)$ is the inverse escape time of a particle from the box, once this is coupled to an external environment. One now couples together several of such boxes: then $E_T(L)$ can serve as an estimate for the typical coupling between levels in neighboring boxes. Therefore, $g(L)$ is an estimate of the strength of hybridizations among states of different boxes: for $g \gg 1$, states of different subsystems get strongly hybridized, and the particles delocalize. On the other hand, for $g \ll 1$, the various subsystems behave almost independently, and particles remain localized in a finite volume.

A scaling theory for the Thouless conductance is constructed checking how quantum corrections modify its dependence on the length scale L. For this purpose, one studies the *β-function*

$$\beta(g) \equiv \frac{d \ln g}{d \ln L}. \tag{2.2.16}$$

The advantage of this quantity is that it is *universal*, in the sense that it does not depend on the particular model one is looking at, but only on the dimensionality of space and on the symmetries of the system. Let us first look at the limit $g \gg 1$: in that regime, macroscopic theory of transport is expected to work, the system behaves like a classical metal, and Eq. (2.2.15) gives the correct scaling $g(L) \propto L^{d-2}$. This implies that

$$\lim_{g \to \infty} \beta(g) = d - 2. \tag{2.2.17}$$

One then considers the opposite limit $g \ll 1$. In this case, hybridizations among different regions of the sample are suppressed, and the system is completely localized: one thus expects the scaling $g(L) \propto e^{-\frac{L}{\xi}}$, ξ being the localization length. The β-function consequently behaves as

$$\beta(g) \approx \ln\left(\frac{g}{g_a(d)}\right) < 0, \quad g \to 0 \tag{2.2.18}$$

where g_a is a constant of $O(1)$.

$\beta(g)$ smoothly interpolates between these two limits, as shown in Fig. 2.2.3. Since smaller g necessarily implies a stronger tendency towards localization, $\beta(g)$ has to be monotonous, at least in absence of spin-orbit interaction. If such a monotonicity holds, these asymptotic behaviors are enough to infer the behavior of the Anderson model as a function of dimensionality d. For $\beta(g) > 0$, the conductance grows with system size: this means that hybridizations become stronger as system size is increased, and therefore the sample is a metal. Conversely, for $\beta(g) < 0$ hybridizations among different parts of the system get weaker as the distance is increased: this implies that no transport at macroscopic distances is possible, and the system is an insulator. For $d = 3$, the limit

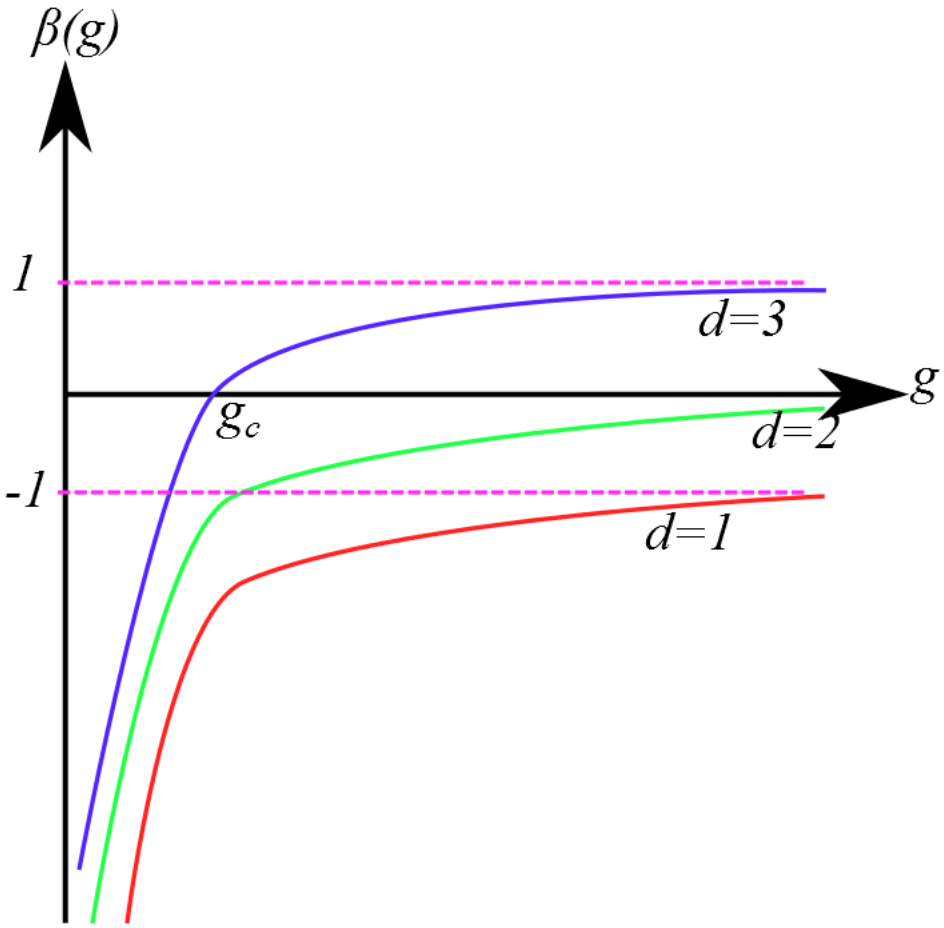

Figure 2.2.3: Qualitative plot of the function $\beta(g)$ for single particle localization, in absence of spin-orbit interaction, for different spatial dimensions. For $d = 1, 2$, the β-function is negative for any finite g, and the conductance flows with system size towards $g = 0$. For $d = 3$, a critical value g_c is present: below that value, the conductance still flows towards 0, and we are still in the insulating phase. For $g > g_c$, the conductance flows towards the value $d - 2 = 1$ predicted by the classic theory of metals: the system is in a metallic delocalized phase.

of the β function is positive for $g \to \infty$, while it is negative for $g \to 0$. In between, there must be an unstable critical point g_c where the β-function vanishes: this is the transition point. For $d = 1$, the β-function can never be positive: this means that the system is always localized, at any disorder strength and temperature. For $d = 2$, no transition is present in the absence of spin-orbit interactions; for GSE systems, however, it can be shown that $\beta(g)$ is no longer monotonous, but rather vanishes at a certain value g_c, becomes positive, and then tends asymptotically to zero. It can be shown that the restoration of the delocalization transition is due to the breakdown of time-reversal symmetry. [15]

2.3 Many-body localization

Up to now, localization has been discussed in terms of single-particle eigenstates, and it is found that transport can break down in the presence of strong disorder. However, in general adding interactions to a model is expected to restore transport, and make the system ergodic: even if the single-particle spectrum is fully localized, one may a priori expect that interactions allow for inelastic hopping among localized states, analogously to the effect of interactions with phonons in the single-particle case. Energy and particles would then be able to spread through the system, and transport and equilibration would ultimately be restored. However, this argument has been shown to be flawed, since it neglects the fact that localized states close in space typically have large energy mismatches. If interactions are weak and short-range enough, they are not able to compensate typical energy differences: particles can not find in their surroundings states from which to absorb the amount of energy they need to hop to a different localized states. Therefore, some properties of the localized phase, like the absence of transport and diffusion, may expected to persist in the presence of interactions.

This conjecture was already present in the original Anderson work [11], and it was seriously addressed by himself and collaborators twenty years later [20]. The problem was stated in terms of perturbation theory in the interaction: one starts with a fully localized Anderson model, creates an excitation above the Fermi energy, and perturbatively computes its lifetime. Such a lifetime was argued to be exponentially long for low temperatures, implying that the conductivity is exponentially small. This was taken as a hint that features of localization may be stable against interactions.

The topic of many-body localization became a very active subject of research recently, after two papers by Basko, Aleiner and Altshuler (BAA) [23] and by Gornyi, Mirlin and Polyakov [22]. These papers are technical, and a full review of their calculations is beyond the purpose of this thesis. Therefore, only a brief sketch of their fundamental idea is provided here. The notation used is the one in the BAA paper. One starts by observing that the main energy scale of the problem is the typical energy spacing between single particle states, the distance of whose localization centers is of the order of the localization length ξ:

$$\delta_\xi \equiv \frac{1}{\nu \xi^d}, \tag{2.3.1}$$

where ν is the single-particle density of states, and d is the spatial dimension. This quantity is the typical energy difference among states which are connected by short-range interactions. Then, a weak short-range interaction is added: the Hamiltonian, expressed in the basis of single-particle eigenstates like in Eq. (2.2.8), now reads

$$H = \sum_{\alpha=1} E_\alpha c_\alpha^\dagger c_\alpha + \frac{1}{2} \sum_{\alpha\beta\gamma\delta} M_{\alpha\beta\gamma\delta} c_\alpha^\dagger c_\beta^\dagger c_\gamma c_\delta. \tag{2.3.2}$$

The matrix elements $M_{\alpha\beta\gamma\delta}$ are assumed to be negligible for states which are far apart either in space or energy., if the latter exceed δ_ξ. Provided that the relations

$$|\overrightarrow{r_\alpha} - \overrightarrow{r_\beta}| \lesssim \xi,\ |\overrightarrow{r_\alpha} - \overrightarrow{r_\gamma}| \lesssim \xi,\ |\overrightarrow{r_\beta} - \overrightarrow{r_\gamma}| \lesssim \xi,\ \text{etc.} \tag{2.3.3}$$

and

$$|E_\alpha - E_\delta| \lesssim \delta_\xi,\ |E_\beta - E_\gamma| \lesssim \delta_\xi \text{ or } |E_\alpha - E_\gamma| \lesssim \delta_\xi,\ |E_\beta - E_\delta| \lesssim \delta_\xi \tag{2.3.4}$$

are fulfilled, one imposes $M_{\alpha\beta\gamma\delta} \sim \lambda\delta_\xi$, with $|\lambda| \ll 1$ being the coupling strength; otherwise, the matrix elements are neglected. Diagonal matrix elements of the form $M_{\alpha\beta\alpha\beta}$ renormalize the energy of the unperturbed states, but do not induce any transition, so are not considered either. Since high energy density is assumed, the sign of λ is not important.

One assumes the system to be prepared in a many-body eigenstate $|\Psi_k\rangle$, then perturbs it by adding one particle in the single particle state α, and constructs perturbation theory in the interaction starting from the resulting state $c_\alpha^\dagger |\Psi_k\rangle$. Let us now apply the interaction to this state: at first order in λ, the Hamiltonian couples the initial state to states with three particle excitations: a hole in state β and two particles in states γ and δ:

$$c_\alpha^\dagger |\Psi_k\rangle \to c_\gamma^\dagger c_\delta^\dagger c_\beta |\Psi_k\rangle . \tag{2.3.5}$$

At second order in λ, two kind of processes are possible: either an extra particle-hole pair is excited, or a particle and a hole recombine in another particle-hole pair. Since the number of available processes of the first kind is much larger than the number of possible processes of the second kind, recombination processes are neglected, and only processes which lead to decay in a larger number of excitations are considered:

$$c_\alpha^\dagger |\Psi_k\rangle \to c_\gamma^\dagger c_\delta^\dagger c_\beta |\Psi_k\rangle \to c_1^\dagger c_2^\dagger c_3^\dagger c_4 c_5 |\Psi_k\rangle \to \dots \tag{2.3.6}$$

One now has to check convergence properties of the resulting perturbative series: if the amplitude of the series coefficients decays fast enough with perturbative order n, only a finite number of excitations is created, and the energy of the starting excitation remains confined in a finite volume. The system is said to be many-body localized (MBL). Conversely, if the decay is too slow, the initial excitation irreversibly decays in a large number of different excitations. In the latter case, energy spreads through the system, and all information about the nature of the initial excitation is lost due to decoherence: the system is ergodic. Working in the continuum, it is possible to use Keldysh formalism to find the following estimation of the transition point:

$$\frac{\lambda T}{\delta_\xi} \ln \frac{1}{\lambda} \sim 1. \tag{2.3.7}$$

The temperature dependence comes from the fact that, the larger the temperature, the larger the phase space available for scattering gets, and therefore the stronger the tendency towards delocalization.

As I will mention in Subsec. 2.3.3, and explain in detail in Chap. 4, the transition in temperature predicted by Eq. (2.3.7) is reduced to a crossover in the thermodynamic limit, due to the effect of rare ergodic regions. As explained in Ref. [29], this was not seen in the BAA paper because this effect is due to processes in which particle-hole excitations scatter without exciting extra particle-hole pairs, which are neglected in their analysis. If correctly taken into account, such processes would give rise to a diverging sub-sequence in the perturbation expansion, which spoils the stability of the localized phase. No real MBL is therefore possible in systems where a transition in temperature is predicted perturbatively: genuine non-ergodicity can only be present in lattice systems where the whole spectrum is localized. Such systems are the topic of the next two Subsections.

2.3.1 Proof for MBL in one dimensional systems

The perturbative arguments I introduced above hint that strong disorder can induce a complete breaking of ergodicity in interacting quantum systems. They involve many approximations which are hard to control, however, and therefore it is not easy to fully determine how robust their conclusions are. More recently, a rigorous proof for the existence of an MBL phase was given by Imbrie [24] for one dimensional lattice systems, with no continuous symmetry, to avoid dealing with massless Goldstone modes. The main idea of the proof consists in taking a disordered Ising spin chain in a weak random transverse field of typical amplitude γ. Then one constructs perturbatively in γ a quasi-local unitary operator that diagonalizes the Hamiltonian. In this approach, it is possible to prove rigorously that perturbation theory converges for small enough γ, under the reasonable assumption of *"limited level attraction"*, i.e., that the probability of finding two energy levels closer than a number δ vanishes at least as a power law for $\delta \to 0$. Apart from the fact that it shows unambiguously the robustness of localization in presence of interactions, the importance of this proof lies in two main points: the first is that it succeeds in showing that rare metallic regions where the disorder is anomalously weak do not spoil the global non ergodicity of the system, as long as they are sufficiently far apart from each other. This was not clear from the original calculation by Basko et al. [23], where such regions are neglected, and remains an open issue for $d > 1$. The second is that, as a result of Imbrie's rotations, it naturally emerges that an extensive set of quasi-local spin operators τ^z exist, which commutes with the Hamiltonian. Here, quasi-local means that their commutators with local operators are finite within a finite region of space, and exponentially small in the distance outside of it. The implications of this fact for the dynamics of the systems are discussed in Subsection 2.3.2. However, this proof has a significant drawback too, namely, it cannot be straightforwardly generalized to dimensions higher than one. At the

moment it is not clear whether the difficulty is just technical, or if it implies that MBL in higher dimensional systems is qualitatively different from its one-dimensional counterpart.

To provide a sketch of the proof, let us consider a one-dimensional spin-$\frac{1}{2}$ Hamiltonian with nearest neighbor XYZ couplings. This is not the model for which the proof was originally formulated, but for the following arguments the difference is not important. The Hamiltonian can be written as

$$H = H_0 + JV. \tag{2.3.8}$$

In the above,

$$H_0 = W \sum_{i=1}^{L} h_i S_i^z \tag{2.3.9}$$

represents a random magnetic field in the z-direction, $h_i \in \left[-\frac{1}{2}, \frac{1}{2}\right]$ being independent random variables with uniform distribution. On the other hand,

$$V = \sum_{i=1}^{L} \left[\gamma_x S_i^x S_{i+1}^x + \gamma_y S_i^y S_{i+1}^y + \gamma_z S_i^z S_{i+1}^z\right] \equiv \sum_{i=1}^{L} V_{i,i+1}. \tag{2.3.10}$$

is the interaction term, with $\gamma_{xyz} \sim O(1)$. The interaction is taken much smaller than the disorder strength, $J \ll W$. Boundary conditions are assumed to be open. For clarity of notation, in this Subsection I call S_i^z the spin operator at site i, whereas $\sigma_i^z = \pm 1$ are its eigenvalues. It is possible to map the Hamiltonian into a system of spinless fermions using a Jordan-Wigner transformation, therefore providing an analogy to the BAA model discussed so far. Of course, for $J = 0$, the Hamiltonian is trivially localized, since each site is unable to exchange energy with the rest of the system.

The strategy of Imbrie's proof consists in applying a sequence of unitary transformations to the Hamiltonian. Such transformation are devised in order to progressively set to zero the non-diagonal elements of the Hamiltonian, thus diagonalizing it. As a starting point, let us set $J = 0$ and consider a classical spin configuration $\left|\{\sigma_i^z\}_{i=1}^N\right\rangle$. Then, let us call $\Delta E_{i,i+1}$ the change in the energy of the system, if spins S_i and S_{i+1} are flipped:

$$\Delta E_{i,i+1}(\{\sigma\}) = 2\left(\sigma_i^z h_i^z + \sigma_{i+1}^z h_{i+1}^z\right). \tag{2.3.11}$$

Now a finite interaction $J \neq 0$ is turned on. A pair $i, i+1$ is called resonant if $\Delta E_{i,i+1} \leq \varepsilon$, where $W \gg \varepsilon \gg J$ is a small (arbitrary) energy scale, intermediate between W and J. Next, the resonant subspace $\mathcal{S} = \{i : i \text{ is involved in at least one resonance}\}$ is defined. $\mathcal{S}$ can be decomposed in blocks of connected resonant spins: since J is assumed to be very small, most of the blocks are composed by two spins only, but in principle blocks of any size L_B can be present, with probability of order $(J/W)^{L_B}$. The key point is that blocks of size L_B are exponentially rare in L_B, and most of the spins are isolated, i.e. they belong to no block. The interaction part of the Hamiltonian can

now be split in three parts:

$$V = \sum_{i,i+1\in\mathcal{S}} V_{i,i+1} + \sum_{i\in\mathcal{S},i+1\notin\mathcal{S}} V_{i,i+1} + \sum_{i\notin\mathcal{S},i+1\in\mathcal{S}} V_{i,i+1} + \sum_{i,i+1\notin\mathcal{S}} V_{i,i+1} \equiv V_R + V_{R-E} + V_E, \quad (2.3.12)$$

where R stands for *"resonant"* and E for *"environment"*. V_R includes all couplings among resonant spins; V_E collects all couplings among isolated spins, which do not belong to any resonant blocks; finally, V_{R-E} represents the coupling between a resonating spin and a neighboring isolated one.

As a first step, the interactions in the typical non-resonant regions are added to H_0:

$$H_0 \to H_1 = H_0 + JV_E. \quad (2.3.13)$$

Since V_E connects only spin configurations whose energy differences are of order $W \gg J$, eigenstates and eigen-energies of H_1 can safely be constructed using non-degenerate perturbation theory in J. Let A be the unitary operator which diagonalizes H_1: without constructing A explicitly (which can however be done, see Ref. [24]), it is possible to qualitatively argue what its action on local spin variables is [28]. Due to the absence of resonances in region E, the mean values of spin operators has to be close to the non-interacting one:

$$|\langle S_i^z \rangle| = 1 - O\left(\frac{J}{W}\right). \quad i \notin \mathcal{S} \quad (2.3.14)$$

In a sense, it is still possible to think to region E in terms of spins sitting at each site, but these *"logical"* spins τ_i are physical spins that are dressed with contributions coming from the surrounding sites. Since in E the problem is fully perturbative, the commutator of τ_i with physical spins has to decay exponentially in the distance:

$$\left[\tau_i^\alpha, S_j^\beta\right] \sim O\left(\left(\frac{J}{W}\right)^{|i-j|}\right), \quad (2.3.15)$$

where $\alpha, \beta = x, y, z$ label the three spin components. Additionally, since A diagonalizes H_1, once we rewrite H_1 in this new basis, no terms that induce spin flips can be present. The only possible couplings that appear are among the T_i^z operators only:

$$H_1 = \sum_i \tau_i^z + \sum_{i,j} J_{i,j}\tau_i^z\tau_j^z + \sum_{n=1}^{\infty}\sum_{i,j,\{k\}} K^{(n)}_{i,\{k\},k}\tau_i^z\tau_{k_1}^z\ldots\tau_{k_n}^z\tau_j^z. \quad (2.3.16)$$

Due the perturbative nature of the construction, all couplings must be exponentially decaying in the distances. I shall call this the *"Huse-Imbrie Hamiltonian"*, and an analysis of its physical properties will be given in Subsec. 2.3.2.

Now let us apply the transformation A to the full Hamiltonian. Since A acts only on spins

living in region E, it has no effects on terms living in the resonating subspace R, which has to be diagonalized separately using degenerate perturbation theory. Since resonances are rare, most of the resonating blocks are formed by a small number $n \sim O(1)$ of spins, and are not able to induce spin flips in the surrounding regions, since their internal level spacing is still of $O(J)$: therefore, they can be included in the Huse-Imbrie description, since they have finite support on a small region only. However, large clusters of $L_B \gg 1$ spins are occasionally present, even though with exponentially small density: inside these clusters, the system looks for all practical points of view ergodic, and can be described by using ETH. One may therefore wonder whether such a large region can act as a bath for the rest of the system, leading to delocalization as the coupling terms V_{R-E} with the localized region are considered. This is however not the case: the presence of a large metallic region indeed thermalizes the spins surrounding it up to a certain length L_s, but does not affect far away regions, since the coupling between the metallic cluster and the far away logical spins is exponentially small in the distance.

To get convinced about this fact, let us look how V_{R-E} is modified under the action of A: in general, due to the exponential tails of the logical spins, a metallic region B gets coupled with all spins in E, but the coupling typically scales as $(J/W)^l$, l being the distance between the spin and the boundary of B. These terms can in principle induce spin flips, but they are able to produce significant hybridizations only if their amplitude is bigger than the level spacing in a region of length $L_B + l$, which scales as 2^{-L_B-l}. So let us define a buffer length L_s by

$$2^{-L_B-L_s} = \left(\frac{J}{W}\right)^{L_s}. \tag{2.3.17}$$

The above reasoning implies that logical spins centered further than L_s from the edge of the ergodic region are not hybridized by the direct coupling to B. Now the chain can be separated in region $\overline{B}$, which includes B and all surrounding spins up to distance L_s, and $\overline{E}$, which is formed by all the rest of the chain. The rotated Hamiltonian can then be written as

$$H' = H_{\overline{B}} + H_{\overline{B}-\overline{E}} + H_{\overline{E}}, \tag{2.3.18}$$

where the terms $H_{\overline{B}-\overline{E}}$ acting on both $\overline{B}$ and $\overline{E}$ are either commuting with $H_{\overline{E}}$ (terms diagonal in the logical spins) or have norm at most $(J/W)^{L_s}$ (terms originating from applying the rotation to V_{R-E}). Using Eq. (2.3.17), this allows to conclude that the eigenstates of H' are close to products of states in $\overline{B}$ and configurations of logical spins in $\overline{E}$. In other words, the delocalizing effect of B is confined to a region of length L_s, whereas MBL is robust outside.

As stated above, this proof does not extend to higher dimensions. The reason is that Eq. (2.3.17) needs to be modified to

$$2^{-(L_B+L_s)^d} = \left(\frac{J}{W}\right)^{L_s}, \tag{2.3.19}$$

which in general has no solution for dimension $d > 1$. The effect of ergodic spots in higher dimensional systems thus remains an interesting open question.

2.3.2 (Quasi-)Local Integrals of Motion in the MBL phase

In the MBL phase, eigenstates do not obey ETH. As is well known, ergodicity does not really hold for non interacting systems, which always possess an extensive set of conserved quantities, i.e. the occupation numbers of the single particle levels, and therefore are in some sense integrable. Average values of local observables in the Anderson model are not correctly described by ETH; since in the MBL phase observable quantities remain close to the non-interacting ones, they violate ETH too [30]. Then, as either the interaction or hopping amplitude are increased, a dynamical phase transition takes place, and thermal behavior is restored. This transition is different from thermodynamic zero temperature quantum phase transitions, which are due to a change of the nature of the ground state as some parameter in the Hamiltonian varies [61]. The MBL transition is due to a change of the nature of the whole spectrum instead, with eigenstates passing from violating ETH to obeying it, and it does not manifest in any thermodynamic quantity, nor is it detectable via standard statistical mechanics techniques.

Currently, a general definition characterizing all possible MBL phases is still lacking (see [26] for a more complete discussion on how many-body localization may be defined rigorously, and [25] for a more intuitive and phenomenological description). While at the single particle level the most natural definition of localization is given in terms of the spatial structure of wave-functions, it is not possible to generalize this definition to the many-body case. From the BAA argument given above, it follows that the first possible definition of MBL is that of *localization in Fock space*: once written in the basis of the eigenstates of the non-interacting Hamiltonian, an MBL state has a finite amplitude over a small fraction of the Hilbert space only, while an ergodic one spans all possible single-particle configurations (due to ETH). This definition is quite slippery, however, since the number of configurations with non-vanishing overlap with the MBL state still grows exponentially with the volume, even though much slower than the dimension of the full Hilbert space. A more useful definition is the absence of any long range transport, which sharply distinguishes MBL systems both from ergodic and integrable ones, since they both always allow for transport, either ballistic, diffusive or subdiffusive. However, from the practical point of view, checking for transport is difficult both from the numerical and analytical point of view, so some other defining property is needed, which allows for easier numerical verification.

A fundamental aspect of MBL, from which many of its other phenomenological properties can be derived, is its hidden integrability: as already stated, many-body localized systems display an extensive and complete set of quasi-local integrals of motions (LIOM), where quasi-local means that their commutators with local operators defined outside a finite spatial region is exponentially small in the distance from such region, as shown in Eq. (2.3.15). [27, 28, 24, 29] As a prototypical

example, it is useful to consider again the spin model (2.3.8). In the non-interacting limit $J = 0$ the conserved charges are just the z-components of the spins, whose eigenvalues are $\{-1, 1\}$. Now let us set $J \neq 0$: as already explained, one can use perturbation theory to construct some "dressed" spins τ_i^z, and rewrite the Hamiltonian in the Huse-Imbrie form (2.3.16). No such construction is possible in the thermal phase: even though one can still construct some conserved operators, they will necessarily be highly non-local and have no physical relevance. The description in terms of LIOMs is very useful to understand many of the physical properties of the MBL phase: therefore, in the remainder of this Subsection, they will be used to explain the most remarkable phenomenological properties of MBL systems.

2.3.2.1 Absence of thermalization and transport

A many-body eigenstate is a simultaneous eigenstate of all LIOMs, and it cannot be thermal: indeed, a microcanonical ensemble is constructed by averaging over all eigenstates in a small energy window, which corresponds in general to very different quasi-particle occupations. As a consequence, the mean value of a generic local operator O on an eigenstate is different from its thermal average, and thus ETH is violated. Additionally, the presence of LIOMs ensures that the d.c. conductivity vanishes in the thermodynamic limit, which follows from the Kubo formula for the conductivity σ associated with the local current density J_r. Following [29], let $J_r(\omega)$ be the current at frequency ω and position r arising in linear response to a homogeneous field E. The spatially averaged current density is then

$$J(\omega) = \frac{1}{V} \sum_r J_r(\omega) \equiv \sigma(\omega) E(\omega). \tag{2.3.20}$$

At finite temperature, the dissipative part of the conductivity is given by

$$\mathrm{Re}\left[\sigma(\omega)\right] = -\frac{1}{V} \sum_r \frac{\mathrm{Im}\left[\Pi(\omega, r)\right]}{\omega}, \tag{2.3.21}$$

where $\Pi(\omega, r)$ is the Fourier transform of the retarded correlation function of the current operator, with Lehmann representation

$$\Pi(\omega, r) = \frac{1}{Z(\beta)} \sum_{m,m'} \sum_{r'} e^{-\beta E_{m'}} \left(1 - e^{-\beta(E_m - E_{m'})}\right) \frac{\langle m' | J_{r'+r} | m \rangle \langle m | J_{r'} | m' \rangle}{\omega + E_{m'} - E_m + i\eta}. \tag{2.3.22}$$

In the above, $Z(\beta)$ is the partition function, and the limit $\eta \to 0$ needs to be taken after the thermodynamic limit. Since

$$\lim_{\omega \to 0} \frac{1 - e^{-\beta\omega}}{\omega} = \beta, \tag{2.3.23}$$

in the d.c. limit one finds

$$\mathrm{Re}\left[\sigma\left(\omega\to 0\right)\right]=\frac{\pi\beta}{V}\sum_{m,m'}\sum_{r,r'}\frac{e^{-\beta E_{m'}}}{Z\left(\beta\right)}\left\langle m'\right|J_{r'+r}\left|m\right\rangle\left\langle m\right|J_{r'}\left|m'\right\rangle\delta_{\eta}\left(E_{m'}-E_{m}\right), \tag{2.3.24}$$

where $\delta_{\eta}\left(x\right)\equiv\pi^{-1}\eta/x^{2}+\eta^{2}$ is a regularized δ function.

For simplicity, let us take the approximation of strictly local LIOMs, i.e., let us assume that each of them commutes exactly with all operators acting outside a region of linear size ℓ. Let us then take two many-body eigenstates m,m' that differ by one logical spin τ_k only, i.e. $\tau_k\left|m\right\rangle=-\tau_k\left|m'\right\rangle$. For a strictly local current operator, and $r\gg\ell$, it follows immediately that at least one of the two matrix elements

$$\begin{cases}\left|\left\langle m'\right|J_{r'}\left|m\right\rangle\right|=\frac{1}{2} & \left|\left\langle m'\right|\left[J_{r'+r},\tau_k\right]\left|m\right\rangle\right|\\ \left|\left\langle m'\right|J_{r'+r}\left|m\right\rangle\right|=\frac{1}{2} & \left|\left\langle m'\right|\left[J_{r'+r},\tau_k\right]\left|m\right\rangle\right|\end{cases}, \tag{2.3.25}$$

since at least one of the two commutators vanishes. Thus, in Eq. (2.3.24) the sum over r can be restricted to $r\lesssim\ell$. Additionally, for any fixed m the sum over m' is restricted to a finite set, since m and m' can not differ by more than $\sim e^{c\ell^{d}}$ integrals of motion, where c is an unimportant constant of $O\left(1\right)$. Thus, once one recalls that $\left\langle m\right|J\left|m\right\rangle=0$ for time reversal invariance, in the thermodynamic limit, once η is sent to zero, the real part of the d.c. conductivity vanishes with probability 1.

This derivation is oversimplified, since the commutators of the logical spins have an exponentially small but finite tail outside of region ℓ^{d}. Since the sum now includes pairs of states whose energy difference $E_{m'}-E_{m}$ is exponentially small too, one may wonder whether the competition between small matrix elements and energy denominators could restore a finite conductivity. However, if this were the case, perturbation theory in the interaction would not have converged, the construction of LIOMs would not have been possible, and the system would not be in an MBL phase. Therefore, it is reasonable to expect that the absence of transport survives, if quasi-locality of LIOMs is correctly taken into account.

2.3.2.2 Statistical properties of the energy levels

Another indicator, often used in numerical simulations to distinguish MBL from thermal phases, regards the spectral statistics of the Hamiltonian. In particular, many authors study the distribution of gaps between consecutive energy eigenvalues. Let

$$\Delta_n\equiv E_n-E_{n-1} \tag{2.3.26}$$

be the energy gap between energy levels n and $n+1$. One then defines the rescaled energy separations

$$s_n\equiv\frac{\Delta_n}{\langle\Delta\rangle}, \tag{2.3.27}$$

$\langle\Delta\rangle$ being the average of Δ_n over the whole spectrum. It is known from random matrix theory that, for Gaussian ensembles, the probability distribution $P(s)$ is the Wigner-Dyson distribution [57]. The most important feature of this distribution is that the probability of finding very small separations $s \ll 1$ vanishes in a power-law fashion:

$$P(s) \propto s^{\beta}, \quad s \ll 1 \tag{2.3.28}$$

where $\beta = 1$ for the GOE, $\beta = 2$ for the GUE and $\beta = 4$ for the GSE. This phenomenon, called *"level repulsion"*, is straightforward to understand. Let us consider a system described by a $N \times N$ Hermitian random matrix with real independent entries, drawn from a Gaussian distribution with variance σ^2 (therefore belonging to the GOE ensemble). Let us suppose that two of its diagonal entries H_{11} and H_{22} are very close to each other, i.e. that $|H_{22} - H_{11}| \ll \sigma$. States $1, 2$ are almost decoupled from the rest of the system, and their dynamics are described by the effective Hamiltonian

$$H = \begin{pmatrix} H_{11} & H_{12} \\ H_{12}^* & H_{22} \end{pmatrix}. \tag{2.3.29}$$

The difference between the two eigenvalues of H is

$$E_2 - E_1 = \sqrt{(H_{22} - H_{11})^2 + |H_{12}|^2}. \tag{2.3.30}$$

If H_{12} is real (and thus H belongs to the GOE), in order for this difference to be small, one has to impose that two independent random variables, $H_{22} - H_{11}$ and H_{12}, are simultaneously small: this yields $P(s) \propto s$, and thus $\beta = 1$. If H_{12} is complex instead, $\mathrm{Re}(H_{12})$ and $\mathrm{Im}(H_{12})$ are independent: one then has to impose that three independent random variables are small, and finds $P(s) \propto s^2$, which means $\beta = 2$. One finds $\beta = 4$ for the GSE with analogous arguments.

Since, by ETH, ergodic Hamiltonians are statistically equivalent to Gaussian random matrices, one expects the energy levels of ergodic systems to follow a Wigner-Dyson distribution. This conjecture has been numerically verified in many cases [68, 69, 70]. For integrable systems the situation is very different: it was conjectured that in this case s follows a Poissonian distribution,

$$P(s) = e^{-s}. \tag{2.3.31}$$

A Poissonian distribution of s can be easily derived if the energies E_n are independent identically distributed (i.i.d.) random variables [57]. Heuristically, the meaning of this conjecture is that, in integrable systems, energy levels are independent from each other: this is due to the fact that, typically, eigenstates very close in energy are labeled by extensively different values of the integrals of motion, and do not repel each other. Since MBL systems share with integrable ones the analogy of having an extensive set of integrals of motion, one can expect their energy levels to be described by the same statistical distribution. This expectation is confirmed in many numerical works (see

for example Refs. [45, 46, 30, 69, 68]). Therefore, one expects that at the MBL transition a change in the form of the distribution, from Poisson to Wigner-Dyson, takes place: numerically this effect can be quantified by the ratio of consecutive level spacings

$$r_j \equiv \frac{\min\left(\Delta_n, \Delta_{n+1}\right)}{\max\left(\Delta_n, \Delta_{n+1}\right)}. \tag{2.3.32}$$

Averaging over the spectrum, one finds for the three Gaussian invariant ensembles

$$r_{\mathrm{GOE}} \approx 0.53, \quad r_{\mathrm{GUE}} \approx 0.60, \quad r_{\mathrm{GSE}} \approx 0.67, \tag{2.3.33}$$

while for the Poisson distribution it can be shown that

$$r_{\mathrm{Poisson}} = 2\ln 2 - 1 \approx 0.39. \tag{2.3.34}$$

Typically, using exact diagonalization one observes a crossover from the Poisson to the Wigner-Dyson value, as quantum fluctuations are increased. That crossover becomes sharper as system size is increased, hinting at a sharp transition in the thermodynamic limit. This quantity can not be used to distinguish MBL from single-particle localization, though, since in both cases s follows a Poissonian distribution. Additionally, since the gap ratio is a non-local quantity, it suffers from finite-size effects.

2.3.2.3 Entanglement properties

Other two interesting features of MBL systems regard their entanglement properties. The first one is the fact that MBL eigenstates obey an *"area law"* entanglement entropy: if the system is prepared in a highly excited eigenstate, and partitioned in two regions A and B as in Fig. 2.1.1, the entanglement entropy S_A will scale as $S_A \propto \partial A$, ∂A being the area of the $d-1$ dimensional surface that separates the two regions. [62] This contrasts with thermal systems, where, as explained in Subsec. 2.1.1, a volume law is expected at finite temperature. Again, this is easily understood in terms of LIOMs: up to exponentially small corrections, the entanglement entropy is proportional to the number of τ_i^z which have support on both regions A and B. This number is obviously proportional to ∂A. The scaling of entanglement entropy for eigenstates is currently one of the most commonly used numerical diagnostics to distinguish between an MBL and a thermal phase (see e.g. [44, 45, 46, 62]). However, like the r parameter, it can not distinguish an MBL system from a non-interacting localized one, since in both case an area-law scaling is present.

The second feature is the growth of entanglement as a function of time, when the system is prepared in an initial condition with no entanglement, i.e., a product state. A prototypical example is an eigenstate of the physical spins $\{S_i^z\}$. Then, the system is partitioned as in Fig. 2.1.1, and S_A is computed as a function of time. If the system is thermal, entanglement grows linearly, $S_A \propto t$

[63, 64]. This comes as the various degrees of freedom of the system get entangled by interaction: the interaction of two spins a, b in general makes them entangled with each other. The subsequent interaction of spin b with another spin c makes c entangled not only with b, but in general with a too. As a consequence, the spread of entanglement is ballistic, with velocity close to the Lieb-Robinson bound [65]. In contrast, in non-interacting localized systems entanglement saturates at a finite value. In this case, entanglement grows while the wavefunctions of the particles sitting next to the boundary between A and B spread up to distances of the order of the localization length. However it cannot spread further, since the particles do not interact among each other. An alternative way to see this is by noticing that, for non-interacting systems, the Huse-Imbrie Hamiltonian (2.3.16) has only the first term.

From this point of view, MBL systems are intermediate between thermal and single-particle localized ones. It was observed numerically [66, 67] that the entanglement growth is unbounded, but logarithmically slow, $S_A \propto \ln t$. Also this behavior has been interpreted in terms of LIOMs [27, 28, 64]: in MBL models, entanglement do spread, since there are higher order terms in the Huse-Imbrie Hamiltonian. However, the interaction between localized quasi-particles decays with distance r as $\exp(-r/\zeta)$, with some length scale ζ of the order of the localization length. Therefore, at time t, only quasi-particles at distance $r \sim \zeta \ln t$ get entangled, as observed in the numerics. This dynamical behavior distinguishes MBL systems not only from thermal, but also from single-particle localized ones. Its obvious drawback is that the entanglement entropy cannot be measured in experiments at the moment, even though recently a protocol has been proposed to extract it experimentally. [64]

2.3.3 Phase diagram of MBL systems

Many-body localization is a very difficult problem, both from the analytical and numerical points of view. The main issue is that MBL is a property of the entire spectrum, not just of the low-energy region. Therefore, most of the techniques commonly used in other areas of condensed matter physics, which are devised to study the ground state and low energy excitations, are not useful in this context. From the analytical side, the only available technique in general is perturbation theory in some small parameter, typically hopping or interaction strength. Despite being conceptually simple and useful in a large variety of situations, it has the obvious downsides of being restricted to the regime of weak quantum fluctuations only, and does not allow for the exploration of the whole parameter range. Additionally, it is insensitive to non-perturbative effects, which can be important in the thermodynamic limit, as discussed in Chap. 4. From the numerical point of view, one has to resort to exact diagonalization, which has the obvious disadvantage of being restricted to very small systems due to the exponential growth of the Hilbert space with system size (even though an extension of DMRG techniques has been proposed for one dimensional systems, which may help to overcome this limitation [71, 72]). Therefore, it is very difficult to extrapolate the observed results

to the thermodynamic limit, due to finite size effects. For these regions, it is not surprising that the phase diagram of MBL systems, and the nature of the transition, are still poorly understood.

An important prediction of the BAA analysis is that, in the continuum, a *"many-body mobility edge"* should exist at any finite hopping, i.e. an energy threshold which separates localized states at low energy density from ergodic ones at high energy density [23, 73]. This is the many-body analogue of the concept of a single-particle mobility edge discussed in Subsec. 2.2.1. This prediction can be understood considering that, the higher the energy density, the more channels are available for scattering, and therefore the easier it is for a quasi-particle excitation to diffuse its energy through the system. In a lattice model, the situation is different, though, since at very small interaction $J \ll 1$ the whole spectrum is localized. Then, for J larger than a certain J_c a mobility edge is expected from perturbation theory to open at zero energy, and the situation would be analogous to the one depicted in Fig. 2.2.2 for the single particle problem.

The BAA analysis is flawed, though, since it neglects the possibility that finite, but large regions of energy density above the putative mobility edge act as a bath for their surrounding localized environment, therefore reinstating transport and thermalization. [29, 41] The mechanism through which ergodicity is restored in terms of this phenomenon will be explained in detail in Chapter 4.

Let us now discuss how this effect modifies the phase diagram. For lattice models, the phase diagram which emerges from my work is shown in Fig. 2.3.1, as a function of energy E and quantum fluctuations t: for very small t, the whole spectrum is localized, and the system is genuinely MBL. This is the regime in which Ref. [24] proved rigorously the existence of MBL for one dimensional systems. Then, at $t = t_c$, an infinite temperature transition takes place, and the spectrum becomes delocalized. For $t > t_c$, no real transition is present as a function of temperature, but there is rather a crossover: for high temperature, the system is ergodic and metallic. For low temperature, the system is in a Griffiths phase, i.e. in a phase in which most of the system is frozen, but transport and equilibration are present due to rare mobile regions that move through the system via resonant hopping. The properties of this *"bad-metal"* regime, like the dependence of conductivity on temperature, or whether transport is diffusive or sub-diffusive, are still largely unknown, and will be subject of future work.

Another interesting consequence of this consideration is that no real MBL is possible in the continuum, since the spectrum can never be fully localized, if the energy density is not bounded. However, the reader shall be cautioned that delocalization by rare regions may take very long times, if starting from a "localized" initial condition. For a realistic experimental setting, this effect might eventually be subdominant as compared to decoherence due to residual coupling to a bath: therefore, for the experimental accessible times the system will for all practical purposes look localized.

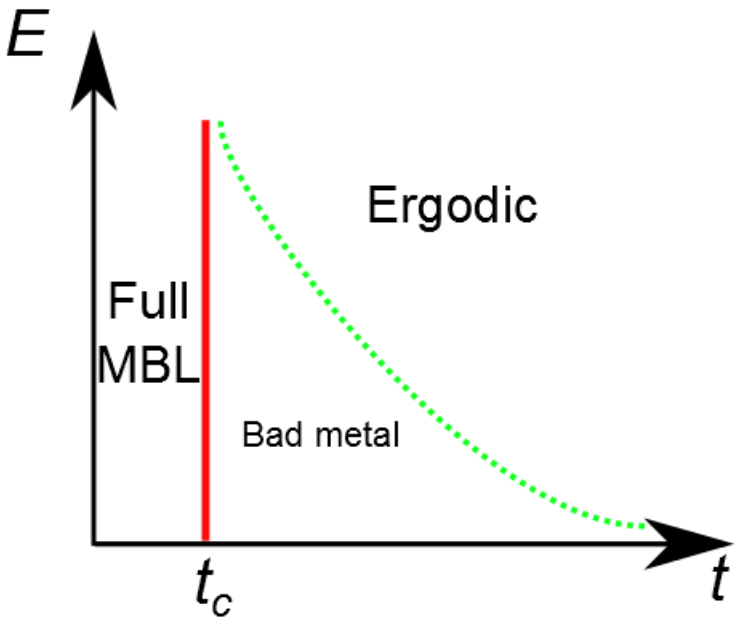

Figure 2.3.1: Phase diagram of an MBL lattice model, as a function of energy E and quantum fluctuations t, for fixed disorder and interaction strengths. For $t < t_c$ the whole spectrum is localized, and the system is fully localized: for $t > t_c$ a crossover line in energy (green dashed line) divides a metallic region from a "bad-metal" regime, in which thermalization and transport are due to the effect of rare regions. On both sides of the transition line (red), there is no transition as a function of energy.

2.3.4 Localization in absence of disorder? A percolation analysis

Up to now, I have described localization as a consequence of the interplay of disorder, hopping and interaction in a quantum Hamiltonian. In particular, I have discussed how disorder tends to localize particles, whereas kinetic energy and interaction tend to favor delocalization, through elastic or inelastic scattering processes. One would be therefore naively lead to think that, in a non-disordered Hamiltonian, localization cannot take place. This conclusion was challenged in the early 80s in the context of diffusion of He^3 atoms in a He^4 crystal. It was found that the diffusion coefficient D of the impurities becomes exponentially small as the concentration ρ is increased [35]. This phenomenon looks very similar to localization, but cannot be interpreted in terms of the mechanisms described so far, since no disorder is present in the system. The key observation, made by Kagan and Maksimov, to understand this phenomenon is that, in the considered system, the interaction strength U among impurities is much larger than the hopping amplitude t. As a consequence, when impurities are injected in random positions on the lattice, the typical energy mismatch one of them needs to overcome in order to hop to a neighboring lattice site is of order U. One can then proceed as in the analysis of the Anderson model and conclude that, for $U \gg t$, neglecting phonon assisted hopping, diffusion is not possible. In a sense, interaction takes the role of the disorder, and the system localizes on its initial random configuration. It is important to notice that the presence of a rigid lattice is essential for this phenomenon: in the presence of phonons, particles can delocalize by phonon-assisted hopping, and therefore the system will eventually relax starting from any initial condition. On a lattice, only discrete displacements are possible instead, and their typical energy cost is finite, so the motion of particles can get blocked if the available kinetic energy is small enough.

The argument sketched in this Subsection has the limitation of relying entirely on perturbative arguments in the hopping, and therefore of being insensitive to non-perturbative effects that restore ergodicity in the thermodynamic limit, analogous to the ones discussed in the previous Subsection to rule out mobility edges. Moreover, there was no analysis of the structure and effect of resonances: in the absence of quenched disorder, there are many exactly degenerate configurations for $t = 0$, if the interactions are short range. For this reason, I will first present the main ideas of the analysis, and then discuss qualitatively how they need to be modified once caveats due to resonances and ergodic regions are taken into account. The role of resonances will then be treated much more carefully in Chap. 3, while delocalization through rare regions is explained in Chap. 4.

2.3.4.1 Localization of strongly interacting impurities in a crystal

The Hamiltonian for the impurities can be written as

$$H = t \sum_{\langle i,j \rangle} c_i^\dagger c_j + \frac{U}{2} \sum_{i,j} \frac{1}{|\vec{r}_i - \vec{r}_j|^\alpha} n_i n_j, \tag{2.3.35}$$

with $\alpha > d$ to ensure the interaction energy per particle ε_{int} to be finite, d being the spatial dimension. In this case, $\varepsilon_{\text{int}} \sim O(U\rho)$, where $\rho \equiv N/V$ is the density. For $\rho \ll t/U$ the impurities are very far apart from each other, their typical interaction energy is much smaller than the hopping strength t and they behave like free particles on a lattice, so no localization is present. For larger density, starting from a random initial configuration, one can identify clusters, which correspond to sets of particles that cannot rearrange internally via resonant transitions, due to interactions among them. The only possible dynamics of a cluster is a rigid displacement of the cluster itself, which requires the simultaneous hopping of all the K particles of the cluster, which appear in perturbation theory as a process of order t^K. Thus, the effective hopping amplitude of the cluster scales as

$$t_{\text{cluster}} \approx t \left(\frac{t}{U}\right)^{K-1}, \tag{2.3.36}$$

i.e. it is exponentially small in the number of constituents. However, the system still acts as an ergodic metal, due to the fact that there is always a finite fraction of space where the density of particles is too low for a rigid cluster to form: these particles are able to diffuse through all areas where no cluster is present, and allow conduction to persist.

As the concentration of particles increases, clusters become larger, and the ergodic low density regions become rarer. To understand the behavior of the system, let us estimate the fraction of space occupied by clusters. A particle belongs to a cluster when the energy $\Delta\varepsilon$ one needs to displace it by one lattice site is much larger than t. This happens if each particle forming the cluster has at least another particle at distance lower than a certain length R_{00}, which is estimated as

$$R_{00} \sim \left(\frac{U}{t}\right)^{\frac{1}{\alpha+1}}. \tag{2.3.37}$$

If a particle is present on a certain site, then all sites within R_{00} from it are "frozen", in the sense that other particles can neither leave it nor enter from outside. Additionally, as stated above, particles inside a frozen region can not rearrange their relative positions, but only rigidly translate all together. The fraction of frozen sites is given by

$$\rho_f \sim \rho R_{00}^3 \sim \rho \left(\frac{U}{t}\right)^{\frac{d}{\alpha+1}}. \tag{2.3.38}$$

As ρ_f reaches a certain critical concentration ρ_∞ (which can be estimated in terms of site-percolation theory, see Ref. [74] for a review, and Ref. [75] for the up to date numerical value of the percolation threshold), an infinite frozen region forms: this identifies a cluster which is unable to move, since it is formed by $K \to \infty$ particles. Since it is neither able to rigidly translate nor to rearrange its internal particle configuration, the presence of the cluster could ensure that ergodicity is broken. This would be so if all particles of the system belonged to the cluster, but, obviously, low density regions where particles are mobile still persist. One must therefore check the effect

of the interaction with mobile particles on the cluster: in Ref. [35] it was argued that scattering between a mobile particle and the cluster is elastic with probability $\gtrsim 1 - O\left(t/U\right)$, since the kinetic energy (of $O\left(t\right)$) the particle can transfer is unable to create excitations within the cluster itself (which have a typical energy cost of $O\left(U\right)$). As a result, the system would macroscopically appear as formed by a large immobile structure, coexisting with rare liquid regions.

2.3.4.2 Flaws of the Kagan-Maksimov analysis

As mentioned above, the analysis of Ref. [35] has two weak points. The first one is that, even in a large supposedly rigid cluster, there are always particles which feel only a weak molecular field generated by the other ones, and are consequently able to rearrange in a resonant way. This happens also in the presence of quenched disorder, however there is an important difference: once some particles have moved, also the effective fields felt by their neighbors change. It may then happen that a particle, which was blocked by a strong field, can get unlocked by this motion, and start moving too. So, in translation invariant systems, resonant spots are not fixed to some definite spatial region, but are in principle able to move [37, 39]. The question naturally arises, whether this mobile resonant spots can travel through the whole system and delocalize it. I found the answer to be negative for one dimensional systems of a particular kind, whereas in higher dimensions the situation is much less clear.

The second issue is that, inside a large enough low density "pond", the system behaves as an ergodic bath, with total energy of the order of the number of particles forming it, and a level spacing which is exponentially small in the volume of the pond. This is the same situation I mentioned in Subsection 2.3.3 above, and that will be discussed in detail in Chapter 4. Under these conditions, it is unavoidable that the bath induces transitions in the particles that surround it: due to such transitions, the pond can resonantly move through the system, changing the configuration of the areas of the percolating cluster it has crossed. Similarly as in disordered MBL systems with mobility edges, delocalization and transport are expected to be reinstated by these rare excitations. However, since thermalization due to rare excitations is expected to be an extremely slow process, one expects the system to appear non-ergodic for very long time scales, even though after a long (but finite) time, thermal behavior will be present. Waiting times may become so long that they are out of reach for experiments, however. This is also what happens in a class of classical non disordered systems, with very slow relaxation dynamics: namely the so called *"structural glasses"*. I will briefly discuss them in the following Section.

2.4 Absence of ergodicity in classical systems: the case of structural glasses

Long before the problem of MBL arose, it was known that very long lived metastable phases of matter exist. Such phases are called *"glasses"*. They are intermediate between crystalline solids and liquids, in the sense that they display mechanical rigidity like a solid, but their structure at the molecular level is completely disordered. The standard protocol to experimentally produce a glass consists in rapidly cooling a liquid to its glass temperature T_g, usually much smaller than the transition temperature T_c to the solid phase [76]. If the quench is fast enough, the system is unable to reach its equilibrium phase (which would be a regular crystal), but remains trapped in some disordered metastable state for very long times. Physical properties are then found to evolve slowly with time, a phenomenon known as *"aging"* [77].

Since the transition to the glass phase is not a thermodynamic transition, T_g is empirically defined as the temperature at which the fluid becomes too viscous to flow in any experimentally accessible timescale, and therefore is a protocol-dependent quantity which does not play any fundamental role in the theoretical description of the phenomenon. For this reason, it is commonly expected that relaxation times at T_g are still finite, but just too large to measure. At this point, the question naturally arises, whether a non zero temperature $T_{\text{ideal}} < T_g$ exists, at which relaxation times are truly divergent. If this is the case, then classical matter displays a genuine non-ergodic phase at finite temperature, in which metastable configurations survive for arbitrary long times; otherwise, ergodicity is always eventually restored by time evolution. The whole physics of glasses then stems from the fact that we are not able to run long enough experiments. This question is somewhat academic, since no equilibration can be observed below T_g, and therefore neither the value T_{ideal} nor the features of a hypothetical "ideal glass" could be measured, but is still very interesting from a conceptual point of view.

An independent quantity which hints that some genuine transition may exist, even though it is extrapolated empirically from experimental data, is the Kauzmann temperature T_K [78]. Let S_{exc} be the part of the entropy of the liquid phase, which is in excess with respect to the entropy of the corresponding crystal. This quantity can be measured down to T_g: extrapolating the resulting curve below the glass temperature, one finds that the excess entropy should vanish linearly at a temperature $T_K \neq 0$, as shown in Fig. 2.4.1 (see Ref. [79] for a compilation of experimental data, and Ref. [80] for a discussion). The popular physical interpretation of this behavior is the following [81]: close to T_g, the system explores an energy landscape which is full of minima, separated by barriers which grow as temperature decreases. At the glass temperature, the system remains trapped in one of these minima, and is not able to escape in measurable timescales. From this picture, the entropy can be divided into two contributions: a term which describes the fast relaxation within one valley, and a second one counting the number of metastable configurations, $S_c \equiv \ln N_{\text{metastable}}$, usually called *"configurational entropy"*. Assuming that the contributions to the

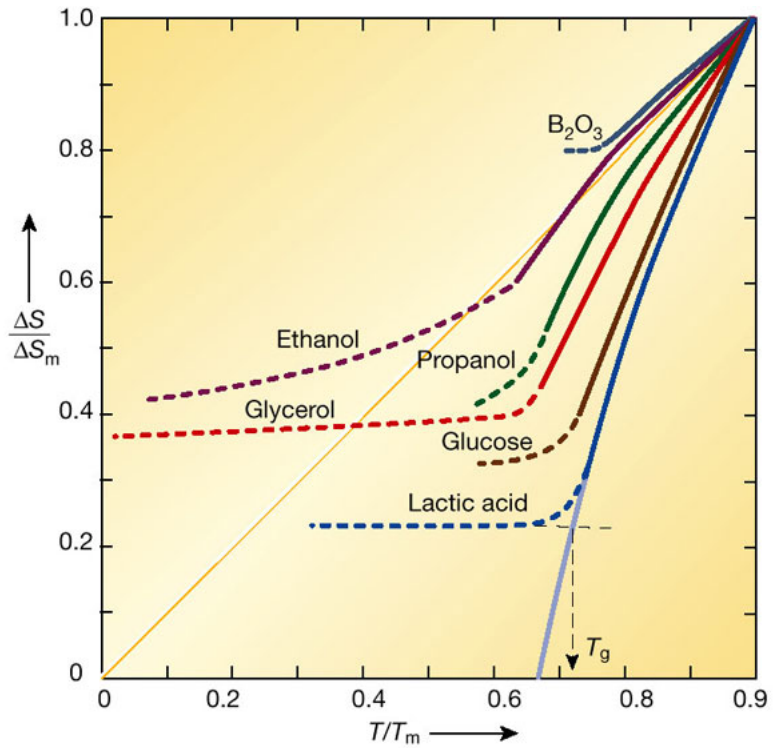

Figure 2.4.1: Excess entropy ΔS of various supercooled liquids with respect to the corresponding regular crystal, as a function of temperature T. The entropy is measured in terms of the melting entropy ΔS_m, while T_m is the melting temperature. Extrapolating from the experimental data (continuous lines) one finds that ΔS should vanish at some finite temperature. However, at T_g relaxation time scales become too large to be measured experimentally, and no further decrease is seen beyond that point (dashed lines). Figure taken from Ref. [80].

entropy coming from vibrations around the minima are similar for the glass and the crystal, one finds $S_{\rm exc} \approx S_c$. The vanishing of S_c at T_K would then imply that a real thermodynamic transition takes place, characterized by a discontinuity in the specific heat. This argument, despite giving a simple physical picture, is however based on the mere extrapolation of experimental data, and should therefore be taken with a grain of salt. Additionally, there is no reason to believe that the Kauzmann temperature, at which a thermodynamic transition might take place, should coincide with the *dynamical* transition point $T_{\rm ideal}$, if it exists at all.

Currently, there are various theoretical approaches which have been proposed to study the physics of glasses. Here I will present only the one which display some direct analogy with the quantum systems I am interested in. This approach consists in studying models whose thermodynamic properties are trivial, but whose *dynamics* are subject to a series of constraints which slow down relaxation towards equilibrium. Put shortly, these *"Kinetically Constrained Models"* (KCM) are characterized by some kind of facilitation process: they describe a system where the majority of degrees of freedom are frozen in time, but some rare relaxation events happen. Once a region in space gets unjammed, it will unlock the dynamics of the surrounding area, therefore triggering

dynamical avalanches that propagate through the system [82]. These models, despite being very simple, display a phenomenology which is consistent with the experimental observations made on glasses. Additionally, since they entirely focus on the dynamical processes which lead to relaxation, they allow for direct comparison with quantum MBL systems. Indeed, it has been proposed that dressing them with quantum fluctuations can lead to translation invariant MBL, see [83, 84]. For these reasons, some of these models will be presented in the following Subsection, and analogies and differences with MBL models will be discussed. For a more complete review, I refer the reader to Ref. [85].

2.4.1 Relaxation by diffusing defects: Kinetically Constrained Models (KCM)

The simplest example of a KCM is the Kob-Andersen model [86]. This model aims at describing a hard sphere system, in the limit of large density. It is a classical lattice gas, with the hard core constraint that no two particles can sit on the same site. Since there is no interaction apart from the hard core constraint, nor any on site potential, the Hamiltonian of the model is trivial. Calling $n_i = 0, 1$ the occupation number at site i,

$$H\left[\{n_i\}\right] = 0. \tag{2.4.1}$$

What makes this model non-trivial is the kinetic constraint that is imposed on the dynamics: a particle can jump to a neighboring site only if both sites occupied before and after the move have less than m neighbors, m being an adjustable parameter. This mimics the steric effect of the neighboring particles, that form a cage when their local density is high enough. Kob and Andersen studied the model on a cubic lattice in $d = 3$, with $m = 4$, and found glassy dynamics and aging at high density. The model was later studied for different values of m, spatial dimension and lattice geometry [87]. The behavior of this model is very intuitive: at low density, particles are typically far away from each other, particles are able to move freely, and the dynamics are fully ergodic. On the other hand, when the filling fraction is close to 1, most of the system gets stuck, since typically particles are not able to move. To describe the evolution of the system, one has to study the dynamics of defects, i.e. extended regions where the density is small. In this model large enough defects are able to move through diffusion and ultimately make the system ergodic, but since they are exponentially rare for typical configurations, any small fraction of the system will look ergodic for exponentially long times (until a defect moves through it).

The main weakness of the Kob-Andersen model is that there is no notion of temperature in it, so it does not allow to describe the experimentally observed dependence of temperature on the slowing-down of the dynamics. To restore the notion of energy, one can modify the Hamiltonian (2.4.1) by introducing a chemical potential. Equivalently, one can consider a system of non

interacting classical Ising variables in a magnetic field h: the Hamiltonian then becomes

$$H\left[\{\sigma_i\}\right] = h\sum_i \sigma_i. \quad \sigma_i = \pm 1 \tag{2.4.2}$$

The dynamical constraint is introduced as in the Kob-Andersen model: a spin σ_i can flip via the usual Metropolis rule, but only if at least k of its nearest neighbors have positive value. This is the well-known Fredrickson-Andersen model [88]. In this model, temperature has two roles, since it determines both the density of mobile defects and their mobility. Overall, defects diffuse through the system, can annihilate when they meet, and can be created from existing defects. At all times, however, the large majority of the system looks completely frozen: thermalization is ultimately present, but it is locally reached by relatively fast rearrangement processes (induced by a defect passing by), followed and preceded by very long waiting times, in which the system is static.

A qualitative description of KCMs can be constructed considering the mobility of sparse defects with density ρ_d, which diffuse anomalously with an exponent z and a temperature dependent diffusion coefficient D [89]. A relaxation time can then be defined as the time at which a finite fraction of the system (typically $1/2$) has been visited by at least one defect. The number of sites visited by a specific defect at time τ is by definition $(D\tau)^{\frac{d_f}{z}}$, where d_f is the fractal dimension of the walk. For a random walk in $d = 3$ one has $d_f = z = 2$: this follows from the fact that, after n steps, the walker is at distance $O\left(\sqrt{n}\right)$ from the origin. Consequently, the number of sites visited in a sphere of radius R scales as R^2. Therefore, the visited number of sites is simply $D\tau$. The relaxation time τ_{rel} can then be estimated as the solution of the equation

$$\rho_d D\tau_{\text{rel}} \approx \frac{1}{2}. \tag{2.4.3}$$

For the Fredrickson-Andersen model, in the case $k = 1$ one finds $\tau_{\text{rel}} \propto e^{\frac{2h}{T}}$, which means that the dynamics follows an Arrhenius law, while for $k > 1$ the behavior is super-Arrhenius. But τ_{rel} diverges only at strictly zero temperature: at any finite temperature, there is always a finite density of macro-defects, which ensure that the system will eventually get thermal in the long time limit. This feature is common to the largest majority of KCMs, even though for some very particular rules a finite temperature transition can be established [90]. Indeed, it is hard to imagine how a full arrest of the dynamics can happen at non-zero temperature: if an infinite long-lived non ergodic classical glass exists, it must be due to extra effects which are not simply obtained by imposing dynamical constraints only.

As it should be evident for the reader at this point, KCMs resemble MBL models from many points of view, since both of them challenge the ergodic paradigm, even in the absence of integrability. However, there are many important differences, too. Probably the most fundamental one is that, for disordered MBL systems, it is possible to prove under quite general assumptions a genuine breakdown of ergodicity, in the sense that equilibration does not set in at arbitrary long

times. This contrasts with glasses, where complete absence of relaxation can be proven in some particular cases [90], but not in general. The analogy becomes much closer if one considers MBL in models without disorder, like the one considered by Kagan and Maksimov, discussed in Subsec. 2.3.4, or the ones that will be presented in Chapter 3. These two kinds of models not only show very similar qualitative behavior (frozen dynamics for very long times, eventually followed by very slow thermalization), but have also in common the fact that relaxation is in both cases due to the effect of very rare mobile regions. There is however an important difference, that does not allow to see translation invariant MBL just as the "quantum version of a KCM": this is the inverted role of temperature. In most classical KCMs, mobility is due to very rare highly excited regions, which move in a cold frozen background; on the other hand, as it will be discussed in Chapter 3, in quantum glasses the immobile regions are at high temperature, whereas the mobile ones are close to the local ground state. How these two opposite situations can be related, and if it is possible to smoothly interpolate between them, remains an open question worth to investigate.

As a last remark, it must be pointed out that, even though KCMs look rather artificial and oversimplified, it is possible to build models in which facilitation emerges naturally from the unconstrained many-body dynamics [91]. As an example, let us consider the following two dimensional plaquette model:

$$H = -J \sum_{i=1}^{L-1} \sum_{j=1}^{L-1} \sigma_{ij}\sigma_{i+1j}\sigma_{ij+1}\sigma_{i+1j+1}, \tag{2.4.4}$$

where as usual the σ are Ising variables. The system evolves through the Metropolis rule. The dynamics of this model can be mapped to a KCM by considering the plaquette variables $p_{ij} \equiv \sigma_{ij}\sigma_{i+1j}\sigma_{ij+1}\sigma_{i+1j+1}$. With this substitution, the Hamiltonian becomes exactly the one of the Fredrickson-Andersen model in Eq. (2.4.2). More interestingly, at low temperature facilitation emerges, too: each time a spin is flipped, it changes the sign of four plaquette variables. It is easy to see that excited plaquettes with $p = 1$ act as a source of mobility, since the energy barriers one must overcome to flip a spin get reduced by their presence. In this particular model, defects can be identified with excited plaquettes.

Chapter 3

Many-body localization without quenched disorder?

As it was shown in the preceding Chapter, both in the single-particle localized case, as well as in many-body systems studied so far (e.g. disordered, weakly interacting fermions and bosons, random quantum magnets,...), non-ergodicity is due to the presence of quenched disorder, which stabilizes the localized phase. The disorder ensures that local rearrangements are typically associated with important energy mismatches, which appear as large denominators in perturbation theory. In turn, those suppress the higher order decay processes, which would be necessary to establish transport and delocalization in an isolated systems, that is not in contact with a thermal bath. The existence of a different mechanism towards localization was also suggested, though, namely that localization may be induced by strong interactions alone, even with a translation invariant Hamiltonian [35]. Several recent works have reconsidered this idea, focusing on the question whether MBL is possible in systems without disorder. This idea has been tested in various physical systems, like one-dimensional Bose-Hubbard models [42, 43, 39, 40], mixtures of heavy and light interacting particles [37, 38, 92], quantum spin chains [83, 93, 84] and three-dimensional topological models. [94] Another notion of localization, characterized by an incomplete volume law entanglement, was conjectured too. [95]

The fundamental idea behind these studies is that quenched disorder is not necessary to localize a strongly interacting system. Instead, self-generated disorder (as a consequence of random, spatially heterogeneous initial conditions) can in principle be sufficient to induce broken ergodicity and absence of diffusion in a quantum many-body system, even if its Hamiltonian is perfectly disorder-free and translation invariant. If these models were fully captured by perturbation theory in the hopping amplitude, their dynamics would genuinely be non-ergodic. As already anticipated in Chapter 2, and more precisely discussed in Chapter 4, for large systems non-perturbative transport in the hopping and thermalization are ultimately restored by the effect of rare mobile regions. The situation should be compared with classical glassy systems at finite T, (such as, e.g., poly-

disperse Lennard-Jones mixtures, or hard sphere liquids), and in particular with their description in terms of KCMs. Despite the fundamental importance of this issue, it will be shown in Chapter 4 that, deep enough in the localized phase, these effects can be neglected for systems and time scales of experimental relevance: therefore, in the present Chapter, they shall not be taken them into account, and my analysis will be based on perturbation theory only.

The kind of models, which I call *"quantum glasses"*, have non-ergodic dynamics for very long times, while being perfectly isolated from external sources of noise, such as thermal baths. Like the usual Anderson insulators, these "glasses" are not robust to thermal noise: the coupling to an external bath introduces dephasing and restores transport in general. Robustness of glassiness and non-ergodicity against thermal noise requires the existence of barriers, which become arbitrarily large when the distance between the considered configurations increases, or very complicated pathways between different parts of configuration space (such as those required for the relaxation of defects in certain topological quantum systems for $T \to 0$ [96]). The former happens in systems which undergo spontaneous symmetry breaking, as well as in many disordered systems with frustrated interactions, such as spin glasses. It also happens in mean field models without disorder. [97] Many such models can be dressed with weak quantum fluctuations, therefore naturally inheriting the glassiness due to classical frustrations, as long as quantum effects are small enough not to overcome the glassy order. [31, 32, 33, 34] While these models exhibit interesting effects arising due to quantum fluctuations (reentrant transition lines, discontinuous glass transitions at low T, etc), the role of quantum effects is secondary to the extent that the glassiness of these systems relies fundamentally on the built-in frustration in their classical configuration space. Here we study a very different type of quantum glass, where classical frustration plays no role: quantum interference is the only driving force that leads to non-ergodic dynamics.

The remainder of this Chapter is organized as follows: in Sec. 3.1, I discuss the essential ingredients of the quantum glasses I am discussing. In Sec. 3.2, a concrete one dimensional Hamiltonian is presented, and I argue by means of perturbation theory that, within a certain parameter range, equilibration starting from a random classical initial condition is exponentially slow in the system size. In Sec. 3.3, I compute some observables which signal the presence of a localized phase, and compare the analytical predictions with numerical simulations, performed using exact diagonalization techniques for small system sizes. Finally, in Sec. 3.5, some potential experimental implementations of the quantum glasses described here are discussed.

3.1 Spontaneously broken ergodicity

Let us first discuss the ingredients necessary to obtain a quantum glass as envisioned above. In Sec. 3.2, an explicit example of one dimensional Hamiltonian possessing all these features is presented.

I consider Hamiltonians which are the sum of two parts,

$$H = H_0 + tH_{\rm hop}. \tag{3.1.1}$$

In the above formula, H_0 describes the "non-hopping part" of the many-body system: the dynamics under H_0 is trivially non-ergodic and localized, and by itself do not allow for any d.c. transport. In this sense, H_0 is the analogue of the disorder potential in a standard single particle Anderson model. In the context of non-disordered, translation invariant Hamiltonians, it is important to note that the absence of hopping leads to an extensive degeneracy in the spectrum, which allows one to choose the highly degenerate eigenbasis of H_0 in the form of localized many-body wavefunctions, which break translation invariance. For the purpose of this discussion, this will be the natural basis from which eigenstates of the full Hamiltonian (3.1.1) are constructed, rather than using a basis which respects translation invariance.

Consider now adding a perturbative "hopping part" $tH_{\rm hop}$ to the Hamiltonian. It is chosen such that it could formally restore ergodicity, in the sense that any state in Hilbert space can be reached from any eigenstate of H_0 by the successive action of appropriate terms appearing in $H_{\rm hop}$ (in analogy to the intersite hopping in the Anderson problem, which in principle could bring a particle anywhere in the lattice). I wish to argue that, for t sufficiently small, the system nevertheless remains non-ergodic and localized for large times, while at higher t an ergodic quantum liquid is expected.

By "non-ergodic" it is meant here that generic, macroscopically inhomogeneous initial conditions will not become homogeneous in an experimentally accessible time: indeed, the required time scale grows exponentially with system size, and saturates to some (very large) value in the thermodynamic limit. This will be shown by perturbatively constructing the eigenstates: with this operation one finds that, at the perturbative level, eigenstates remain close to the spatially inhomogeneous eigenstates of the system at $\tau = 0$. The reader is once again cautioned that the real eigenstates can not be constructed with perturbation theory in large systems: the correct procedure to construct the eigenstates in the thermodynamic limit is presented in Chapter 4, and closely resembles the Imbrie construction. As already stated, to be able to experimentally distinguish between the two constructions one needs to wait for times, which are probably out of reach: for all practical purposes, the physics of quantum glasses can be described by using the simpler approach taken in this Chapter.

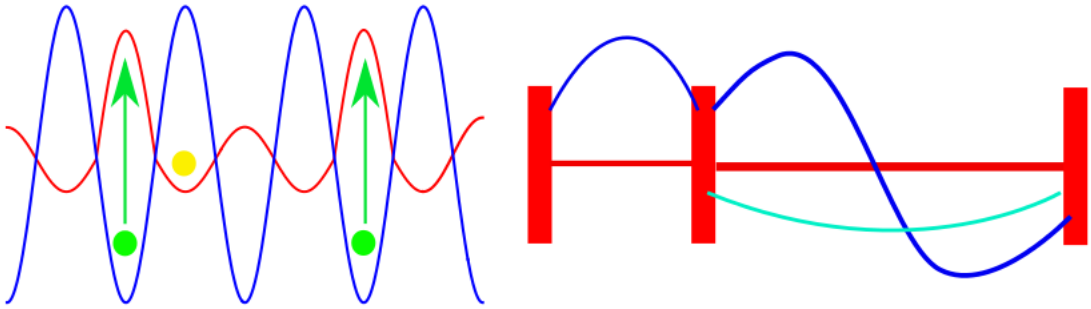

Figure 3.2.1: *Left:* A simple 1d model exhibiting self-induced many-body localization: two atomic species on commensurate lattices with different hopping amplitudes. Heavy particles (green) impede the hopping of light particles (yellow). Those act as effective springs between the heavy particles, and localize them by creating a complex energy landscape for them. *Right:* The non ergodic Hamiltonian H_0. The barriers divide the chain into independent intervals, where the fast particles occupy the free particle states.

3.2 An example of quantum glass in 1d

3.2.1 Inhibited hopping model

To exemplify and analyze the general phenomenon of non-disordered, self-localizing quantum glasses, let us consider a simple 1d model containing two kinds of fermions: a "fast" species a and a "slow" species c. The presence of a slow particle is assumed to hinder the propagation of the fast particles, cf. Fig. 3.2.1. Physically, this may arise due to a strongly enhanced tunneling barrier for a fast particle in the presence of a c particle, which I therefore call a *"barrier"* henceforth. The considered Hamiltonian takes the form (3.1.1), with

$$\begin{aligned} H_0 &= -J\sum_j \left(a_{j+1}^\dagger a_j + a_j^\dagger a_{j+1}\right)(1-n_j)\,, \\ tH_{\rm hop} &= -t\sum_j \left(e^{i\phi/L}c_{j+1}^\dagger c_j + e^{-i\phi/L}c_j^\dagger c_{j+1}\right), \end{aligned} \tag{3.2.1}$$

where $n_j = c_j^\dagger c_j$. The barriers move with very small kinetic energy $t \ll J$, as compared to the hopping strength J of the fast particles. Note that, in the hopping part $H_{\rm hop}$, a weak hopping of a in the presence of a barrier could also be added, without altering the qualitative conclusions. Note that the barriers could be could equally well be taken to be hard-core bosons. This choice does not affect the spectrum or localization properties, but only the non-local (in space and time) correlation functions.

The index $j = 1, ..., L$ labels both the lattice sites, which host the fast particles, and the links between them where barriers reside, cf. Fig. 3.2.1. Furthermore, periodic boundary conditions

are used to make the system translation invariant, but a magnetic flux ϕ for the slow particles is inserted, so as to break inversion symmetry. This removes the related spectral degeneracy, which simplifies the analysis. The number of particles $N_{a,c}$ and their respective densities $\rho_{a,c} = {}^{N_{a,c}}/_{L}$ are fixed. This model is somewhat reminiscent of Falicov-Kimball models, where localized particles create a potential for inert fast particles (for a review, see Ref. [98] and references therein). However, here I am not interested in the thermodynamic properties, such as the ground state, but rather in dynamical questions: giving the heavy particles a finite mass, I rather investigate the coherent dynamics of the whole system and its ergodicity and transport properties.

The physical essence of the model is retained upon "integrating out" the light a particles and substituting them by repulsive strings, which yields the effective Hamiltonian

$$H_{\text{eff}} = H_0^{\text{eff}} + tH_{\text{hop}} \equiv U \sum_{j=1}^{L} \sum_{l=1}^{L-1} v(l)\, n_j n_{j+l} \prod_{k=1}^{l-1} (1 - n_{j+j}) - t \sum_{j=1}^{L} \left(e^{i\phi/L} c_{j+1}^{\dagger} c_j + e^{-i\phi/L} c_j^{\dagger} c_{j+1} \right), \tag{3.2.2}$$

where $v(l) = l^{-\beta}$. An exponent $\beta = 2$ mimics Eq. (3.2.1) best at low energies. Indeed, a single fast particle trapped is taken between each pair of successive barriers and it is assumed to remain in its ground state. The effective repulsion then decays as a power law with exponent $\beta = 2$. The interaction constant U is proportional to the hopping constant J of the fast particles. The advantage of this model is that, since it contains only one kind of particle, its Hilbert space dimension scales much less fast with system size L, with respect to the model (3.2.1). Therefore, it is much more suitable for numerical studies: for this reason, from now on I will often refer to this simpler effective model.

3.2.2 Properties of the non-hopping Hamiltonian H_0

For $t = 0$, the barriers can not move. Hence, the fast particles remain confined between them and do not interact with other particles outside their own interval. Thus, there is trivially no long range transport of energy of particles, and the system is non-ergodic. Each interval between two consecutive barriers hosts a *discrete* set of energy levels for the fast particles. In the simple model above, for intervals of length l, these are just standing waves with wavevectors $k_m = {}^{m\pi}/_{l+1}$, for $m = 1, ..., l$, wavefunctions $\psi_j^{(m,l)} = \sqrt{\frac{2}{l+1}} \sin(k_m j)$ and energy $E_{l,m} = -2J \cos(k_m)$, but these specific forms are inessential for the subsequent considerations, except for the fact that the level spacings within a certain interval are of order $O(J)$ and depend on l. In fact accidental degeneracies of different level spacings are explicitly neglected, as they are non-generic and can be removed by simple modifications of the Hamiltonian for the fast particles. Under these circumstances, a barrier can only move with a concomitant energy change in the spectrum of the fast particles, unless the barrier motion does not alter the distribution of interval lengths. If one neglects that latter exception, one realizes that fast particles placed in a random arrangement of barriers create an

inhomogeneous energy landscape for the barriers, which plays the role of disorder in standard non-interacting and interacting localization problems. At first sight it thus appears almost obvious that when barriers acquire a small but finite hopping t, the latter can not compete with the much larger roughness in the energy landscape, and thus the motion of the barriers becomes strongly localized. However, this view, even though basically correct, is oversimplified and misses an important potential caveat: the non-hopping Hamiltonian H_0 has an extensively degenerate spectrum. This is so because any permutation of the intervals (as defined by consecutive barriers) does not cost any energy at $t = 0$ if the internal state of fast particles is permuted together with the intervals. Thus, one has to be careful in dealing with these resonances before one can assert self-induced localization.

Additionally, I will only be able to argue for localization of the most abundant, typical initial conditions, while it will be shown that initial conditions with extensive correlations are not localized. This implies that in this model perturbation theory predicts localized states at high temperature to coexist with low temperature delocalized states for any finite value of t. It will be shown in Chapter 4 that this coexistence is not possible in the thermodynamic limit, though, as already hinted when discussing the phase diagram of disorder-driven MBL: for this reason, in the thermodynamic limit quantum glasses always eventually thermalize. At the perturbative level, however, the non trivial aspect of this analysis consists thus in showing that the extensive degeneracy of H_0 is lifted by the introduction of the hopping in such a way that strong resonances and system-spanning hybridizations are avoided for *typical*, random initial conditions.

An interesting property of H_0 is its local "integrability", i.e., the existence of an extensive set of mutually commuting, local conserved quantities. In the above model, apart from the trivially conserved barrier positions, $c_i^\dagger c_i$, the conserved quantities associated with the levels of fast particles take the form

$$S_{i,l;m} = c_i^\dagger c_i c_{i+l}^\dagger c_{i+l} \left[\prod_{j=1}^{l-1} \left(1 - c_{i+j}^\dagger c_{i+j} \right) \right] \gamma_{i,l;m}^\dagger \gamma_{i,l;m}, \tag{3.2.3}$$

where γ are the annihilation operators for fast particle states confined by two barriers located at the links i and $i + l$,

$$\gamma_{i,l;m} = \sum_{j=1}^{l} \psi_j^{(l;m)} a_{i+j}. \tag{3.2.4}$$

With these integrals of motion, H_0 can be compactly written as

$$H_0 = \sum_{i=1}^{L} \sum_{l=1}^{L} \sum_{m=1}^{l} E_{l;m} S_{i,l;m}. \tag{3.2.5}$$

In this sense, the operators S are the equivalent of the physical spins (or occupation numbers of single particle eigenstates) in the disorder driven MBL models, see Subsection 2.3.2 above. One may wonder whether, starting from them, it is possible to analogously construct some dressed

logical spins T, as soon as a finite t is turned on. The answer is negative: in this context, it is not possible to find an extensive set of quasi-local conserved operators, because delocalized states are always present in the spectrum. At the moment, it is not known how to extend the LIOM construction to cases where perturbation theory predicts the existence of a mobility edge (see also the discussion in [29]). This possibly reflects the fact that mobility edges are not stable in the thermodynamic limit, and therefore such an extension is probably not possible.

3.2.3 Perturbative construction of the eigenstates of H_0^{eff} and H_{eff}

In a generic high energy eigenstate of H_0^{eff} (with energy density of order $O(U)$ above the ground state), the intervals between nearest neighbor barriers have lengths l, which are exponentially distributed according to the probability distribution

$$P(l) = (1-\rho)^{l-1}\rho, \tag{3.2.6}$$

with mean length $\bar{l} = 1/\rho$. In the above, ρ is the mean density of barriers. Let us now discuss how such eigenstates deform when a finite but small hopping for barriers is turned on. The same description can be applied to the full Hamiltonian H too, with only some unimportant small changes, which have no impact on the physics discussed here.

3.2.3.1 Broken translational invariance

The aim of this Subsection is to show that the approximated eigenstates, which can be constructed using perturbation theory, remain "localized" close to the eigenfuctions of H_0. The starting point is the eigenbasis of H_0 discussed above, which explicitly breaks translation invariance. The strategy is to show that the higher we push the perturbation theory in t, the smaller the fraction of states which remain degenerate at the given order of perturbation theory. Nevertheless, the degeneracy associated with translation always survives. For typical, that is, random eigenstates, that degeneracy will only be lifted at a perturbative order proportional to the system size L. All other degeneracies are lifted fairly rapidly, and persist typically at most to an order which grows logarithmically with L, due to rare subsequences of barrier intervals.

The extensive degeneracy between eigenenergies is lifted at various levels. In general, one needs to use degenerate perturbation theory. Let us consider the eigenstate $\left|\chi_m^{(0)}\right\rangle$ of H_0. At the k-th order in perturbation theory, one considers all the states $\left|\chi_n^{(k-1)}\right\rangle$, constructed at the previous stage, which have matrix elements with $\left|\chi_m^{(k-1)}\right\rangle$ at this order. If the relevant matrix element is much smaller than the energy difference between the two states (as obtained at $(k-1)$-th order), one considers the state *off-resonance* with $\left|\chi_m^{(k-1)}\right\rangle$ and treat it using non-degenerate perturbation theory. If, in contrast, the matrix element is dominant, it is necessary to write

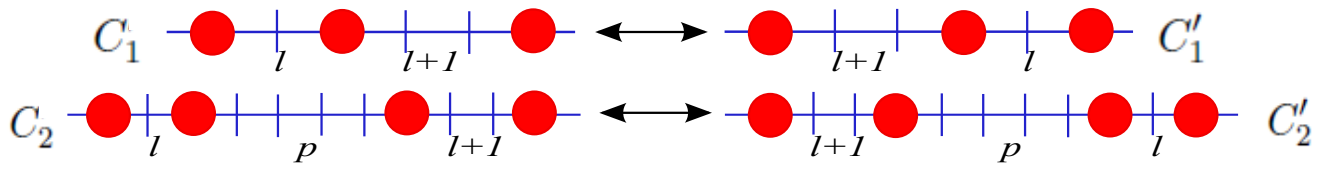

Figure 3.2.2: Examples of the most common type of resonances. The configurations C_1 and C_1' (top) hybridize at first order of degenerate perturbation theory in t, while C_2 and C_2' (bottom) hybridize at second order. Moving the middle particle(s) to the right costs no energy.

an effective Hamiltonian in the resonant subspace, with matrix elements of order $O\left(t^k\right)$ as non-diagonal elements, and the energies evaluated up to $O\left(t^{k-1}\right)$ as the diagonal entries.

The core of the argument consists in showing that by applying perturbation theory to a random eigenstate of H_0, its random barrier configuration ensures the lifting of degeneracies at low perturbative orders. The degeneracy, which is present in H_0^{eff} due to invariance of the energy under permutation of interval lengths, is lifted due to perturbative shifts in the eigenenergies, which are sensitive to the actual sequence of intervals. The goal is to show that, when at higher order the initially degenerate configurations are connected by non-zero matrix element between each other, they are no longer in resonance, since their degeneracy has already been lifted by an amount which parametrically exceeds the typical matrix element. As we will show, for small t resonances become rapidly rarer as perturbative order is increased. Thus, perturbation theory will converge, and the perturbative eigenstate $|\chi_m\rangle$ remains close to $\left|\chi_m^{(0)}\right\rangle$. By the latter, I mean that expectation values of local observables (such as the position of barriers) remain close to their values on the unperturbed states - except rare spatial regions where significant hybridizations take place. Note that this notion of closeness does not imply that $\left\langle\chi_m\left|\chi_m^{(0)}\right.\right\rangle$ is finite; indeed, such an overlap trivially decays exponentially with system size, for any finite t. The important point is rather that $\left|\chi_m^{(0)}\right\rangle$ hybridizes with far less states in Hilbert space than a wavefunction, whose pure state realizes a local Gibbs ensemble, would do.

3.2.3.2 Lifting of degeneracies

The extensive degeneracy between eigenenergies is lifted at various levels. At first order in perturbation theory the only degenerate eigenstates of H_0 that can be connected by tH_{hop} are configurations where one barrier moves such that the two adjacent intervals exchange lengths from $(l, l+1)$ to $(l+1, l)$.The simplest kind of such resonances are shown in Fig. 3.2.2: the configurations C_1, C_1' are classically degenerate. The off-diagonal element $t\left\langle C_1'\right| H_{\text{hop}}\left|C_1\right\rangle$ is non-zero and induces a level splitting of $O(t)$. One then has to restart perturbation theory from the following hybridized states:

$$|C, \pm\rangle = \frac{|C\rangle \pm \left|C'\right\rangle}{\sqrt{2}}. \tag{3.2.7}$$

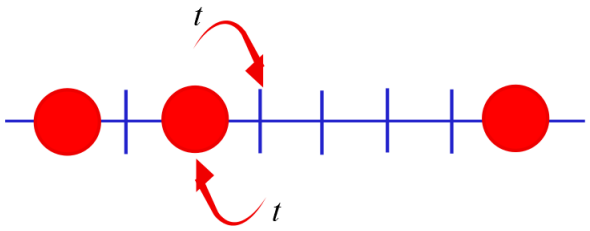

Figure 3.2.3: The energy of eigenstates are shifted by contributions of order $O\left(t^2/J\right)$ by the virtual hop of barriers. These virtual processes lift the largest part of the degeneracies in the many-body spectrum.

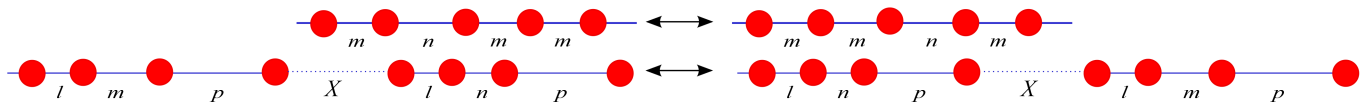

Figure 3.2.4: Pairs of configurations where the exchange of an interval of length m and n do not change the set of pairs of adjacent intervals in the sequence. Eigenstates which differ only by such local rearrangements remain degenerate at order t^2 in perturbation theory.

Apart from these local first order splittings, the most generic lifting of degeneracies takes place at second order in t. This happens in two ways: first, analogously to what happens at first order, some local resonant contributions of the form $C_2 = (l, p, l+1), C_2'(l+1, p, l)$, with $p \notin \{l-1, l, l+1\}$, get hybridized. Such configurations are shown in Fig. 3.2.2, and give rise to hybridized states of the same form of Eq. (3.2.7). The second, and more generic, type of lifting is due to barriers moving virtually back and forth, as shown in Fig. 3.2.3. These processes lead to energy shifts of $O\left(t^2/J\right)$ per moving barrier and remove a large part of the exact degeneracies present at $t = 0$.

Nevertheless, certain configurations remain degenerate at higher orders of perturbation theory. These correspond to sequences of intervals, which can be permuted in such a way that each interval has neighbors of the same lengths as before the permutation. This ensures that the second order shifts of the energy are exactly the same in the two sequences. The most abundant type of configurations which are not split at second order corresponds to sequences of the form

$$|m, n, m, m\rangle\,;\ |m, m, n, m\rangle\,, \tag{3.2.8}$$

as shown in Fig. 3.2.4. Here m, n are interval lengths such that $|m - n| > 2$, otherwise the two configurations would hybridize at second order, which would already lift their degeneracy. The occupation of fast particle levels within corresponding intervals of the same lengths is again assumed to be equal.

In order to ensure the convergence of the perturbative expansion, the probability per unit length, that degeneracies survive, needs to be small enough and to decrease sufficiently fast with

increasing order at which perturbation is lifted. Otherwise neighboring degenerate regions would hybridize and form a delocalized band of excitations. Let us therefore estimate the probability P_{mnmm} of degenerate configurations as in (3.2.8) to appear in a given location in the sequence of intervals in a random eigenstate of H_0. Those configurations can be checked to be the most abundant type of degeneracies. The average distance between such degenerate regions will be $d_{\text{deg}} \approx P_{mnmm}^{-1}$. The degeneracy of these configurations is in general lifted at order $O(t^4)$. On the other hand, we expect a matrix element between two degenerate regions to appear typically at order $t^{d_{\text{deg}}-3}$, since a matrix element is created by the forward motion of the $d_{\text{deg}}-3$ barriers located between the resonant regions. Therefore, if t is sufficiently small, such two regions will almost always be off-resonance, if $d_{\text{deg}} > 7$. I will show that this condition is indeed well satisfied in general for this model. For other complex models an analogous calculation may be more involved, and the existence of a quantum glass phase may be less evident than in the present toy model.

The probability P_{mnmm} of either of the configurations (3.2.8) to appear in a given location of the sequence of intervals is easily calculated to be

$$P_{mnmm} = 2\sum_{S=1}^{\infty} P(S)^3 \sum_{S',|S'-S|>2} P(S') = \frac{2}{3}\rho_c^2 + O\left(\rho_c^3\right), \tag{3.2.9}$$

where I explicitly use the independence of successive interval lengths. The asymptotics $P_{mnmm} \sim \rho_c^2$ for small barrier density ρ_c^2 arise because the first and the last interval lengths are not free, but must be equal to one of the two lengths in the middle. For $\rho_c = 1/2$, which is nearly optimal for such degeneracies to occur, I still find a very small probability $P_{mnmm} \simeq 0.034$, which implies a large typical separation between resonant regions by $d_{\text{deg}} \approx 30 \gg 7$.

Configurations which remain degenerate at yet higher order are even rarer. The most abundant pairs whose degeneracy is not lifted at order $O(t^{2n})$ correspond to sequences of intervals which can be permuted in such a way that all sets of $n+1$ consecutive intervals are present in both configurations (possibly up to spatial inversion of the sequence). As an example, the most probable configurations that are not split at order t^4 are of the form:

$$|l,m,n,m,m,l\rangle\,;\ |l,m,m,n,m,l\rangle\,, \tag{3.2.10}$$

with the restrictions $|m-n|, |m-l| > 4$. At small ρ_c, the density of these configurations is of order ρ^{n+1}. Since the inverse of this small quantity controls the power of t at which matrix elements couple neighboring degeneracies, hybridizations between such regions are exceedingly rare and remain strongly localized.

From the above arguments it becomes clear that the degeneracy of H_0^{eff} is lifted at higher orders in perturbation theory in the barrier hopping t, and that the quantum fluctuations induce an effective disorder, which takes the same role as quenched disorder in other many-body systems considered previously. Having reached this stage, one can repeat the same type of arguments as

in those systems [23] to conclude that for sufficiently small t perturbation theory should converge and the perturbed eigenstates remain close to the inhomogeneous initial states. [24]

3.3 Dynamical properties of quantum glasses

3.3.1 Miniband structure of the spectrum

Up to now, arguments about the properties of ideal quantum glasses in the thermodynamic limit have been presented, as long as non-perturbative effects are neglected. However, one should be careful when reasoning about finite size systems, where translational invariance is eventually restored, as mentioned above. Indeed, the degeneracy between a sequence of intervals and its rigid translations by a certain number of lattice sites is never lifted to any order in perturbation theory. However, when t is small, the matrix element connecting two such configurations is of order $t^{\rho L}$, since all barriers need to be moved. This matrix element gives rise to an exponentially small splitting between the L hybridizing, rigidly rotated configurations. Consequently, the characteristic time needed to observe the effect of this hybridization is inversely proportional to this matrix element, and thus diverges exponentially with the system size L. Nevertheless translational invariance is restored in such finite size systems when averages are taken over times exceeding the hybridization time.

As stated above, for any finite L, the eigenstates can be chosen to be eigenvectors of the discrete translation operator T. For infinitesimal hopping t, the eigenstates organize in momentum *minibands*. These are essentially formed by hybridizations of a classical eigenstate of $H_0^{\text{eff}} |C\rangle$ with all its translations around the ring, $T^j |C\rangle$, for $j = 0, 1, 2, ..., L-1$. Typical states correspond to configurations $|C\rangle$ in which sites are occupied randomly by barriers, with probability ρ. The eigenstates of such minibands take the form

$$|C, P_n\rangle \approx \frac{1}{\sqrt{L}} \sum_{j=0}^{L-1} e^{ijP_n} T^j |C\rangle , \tag{3.3.1}$$

where P_n is the total momentum. The hopping Hamiltonian connects typical configurations $|C\rangle$ and its translations only at very high order in perturbation theory. This leads to an exponentially narrow dispersion of the band

$$\varepsilon_n = -2t_{\text{eff}} \cos P_n, \; P_n = (2\pi n + \phi)/L, \tag{3.3.2}$$

where t_{eff} is the effective hopping of the center of mass of this state. The magnetic flux ϕ was introduced in the Hamiltonian (3.2.1). For small hopping t it is exponentially small in system size. This is estimated in more detail in Eq. (3.3.51) below. This behavior has important consequences for the dynamics: after preparing the system in an inhomogeneous initial configuration, the time

scale to relax to a homogeneous state (if averaged over time) is proportional to t_{eff}^{-1}, which diverges in the thermodynamic limit.

The description of Eq. (3.3.1) is oversimplified, however, since it neglects the presence of *resonances*, like the one discussed in Subsec. 3.2.3.2. Let us take as an example the configurations $|C_1\rangle, |C_1'\rangle$ shown in Fig. 3.2.2: when such a resonant pair is met, one has to construct a miniband by translating the hybridized states (3.2.7), which brings to the form

$$|C, P, \pm\rangle \approx \frac{1}{\sqrt{L}} \sum_{j=0}^{L-1} e^{ijP} T^j \frac{|C\rangle \pm |C'\rangle}{\sqrt{2}}. \tag{3.3.3}$$

Such states can be seen as the admixture of two of the minibands described by Eq. (3.3.1). This can be easily generalized to the case in which n resonances are present (labeled $i = 1, 2, ..., n$). Each of them hybridizes a finite number r_i of locally differing, degenerate configurations. The eigenstates then take the form

$$|C, P, \alpha_i\rangle \approx \frac{1}{\sqrt{L}} \sum_{k=0}^{L-1} e^{iPk} T^k \prod_{i=1}^{n} \left(\sum_{m_i=1}^{r_i} \psi_{m_i}^{\alpha_i} R_i^{(m_i)} \right) |C\rangle \tag{3.3.4}$$

where the $\{\alpha_i\}$ label the possible states of the i'th resonance. Those are described by amplitudes $\psi_{m_i}^{\alpha_i}$ multiplying local operators $R_i^{(m_i)}$ that rearrange the classical configuration at the resonant spot.

The restriction to exactly degenerate configurations applies for very small t only. At larger hopping, states with finite energy differences of $O(t)$ hybridize as well. Nevertheless, the crucial point of the analysis of Subsec. 3.2.3.2 is that at perturbative level in t no system spanning hybridizations are expected. This is expected despite the fact [92] that in the thermodynamic limit the exponentially many minibands (3.3.1) overlap in energy, because the matrix elements between most minibands are even much smaller than the level spacings resulting from band overlaps.

3.3.2 Diverging susceptibility to infinitesimal disorder

In order to verify the phenomenon of self-induced MBL, it is useful to exploit a specific property of non-disordered systems: namely, that dynamical localization of typical quantum states and the spontaneous breaking of translation invariance are essentially equivalent, as we argued above. From a numerical point of view this is very convenient, since the sought phenomenon can be phrased in the familiar language of spontaneous symmetry breaking. In this way, we avoid the identification of many-body localization by other observable, which are harder to analyze. Those include the observation of freezing via Edwards-Anderson like order parameters [30], or the analysis of many-body level statistics. [21, 69] The latter is, however, based on the conjecture that a delocalization transition in a many-body system is concomitant with a change from Poisson to Wigner-Dyson

statistics, as explained in Subsection 2.3.2. Even if this conjecture is true and also applies to the non-disordered systems considered here, one nevertheless would expect the corresponding observables to suffer from stronger finite-size effects than in systems with quenched disorder. Therefore, it is very useful to have an alternative route to detecting many-body localization.

In order to probe for spontaneous translational symmetry breaking, one proceeds in the usual way. One introduces a small symmetry breaking term H_{SB} in the Hamiltonian,

$$H_{\mathrm{eff}} \to H_{\mathrm{eff}} + H_{\mathrm{SB}}, \tag{3.3.5}$$

and asks whether the induced symmetry breaking persists as the strength of the perturbation W tends to zero, after the thermodynamic limit has been taken. To break the translational symmetry externally, a weak disorder potential

$$H_{\mathrm{SB}} = \sum_i \varepsilon_i c_i^\dagger c_i \tag{3.3.6}$$

is applied, where ε_i are independent, identically distributed random variables, taken from a centered box distribution of unit width. In order to probe dynamical translational symmetry breaking, I define for any quantum state Ψ the observable

$$\Delta\rho_\Psi^2 \equiv \frac{1}{L}\sum_{j=1}^{L} \left[\langle\Psi|\left(n_{j+1}-n_j\right)|\Psi\rangle\right]^2, \tag{3.3.7}$$

which is a measure of the spatial inhomogeneity of the density of barriers. This observable vanishes for any translation invariant state, and can be measured in cold-atom experiments using microscopy techniques. [18, 19, 99] Translational invariance is present in the long time average over the dynamics, even without considering rare regions effects, if the inhomogeneity of typical many-body *eigenstates* vanishes in the limit $W \to 0$. This is expected to happen if the barriers are sufficiently mobile, i.e., for $t > t_c$, where t_c is the critical hopping strength. In contrast, translational symmetry is spontaneously broken at the perturbative level in the dynamics starting from a random typical classical configuration C, if infinitesimal disorder induces a finite inhomogeneity of eigenstates in the thermodynamic limit, i.e., if

$$\lim_{W\to 0}\lim_{L\to\infty} \Delta\rho^2(\epsilon) \neq 0, \tag{3.3.8}$$

where

$$\Delta\rho^2(\epsilon) = \overline{\langle\Delta\rho_\Psi^2\rangle}_{\Psi,\epsilon}, \tag{3.3.9}$$

is averaged over both eigenstates with energy densities in a narrow range around ϵ (as denoted by the square brackets) and over the disorder (as denoted by the overline). The critical values t_c, where the quantum glass breaks down and ergodicity and transport are restored, are expected to depend on ϵ, since the occupation probability of fast particle levels will affect the motion of the

slow barriers.

The effect of a weak disorder potential can be analyzed using perturbation theory in W. In contrast to the analysis of the previous Section, here I start with the translational invariant eigenbasis, which simultaneously diagonalizes the momentum. To first order, the n-th eigenstate $|\Phi_n\rangle$is perturbed by the following hybridizations:

$$|\Phi_n\rangle \to \left|\Phi_n^W\right\rangle = |\Phi_n\rangle + \sum_{m\neq n} \frac{\langle\Phi_m| H_{\rm SB} |\Phi_n\rangle}{E_m - E_n} |\Phi_m\rangle + O\left(W^2\right), \tag{3.3.10}$$

where E_n is the energy of state $|\Phi_n\rangle$ at zeroth order in W. Recalling that $\Delta\rho^2_{\Phi_n} = 0$, we find the quadratic response

$$\Delta\rho^2_{\Phi_n^W} = \frac{4W^2}{L}\sum_{i=1}^{L}\left[{\rm Re}\sum_{m\neq n}\frac{\langle\Phi_m| H_{\rm SB} |\Phi_n\rangle}{E_m - E_n}\langle\Phi_m|\left(n_{i+1}-n_i\right)|\Phi_n\rangle\right]^2 + O\left(W^4\right). \tag{3.3.11}$$

The response is dominated by the states of the miniband $|\Phi_n\rangle$ belongs to, as explained in Subsec. 3.3.1. To estimate this quantity, one first notices that the matrix elements appearing in Eq. (3.3.11) are gently behaved as a function of system size. One easily finds that $\langle\Phi_m|\left(n_{i+1}-n_i\right)|\Phi_n\rangle = O\left(1\right)$does not scale with L, while $\langle\Phi_m| H_{\rm SB} |\Phi_n\rangle \sim {}^1\!/\!\sqrt{L}$, since it is a sum of L uncorrelated random variables. In contrast, the energy denominators $E_m - E_n$ are very small, since they are of the order of the (exponentially small in L) effective hopping $t_{\rm eff}$. Accordingly, we expect that the eigenstate susceptibility to disorder grows exponentially in system size, as

$$\frac{d\sqrt{\Delta\rho^2}}{dW} \sim t_{\rm eff}^{-1} \sim \left(\frac{c}{(t/U)^\alpha}\right)^L. \tag{3.3.12}$$

In the above expression, c is a constant, which depends on the details of the initial configuration, and is estimated for a typical initial condition in Subsec. 3.3.5 below. The exponent $\alpha \lesssim \rho_c$ takes care of the occasional local resonances, which allow for faster tunneling processes, and is estimated in Subsec. 3.3.4.

The exponentially large response to infinitesimal disorder is a genuine many-body phenomenon. This contrasts with free particles, which also localize at infinitesimal disorder, at least for $d \leq 2$, but with a susceptibility ${}^d\!\sqrt{\Delta\rho^2}/\!_{dW}$ that grows only as a power-law in system size.

I have confirmed the above expectations numerically by computing the inhomogeneity $\sqrt{\Delta\rho^2}$ in the presence of a very small disorder W. I exactly diagonalized systems of sizes $L = 4, 6, 8$ with a fixed density of fast particles and barriers, $\rho_a = \rho_c = {}^1\!/\!_2$. The results are averaged over 100 realizations of the disorder and over a small energy window centered at energy density ${}^E\!/\!_L = {}^J\!/\!_4$. $\sqrt{\Delta\rho^2}$ is averaged over 10 eigenstates for $L = 4, 6$ and over 20 eigenstates for $L = 8$. The results are shown in Fig. 3.3.1 for $t = t_0 = 0.01U$.

It can be seen from the plot that the average susceptibility to disorder increases exponentially

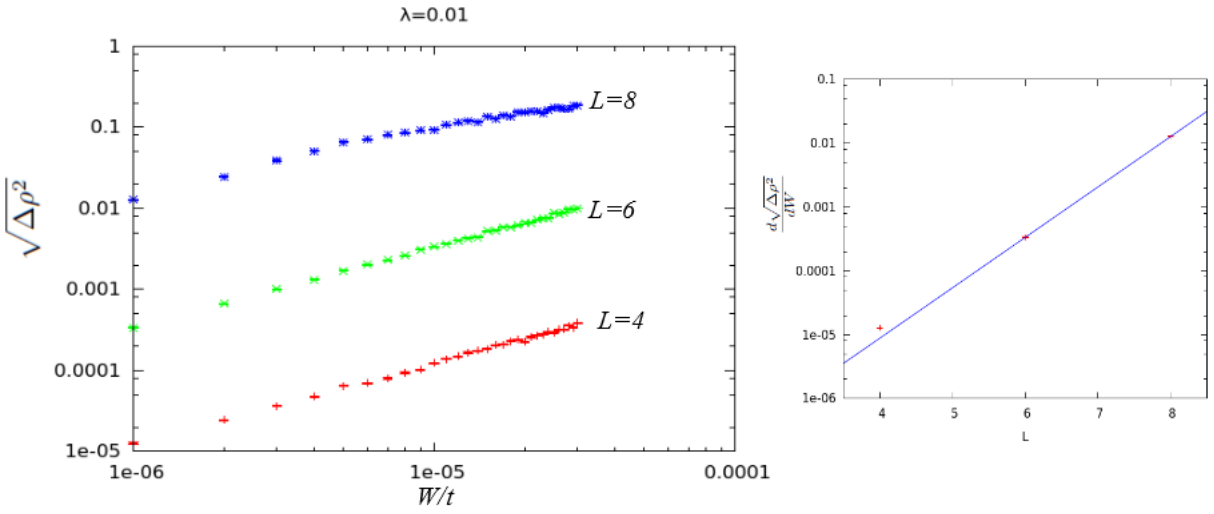

Figure 3.3.1: Left: Disorder averaged spatial inhomogeneity $\sqrt{\Delta\rho^2}$ ($\epsilon = J/4$) induced by a very weak disorder potential of strength $W \ll t$ in a strongly localized system with hopping $t = 0.01J$. The initial response is linear in W, with a susceptibility $d\sqrt{\Delta\rho^2}/dW$ that diverges exponentially in system size. This demonstrates that in the thermodynamic limit the many-body eigenstates spontaneously break translational symmetry at the perturbative level, and thus violate the eigenstate thermalization hypothesis. Right: the fit of the disorder averaged susceptibility yields the exponential behavior $d\sqrt{\Delta\rho^2}/dW \propto a^L$ with $a = 6.2$ at $t = 0.01U$.

with the system size. Fitting the average susceptibility to the expected behavior (3.3.12) yields the value $c/(t_0/U)^\alpha \simeq 6.2$. From this we can obtain a rough estimate for the critical value of the barrier hopping, by assuming that Eq. (3.3.12) holds approximately up to the delocalization transition. Since the susceptibility to disorder must stop growing exponentially with L in the ergodic phase, we may estimate the critical hopping from the requirement $c/(t_c/U)^\alpha \approx 1$, which yields $t_c \approx 0.4U$. This is consistent with the expectation that the delocalization or quantum glass transition takes place when the barrier hopping strength t becomes comparable to the hopping for fast particles J. This is in good agreement also with the estimation of the critical hopping from real time dynamics, done in Subsec. 3.3.3 below, and with results from other authors. [92]

3.3.3 Temporal decay of spatial inhomogeneity

Let us now take the effective model (3.2.2), prepare the system in a classical initial configuration C, and consider its time evolution. This allows to check for the most fundamental signature of ideal quantum glassiness, which is, the divergence of relaxation times with system size. Considerations are first restricted to the case in which $|C\rangle$ has no resonant spots, which allows for exact calculations. As an observable to characterize localization properties of translation invariant systems, I use again the average spatial inhomogeneity defined in Eq. (3.3.7), computed on $|\Psi\rangle \equiv |\psi(\tau)\rangle \equiv e^{-iH\tau}|C\rangle$, the state time evolved from the classical initial configuration $|C\rangle$. Be-

low, also its time average, $\left\langle \Delta\rho_\psi^2 \right\rangle (T) \equiv T^{-1} \int_0^T d\tau \Delta\rho_\psi^2 (\tau)$, which will be insensitive to quantum revivals in finite systems, will be considered. In the absence of resonances, the only eigenstates which have significant overlap with C are the states in the miniband described by Eq. (3.3.1), with energies given by Eq. (3.3.2). Expanding in those eigenstates, labeled by n, m, one obtains

$$\begin{aligned}
\Delta\rho_\psi^2 (\tau) &= \frac{1}{L} \sum_{j=1}^{L} \left[\sum_{n,m} e^{i(\varepsilon_n - \varepsilon_m)\tau} \langle C| n\rangle \langle m| C\rangle \langle n| (n_{j+1} - n_j) |m\rangle \right]^2 \\
&= \frac{1}{L} \sum_{j=1}^{L} \sum_{n,m} \sum_{n',m'} e^{i[(\varepsilon_n + \varepsilon_{n'}) - (\varepsilon_m + \varepsilon_{m'})]\tau} \langle C| n\rangle \langle m| C\rangle \langle n| (n_{j+1} - n_j) |m\rangle \\
&\times \langle C| n'\rangle \langle m'| C\rangle \langle n'| (n_{j+1} - n_j) |m'\rangle , \qquad (3.3.13)
\end{aligned}$$

where the overlaps with the initial configuration are given by

$$\langle C| n\rangle = \frac{1}{\sqrt{L}} \qquad \forall n.$$

Since the operators n_i are diagonal in the basis of classical configurations, the matrix elements of the site occupations are

$$\langle n| n_j |m\rangle = \frac{1}{L} \sum_{k,k'=0}^{L-1} e^{i\frac{2\pi}{L}(m+\phi)k} e^{-i\frac{2\pi}{L}(n+\phi)k'} \langle C| T^{-k'} n_j T^k |C\rangle = \frac{1}{L} \sum_{k=0}^{L-1} e^{i\frac{2\pi}{L}(m-n)k} \langle C| n_{j+k} |C\rangle , \qquad (3.3.14)$$

where T is the translation operator. Then the expression for the inhomogeneity becomes

$$\begin{aligned}
\Delta\rho_\psi^2 (\tau) &= \frac{1}{L^5} \sum_{j=1}^{L} \sum_{m,n=0}^{L-1} \sum_{m',n'=0}^{L-1} e^{i[(\varepsilon_n + \varepsilon_{n'}) - (\varepsilon_m + \varepsilon_{m'})]\tau} \qquad (3.3.15) \\
&\times \sum_{k=0}^{L-1} \sum_{k'=0}^{L-1} e^{i\frac{2\pi}{L}(m-n)k} e^{i\frac{2\pi}{L}(m'-n')k'} \langle C| (n_{j+k+1} - n_{j+k}) |C\rangle \langle C| (n_{j+k'+1} - n_{j+k'}) |C\rangle .
\end{aligned}$$

One can now define the auto-correlation function of the initial density,

$$G(k - k') \equiv \frac{1}{L} \sum_{j=1}^{L} \langle C| n_{j+k} |C\rangle \langle C| n_{j+k'} |C\rangle , \qquad (3.3.16)$$

and rewrite Eq. (3.3.15) as

$$\begin{aligned}
\Delta\rho_\psi^2 (\tau) &= \frac{1}{L^4} \sum_{m,n=0}^{L-1} \sum_{m',n'=0}^{L-1} e^{i[(\varepsilon_n + \varepsilon_{n'}) - (\varepsilon_m + \varepsilon_{m'})]\tau} \sum_{k=0}^{L-1} \sum_{k'=0}^{L-1} e^{i\frac{2\pi}{L}(m-n)k} e^{i\frac{2\pi}{L}(m'-n')k'} \\
&\times \left[2G(k - k') - G(k - k' - 1) - G(k - k' + 1) \right] . \qquad (3.3.17)
\end{aligned}$$

In the thermodynamic limit, one can take a continuum limit and measure time naturally in units of the inverse of the inverse of the center of mass hopping $\lambda_{\text{eff}}^{-1}$. I assume an essentially random initial configurations of the barriers of density ρ, and compute the function $G(k-k')$. Such a function is made by two terms: for $k=k'$, the sum over the sites of the chain is equal to the number of particles, which means that

$$G(0)=\rho. \tag{3.3.18}$$

On the other hand, for $k\neq k'$, $G(k-k')$ is the sum of L independent random variables with the following distribution:

$$\langle C|\, n_{j+k}\,|C\rangle\,\langle C|\, n_{j+k'}\,|C\rangle=\begin{cases}1 & \text{w. p. } \rho^2\\ 0 & \text{w. p. } (1-\rho^2)\end{cases}. \tag{3.3.19}$$

For large L the central limit theorem can be applied, and this leads to the result

$$G(k-k')=\rho^2+\frac{W(k-k')}{\sqrt{L}},\qquad k\neq k' \tag{3.3.20}$$

where $W(k-k')$ is a Gaussian random variable with mean value $\mu=0$ and variance $\sigma^2=\rho^2(1-\rho^2)$. In the thermodynamic limit, the random term becomes negligible, and one finds

$$G(k-k')=\rho(1-\rho)\,\delta_{k-k',0}+\rho^2. \tag{3.3.21}$$

The summation over the indexes k, k' in Eq. (3.3.17) can now be performed:

$$\begin{aligned}\frac{1}{L}\sum_{k=0}^{L-1}\sum_{k'=0}^{L-1}e^{i\frac{2\pi}{L}(m-n)k}e^{i\frac{2\pi}{L}(m'-n')k'}\left[2G(k-k')-G(k-k'-1)-G(k-k'+1)\right] &= \\ \frac{1-\cos\left[\frac{2\pi}{L}(m'-n')\right]}{L}2\rho(1-\rho)\sum_{k=0}^{L-1}e^{i\frac{2\pi}{L}(m+m'-n-n')k} &= \\ 2\rho(1-\rho)\left\{1-\cos\left[\frac{2\pi}{L}(m-n)\right]\right\}\delta_{m',m-n-n'} &\quad .\end{aligned} \tag{3.3.22}$$

Next one sums over the index m', and finds

$$\Delta\rho_{\psi}^2(\tau)=\frac{2\rho(1-\rho)}{L^3}\sum_{m,n=0}^{L-1}\left\{1-\cos\left[\frac{2\pi}{L}(m-n)\right]\right\}\sum_{n'=0}^{L-1}e^{i\left[(\varepsilon_n+\varepsilon_{n'})-\left(\varepsilon_m+\varepsilon_{m-n-n'}\right)\right]\tau}. \tag{3.3.23}$$

The continuum limit can now be performed, replacing the discrete indexes n,n',m with continuous

variables q_1, q_2, q_3:

$$\frac{\Delta\rho_\psi^2(\tau)}{\Delta\rho_\psi^2(0)} = \int_0^{2\pi} \frac{dq_1 dq_2 dq_3}{(2\pi)^3} \left[1-\cos(q_1-q_2)\right] \exp\left\{2i\tau\left[\cos q_1 - \cos q_2 + \cos q_3 - \cos(q_2-q_1-q_3)\right]\right\}, \tag{3.3.24}$$

which, performing the change of variables

$$\begin{cases} q_+ = & \frac{q_1+q_2}{2} \\ q_- = & \frac{q_2-q_1}{2} \end{cases}, \tag{3.3.25}$$

becomes

$$\begin{aligned} \frac{\Delta\rho_\psi^2(\tau)}{\Delta\rho_\psi^2(0)} &= \int_{-\pi}^{\pi} \frac{dq_-}{2\pi} \int_0^{2\pi} \frac{dq_+ dq_3}{(2\pi)^2} \left[1-\cos(2q_-)\right] \\ &\times \exp\left\{2i\tau\left[2\sin q_+ \sin q_- + \cos q_3 - \cos(2q_-)\cos q_3 - \sin(2q_-)\sin q_3\right]\right\}. \end{aligned} \tag{3.3.26}$$

The integration over q_+ can now be performed:

$$\int_0^{2\pi} \frac{dq_+}{2\pi} \exp\left(4i\tau \sin q_+ \sin q_-\right) = J_0\left(4\tau\left|\sin q_-\right|\right), \tag{3.3.27}$$

where J_0 is the Bessel function of the first kind. Next I integrate over q_3:

$$\int_0^{2\pi} \frac{dq_3}{2\pi} \exp\left\{2i\tau\left[\cos q_3 - \cos(2q_-)\cos q_3 - \sin(2q_-)\sin q_3\right]\right\} = J_0\left(4\tau\left|\sin q_-\right|\right). \tag{3.3.28}$$

Renaming $q_- \equiv q$ to simplify the notation, inserting again the effective hopping explicitly, and applying some trigonometric relations, one finally finds the expression

$$\frac{\Delta\rho_\psi^2(\tau)}{\Delta\rho_\psi^2(0)} = \int_{-\pi}^{\pi} \frac{dq}{2\pi} J_0^2\left(4\tau\lambda_{\text{eff}}\left|\sin q\right|\right) \sin^2 q. \tag{3.3.29}$$

For times $\tau \ll \lambda_{\text{eff}}^{-1}$, one finds essentially no relaxation:

$$\frac{\Delta\rho_\psi^2(\tau)}{\Delta\rho_\psi^2(0)} = 1 - 6\left(\tau\lambda_{\text{eff}}\right)^2 + O\left(\left(\tau\lambda_{\text{eff}}\right)^4\right), \tag{3.3.30}$$

reflecting the absence of local resonances. For large times, if no time average is taken, the inhomogeneity oscillates, with an envelope decaying as $\Delta\rho_\psi^2(\tau) \propto \tau^{-1}$.

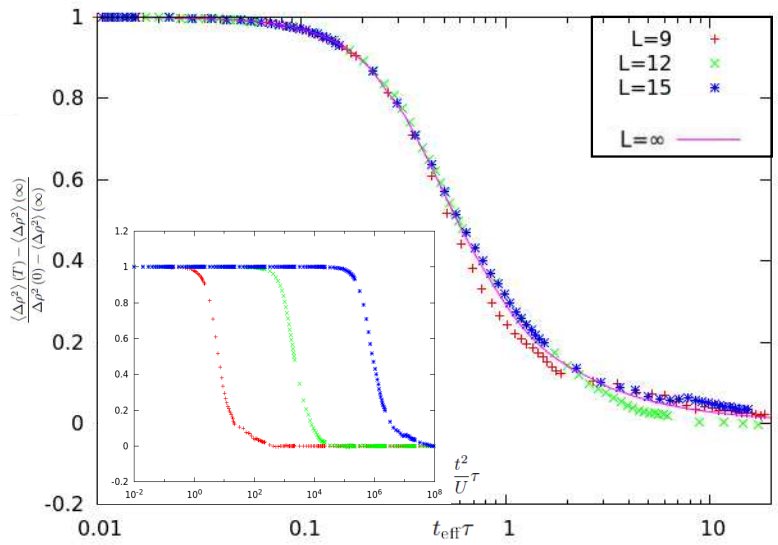

Figure 3.3.2: Relaxation of inhomogeneity in the density, in the absence of resonances. Time is rescaled by the exponentially large sample dependent $t_{\rm eff}^{-1}$. The solid line is the analytical result (3.3.29) for the thermodynamic limit. *Inset*: the same numerical data without rescaled time shows that the density inhomogeneity persists for times which diverge with the system size.

Now let us move back to finite systems, and compute the time averaged inhomogeneity in the limit of long times: in this regime, the only terms which are non-vanishing are those with $\varepsilon_n + \varepsilon_{n'} = \varepsilon_m + \varepsilon_{m'}$. Since with finite hopping and magnetic flux the spectrum of H is non-degenerate, the asymptotic limit for the time averaged inhomogeneity reads

$$\begin{aligned}
\left\langle \Delta\rho_\psi^2 \right\rangle (\infty) &= \frac{1}{L^5} \sum_{j=1}^{L} \sum_{k=0}^{L-1} \sum_{k'=0}^{L-1} \langle C| \, n_{j+k} \, |C\rangle \, \langle C| \, n_{j+k'} \, |C\rangle \sum_{n \neq m=0}^{L-1} \left(e^{i\frac{2\pi}{L}(m-n)(k+k')} + e^{i\frac{2\pi}{L}(m-n)(k-k')} \right) \\
&= \frac{1}{L^3} \sum_{j=1}^{L} \sum_{k=0}^{L-1} \left[\left(\langle C| \, (n_{j+k+1} - n_{j+k}) \, |C\rangle \right)^2 - \langle C| \, (n_{j+k+1} - n_{j+k}) \, |C\rangle \, \langle C| \, (n_{j-k+1} - n_{j-k}) \, |C\rangle \right] \\
&= \frac{\Delta\rho_\psi^2 \, (0)}{L}. \qquad (3.3.31)
\end{aligned}$$

In Fig. 3.3.2, the above calculations are compared with numerical data from exact diagonalization of finite systems, initialized in a configuration C of $N = \rho L$ particles, with $\rho = 1/3$. The numerics are restricted to configurations that do not exhibit resonances at any order in perturbation theory. A very small hopping $t = 10^{-3}U$ is used. For each data set, time is rescaled with the appropriate center-of-mass hopping, $t_{\rm eff}\,(C)$. The long time average $\left\langle \Delta\rho_\psi^2 \right\rangle (\infty)$ has been subtracted, so that all curves tend asymptotically to zero. Despite the small sizes, the agreement with Eq. (3.3.29) for the thermodynamic limit is very good.

3.3.4 Effect of local resonances

Let us now discuss the role of local resonances in the configurations C. It is still expected that, at small enough t, the effective hopping of the center of mass of a generic configuration C scales as $t_{\text{eff}} \propto t^{\alpha N}$. Resonances simply reduce the exponent α with respect to the naive expectation $\alpha = 1$. To understand the origin of this effect, let us consider the simple case of three particles on a ring. We call the three inter-particle distances l_1, l_2, l_3. In general, the effective hopping in the system is proportional to t^3/U^2, since to translate the entire system all particles must be moved by one site. Now let us analyze the resonant case $l_2 = l_1 + 1$. As illustrated in Fig. 3.2.2, there are two degenerate configurations, which form the hybridized states

$$|\psi_\pm\rangle \approx \frac{|l_1, l_1+1, l_3\rangle \pm |l_1+1, l_1, l_3\rangle}{\sqrt{2}} \tag{3.3.32}$$

with an energy splitting of order $O(t)$. It is straightforward to see that a matrix element between $|\psi_\pm\rangle$ and the translated wavefuctions $T|\psi_\pm\rangle$ appears already at second order in t, not only at third order. This implies that the effective hopping of this configuration is only of order t^2/U.

An alternative way of understanding this result is as follows. If two resonant intervals are present, the ensuing degeneracy of the spectrum is split at first order in perturbation theory if the intervals are direct neighbors. If they are not adjacent to each other and if they are surrounded by intervals of different lengths, the splitting is generically of second order $\sim t/U$. In the calculation of the effective hopping, such lifted resonances appear as small denominators, which increase the transition amplitude by one or two factors of U/t, respectively. This argument is easily generalized to configurations with multiple, spatially distant resonances.

Apart from increasing the effective hopping of the system, resonances result also in fast, partial relaxation processes through admixture. This diminishes the inhomogeneity plateau in $\langle \Delta\rho^2 \rangle$ by an amount proportional to the density $\sim \rho$ of resonating configurations. This effect is seen in Fig. 3.3.3, where the evolution of the inhomogeneity is plotted for configurations which include a resonance at first order in t.

Let us now determine the exponent α at leading order in the density $\rho \ll 1$, within perturbation theory. The simplest type of resonance is a pair of two consecutive intervals with lengths $(l, l+1)$ or $(l+1, l)$, as shown in Fig. 3.2.2. The probability of finding an interval of length l in a random configuration of density ρ is given by Eq. (3.2.6). There are

$$N_{1\text{res}} = 2N\rho^2 \sum_{l=1}^{\infty} (1-\rho)^{2l-1} + O\left(\rho^2\right) = \rho N + O\left(\rho^2\right) \tag{3.3.33}$$

such resonances in a typical configuration C, where corrections due to overlapping pairs are neglected. The factor of 2 accounts for both possibilities $(l, l+1)$ and $(l+1, l)$. As discussed above, local configurations like this hybridize at first order in perturbation theory. Accordingly they

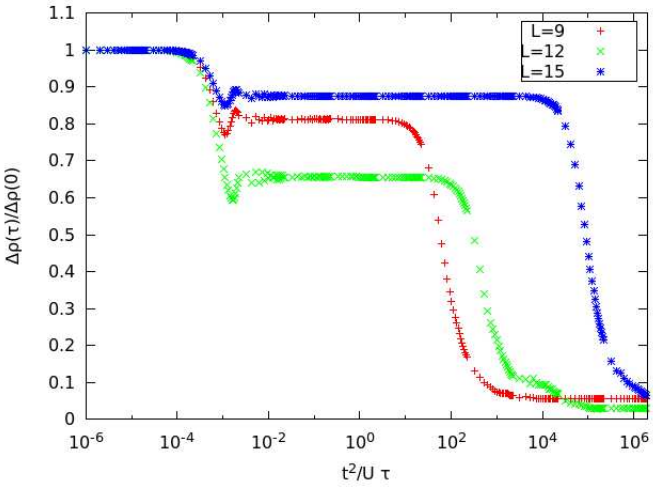

Figure 3.3.3: Time evolution of the inhomogeneity for configurations containing first order resonances. The samples of length $L = 9, 15$ have only one particle involved in the resonance; for $L = 12$ two particles are involved. The presence of local resonances leads to partial relaxation processes at short time scales $\tau \approx O\left(t^{-1}\right)$. Moreover, by comparing the plot with the inset of Fig. 3.3.2, one sees that the global relaxation times $\sim t_{\text{eff}}^{-1}$ are reduced by a factor t/U for particle involved in resonances. As resonances are rare, this effect does not alter the fact that t_{eff}^{-1} diverges exponentially in the thermodynamic limit.

reduce the power of t in the effective tunneling by one each, which yields

$$(\Delta\alpha)_{1 \text{ res}} = -\rho + O\left(\rho^2\right). \tag{3.3.34}$$

The dominant reduction of α is, however, due to sequences of interval lengths of the form

$$(l, p_1, p_2, ..., p_m, l+1), \tag{3.3.35}$$

where the $p_{i=1,...,m} \notin \{l-1, l, l+1\}$ are non resonant with l or $l+1$. If $m > 1$, such configurations do not lead to strong hybridizations though, and thus they do not significantly contribute to the fast relaxation of the density inhomogeneity, $\Delta\rho^2$, which occurs before the long time plateau. Nevertheless, they increase the effective hopping by introducing a small denominator in perturbation theory. Such a denominator is generically of order t^2, due to self-energies that arise at second order in perturbation theory, as discussed in Subsec. 3.2.3.2. If two separated pairs $(l, l+1)$ and $(l', l'+1)$ are interlaced, only one of them can be used to create a small denominator, however. The maximal number of resonances encountered in perturbation theory will usually be obtained by retaining the shorter of the two pairs.

Let us now estimate the total number of resonant pairs of the form (3.3.35), which are not interlaced by shorter resonances. To leading order the probability of finding such a sequence formed by $m+2$ intervals can be estimated as ρ, multiplied by the probability that there are

no resonant sequences of shorter length which interlace it. To compute this probability, we first impose the requirement that the interval of length $l+1$ is not in resonance with the m intervals that follow it, which yields a factor $(1-\rho/2)^m$. Next, we impose the requirement that the interval p_m is not in resonance with either $l+1$ nor with any of the subsequent $m-1$ intervals, which yields another factor $(1-\rho/2)^m$. The preceding interval p_{m-1} can be in resonance with the interval p_m (since that resonance would be nested inside the considered one), but not with $l+1$ or the following $m-2$ intervals. This yields a factor $(1-\rho/2)^{m-1}$. This procedure is iterated up to interval p_1, and then the resulting probability is squared, since the same conditions applies to the left of the sequence, too. This leads to

$$N_{2\text{ res}} \approx= N\rho\left(1-\frac{\rho}{2}\right)^{2m}\prod_{j=1}^{m}\left(1-\frac{\rho}{2}\right)^{2j} N\rho\left(1-\frac{\rho}{2}\right)^{m^2+3m} \simeq N\rho e^{-\frac{\rho}{2}\left(m^2+3m\right)}. \tag{3.3.36}$$

The corresponding reduction in the exponent α can be estimated by summing the above over m and approximating the sum as an integral:

$$\left(\Delta\alpha\right)_{2\text{ res}} \simeq -2\rho\int_1^\infty dm e^{-\frac{\rho}{2}\left(m^2+3m\right)} = -\sqrt{2\pi\rho}+O\left(\rho\right), \tag{3.3.37}$$

where the factor 2 is due to the fact that each resonance typically increases the effective hopping by a factor $O\left(t^{-2}\right)$. This yields the dominant reduction of the tunneling exponent, $\alpha = 1-\sqrt{2\pi\rho}$.

Note that the effective hopping could be computed by moving all particles either to the left or to the right. One might thus worry that the above result depends on this choice. However, one can check that in either construction the maximal number of small denominators encountered in calculating the perturbative matrix element is the same.

3.3.5 Estimation of the effective hopping

The inset of Fig. 3.3.2 illustrates the long-time plateau of inhomogeneity, whose length diverges exponentially in the thermodynamic limit. The latter is due to the exponential smallness of t_{eff}, $\ln t_{\text{eff}} \propto -L$.

Let us estimate this effective hopping. I first consider a configuration C which exhibits no resonances at any order of perturbation theory. This means that the displacement of any subset of $n < N$ particles by one site (all in the same direction) does not lead to a configuration whose classical energy is degenerate with that of C. This restriction is equivalent to requiring that no two intervals between successive particles differ by one lattice spacing only. Such a request is realistic only for small number of particles $N \ll \rho^{-1}$: for larger systems, one has to take care of the effect of resonances, as explained in the previous Subsection. Neglecting for the moment resonant configurations, the effective hopping t_{eff} is computed using degenerate perturbation theory in t.

One needs to sum over all possible orders in which N particles can be moved forward by one site each and divide the hopping matrix elements by the corresponding intermediate energies. This leads to the expression

$$t_{\text{eff}} \equiv t \sum_{P \in S(N)} \prod_{i=1}^{N-1} \frac{t}{\sum_{j=1}^{i} \Delta V^{\text{exact}}_{P(j).P}}. \tag{3.3.38}$$

P runs over all permutations of N elements, and $\Delta V^{\text{exact}}_{P(j).P}$ is the energy shift associated with the displacement of particle $P(j)$. It has an explicit dependence on the permutation P, as the energy shift depends on whether or not particles $P(j) \pm 1$ have already moved when particle $P(j)$ moves:

$$\frac{\Delta V^{\text{exact}}_{P(j),P}}{U} = \begin{cases} v\left(l_{P(j)} + a\right) - v\left(l_{P(j)}\right) + v\left(l_{P(j)+1} - a\right) - v\left(l_{P(j)+1}\right) \\ \text{if neither } P(j) \pm 1 \text{ have moved before step } j; \\ v\left(l_{P(j)} + a\right) - v\left(l_{P(j)}\right) + v\left(l_{P(j)+1}\right) - v\left(l_{P(j)+1} + a\right) \\ \text{if only } P(j) + 1 \text{ has moved before step } j; \\ v\left(l_{P(j)}\right) - v\left(l_{P(j)} - a\right) + v\left(l_{P(j)+1} - a\right) - v\left(l_{P(j)+1}\right) \\ \text{if only } P(j) - 1 \text{ has moved before step } j; \\ v\left(l_{P(j)}\right) - v\left(l_{P(j)} - a\right) + v\left(l_{P(j)+1}\right) - v\left(l_{P(j)+1} + a\right) \\ \text{if both } P(j) \pm 1 \text{ have moved before step } j. \end{cases} \tag{3.3.39}$$

Here $l_j \equiv |r_j - r_{j-1}|$ is the distance between particles j and $j-1$, while a is the lattice spacing. The interaction $v(l)$ is the one appearing in the effective Hamiltonian (3.2.2).

Let us first discuss the sum over permutations qualitatively. Even though there are $N!$ terms, most of them have denominators that grow factorially as well. Given that the ΔV have essentially random signs, typical denominator products scale as $\sqrt{N!}$ and have random signs, too. This compensates the factorial number of (randomly signed) terms and leaves us with a merely exponentially growth with N.

Finding an analytic estimate for the effective hopping is a very difficult task, since one has to take into account non-trivial interference effects among different ways in which particles can be moved. However, in the low density limit $\rho \ll 1$, at least the scaling of the effective hopping with ρ can be obtained, in the absence of resonances. I shall later explain in Sub-Subsec. 3.3.5.2 what the effect of resonant pairs of intervals is. To find this scaling, one first needs to rewrite Eq. (3.3.38) by applying the middle value theorem to the energy denominators $\Delta V^{\text{exact}}_{P(j),P}$. This yields the expression

$$\frac{\Delta V^{\text{exact}}_{P(j),P}}{U} = \begin{cases} a\left[v'\left(l_{P(j)} + a\vartheta^{+}_{P(j)}\right) - v'\left(l_{P(j)+1} - a\vartheta^{-}_{P(j)+1}\right)\right] \\ \text{if neither } P(j) \pm 1 \text{ have moved before step } j; \\ a\left[-v'\left(l_{P(j)} + a\vartheta^{+}_{P(j)}\right) - v'\left(l_{P(j)+1} - a\vartheta^{-}_{P(j)+1}\right)\right] \\ \text{if only } P(j)+1 \text{ has moved before step } j; \\ a\left[v'\left(l_{P(j)} + a\vartheta^{+}_{P(j)}\right) + v'\left(l_{P(j)+1} - a\vartheta^{-}_{P(j)+1}\right)\right] \\ \text{if only } P(j)-1 \text{ has moved before step } j; \\ a\left[-v'\left(l_{P(j)} + a\vartheta^{+}_{P(j)}\right) + v'\left(l_{P(j)+1} - a\vartheta^{-}_{P(j)+1}\right)\right] \\ \text{if both } P(j) \pm 1 \text{ have moved before step } j. \end{cases} . \tag{3.3.40}$$

In the above, $0 \leq \vartheta^{\pm}_j \leq 1$ are numbers which depend on the lengths l_j and the form of the interaction $v(l)$. One can now consider these $\vartheta^{\pm}_j$ as free variables, and expand the energy denominators in them. This is equivalent to an expansion in powers of a. From the expression above, it is easy to see that each energy denominator can be written as a sum of terms of the form

$$U\Delta E_{i,j} \equiv Ua\left[v'\left(l_i + a\vartheta^{+}_i\right) - v'\left(l_j - a\vartheta^{-}_j\right)\right]. \tag{3.3.41}$$

The ΔE_{ij} are the fundamental objects that are studied in this Subsection. Expanding the inverse of these denominators, one finds

$$\frac{1}{\Delta E_{i,j}} \equiv \frac{1}{a\left(v'\left(l_i + a\vartheta^{+}_i\right) - v'\left(l_j - a\vartheta^{-}_j\right)\right)} = \frac{1}{a\left(v'(l_i) - v'(l_j)\right)} + \frac{1}{2}\frac{\vartheta^{+}_i v''(l_i) + \vartheta^{-}_j v''(l_j)}{\left(v'(l_i) - v'(l_j)\right)^2} + O\left(a\vartheta^2\right). \tag{3.3.42}$$

It is easy to check that the zeroth order terms in the ϑs $\Delta E^{(1)}_{i,j} \equiv a\left(v'(l_i) - v'(l_j)\right)$ do not depend on the permutation P explicitly. This is because, when two consecutive particles are moved, the contribution to the energy denominator due to the interval separating them gets canceled in the sum. As an example, let us suppose that particles j and $j+1$ are moved: the corresponding energy denominator $\Delta E^{(1)}_{j-1j+1}$ can be written as

$$\Delta E^{(1)}_{j-1,j+1} = a\left[v'(l_{j-1}) - v'(l_{j+1})\right] = \Delta E^{(1)}_{j-1j} + \Delta E^{(1)}_{jj+1}, \tag{3.3.43}$$

which is exactly the sum of the energy differences arising from the motion of particles j and $j+1$. This property holds only for $\vartheta^{+}_j = \vartheta^{-}_j = 0$: when $\vartheta^{\pm}_j \neq 0$, a dependence on the order in which particles are moved (i.e. from the permutation P) is restored.

At this point, one may think that, retaining the zeroth order terms in the ϑs only, it should be possible to compute an analytic estimate for the effective hopping, in the limit of low density. This is not the case, however, since this procedure neglects the important constraint $\sum_i \Delta E^{(1)}_{i,i+1} = 0$, which induces a cancellation in the expansion. To see this, let us compute the effective hopping at

zeroth order, and observe that for N numbers $A_1, A_2, ..., A_N$, it holds that

$$\sum_{P\in S(N)}\prod_{i=1}^{N}\frac{1}{\sum_{j=1}^{i}A_{P(j)}}=\prod_{i=1}^{N}\frac{1}{A_i}, \tag{3.3.44}$$

which can be easily proven by induction. This result can now be applied to Eq. (3.3.38). Since

$$\Delta V^{\text{exact}}_{P(j),P}(a)=a\Delta E^{(1)}_{P(j),P(j)+1}+O\left(a^2\right), \tag{3.3.45}$$

taking $A_i=a\Delta E^{(1)}_{i,i+1}$ one finds

$$t_{\text{eff}}\simeq t_{(1)}\equiv t^N\left(\prod_{i=1}^{N}\frac{1}{a\Delta E^{(1)}_{i,i+1}}\right)a\sum_{j=1}^{N}\Delta E^{(1)}_{j,j+1}. \tag{3.3.46}$$

Neglecting for a moment the sum appearing in the numerator, the product term scales exponentially with N, as expected. One can estimate how this expression scales with ρ by recalling that the typical interparticle distance scales as $l_{\text{typ}}\sim\rho^{-1}$, as follows from the distribution (3.2.6). One then finds that, typically, $\Delta V^{(1)}\sim v'\left(l_{\text{typ}}\right)\sim\rho^{\beta+1}$: the logarithmic average of t_{eff} should then scale as

$$\ln\left(\frac{t_{(1)}}{t}\right)_{\text{typ}}\sim(N-1)\left[\ln t-(\beta+1)\ln\rho-\ln a+\tilde{c}_\beta\right], \tag{3.3.47}$$

where all N interparticle lengths $l_1,\ldots,l_N$ that enter in the expression (3.3.46) are averaged over the distribution (3.2.6). $\tilde{c}_\beta$ is a constant of $O(1)$, which depends on the exponent β of the interaction. However, the prefactor of N in the exponent is not estimated correctly by this calculation, since the sum $\sum_{j=1}^{N}\Delta E^{(1)}_{j,j+1}$ vanishes exactly, as stated above. This implies that terms of higher order in a (or equivalently in the ϑs) must be retained to obtain a finite result.

To find the correct scaling of the effective hopping with the density, one needs to find at which order in the $\vartheta^{\pm}_j$ the first non vanishing-contribution appears. It turns out that t_{eff} vanishes exactly if there are two intervals i,j whose associated $\vartheta^{\pm}$ are set to zero:

$$\vartheta^{\pm}_i=\vartheta^{\pm}_j=0\Rightarrow t_{\text{eff}}=0.\quad i\neq j \tag{3.3.48}$$

Before proving this statement, it is important to point out that this property unambiguously fixes the scaling of the effective hopping with the density. Indeed, it implies that the lowest order contribution to the expansion is a polynomial of order $N-1$ in the ϑs, and consequently of order $O\left(a^0\right)$ in the lattice spacing (as follows from Eq. (3.3.42)):

$$t_{\text{eff}}=\sum_{n=1}^{N}\prod_{i\neq n}\sum_{\sigma_i=\pm}c_i\vartheta_i^{\sigma_i}+O\left(a\vartheta^N\right). \tag{3.3.49}$$

One must impose in the sum above the extra constraint that at least one σ_i in each product of ϑs must be $+$, and at least one must be $-$, but this has no consequence on the scaling form we are interested in. What really matters is that each $\vartheta_i^{\sigma_i}$ comes together with a factor c_i, which can be read from Eq. (3.3.42) to be

$$c_i = \frac{v''(l_i)}{\left(v'(l_i) - v'\left(l_{k(i)}\right)\right)^2} \sim O\left(\rho^{-\beta}\right), \tag{3.3.50}$$

$k(i) \neq i$ being an interval, which it is not possible to identify through this approach. This is not important, however, since all interval lengths typically scale with density in the same way. Therefore, the logarithmic average of the full expression (which involves products of $N-1$ such factors) must scale as

$$\ln\left(\frac{t_{\text{eff}}}{t}\right)_{\text{typ}} \sim (N-1)\left[\ln t - \beta \ln \rho + c_\beta\right]. \tag{3.3.51}$$

Two important facts need to be noticed, when this scaling form is compared with the naive one (3.3.47). The first one is that the correct form is smaller by a factor ρ^{N-1} with respect to the naive one: this very strong suppression is a manifestation of the interference among different paths, and implies that the collective motion of the particles is much slower than predicted from Eq. (3.3.46), and similar estimates in Ref. [35]. The second one is that there is no explicit dependence from the lattice spacing a.

Now I just need to prove that t_{eff} indeed vanishes when I pick two intervals i, j and set $\vartheta_{i,j}^{\pm} = 0$. Intervals i and j partition the system into two disjoint sets, $A = \{i+1, i+2, \ldots, j\}$ and $B = \{j+1, j+2, \ldots, N, 1, \ldots, i\}$. If $\vartheta_{i,j}^{\pm} = 0$ energy denominators arising from moving subsets $A' \subset A$ and $B' \subset B$ are exactly equal to the sum of the energy differences due to moving only one subset,

$$\Delta E_{A',B'} = \Delta E_{A'} + \Delta E_{B'}. \tag{3.3.52}$$

This property is trivial if subsets A', B' are not in contact with each other, i.e. if there is no particle $k \in A'$ such that either particle $k+1$ or $k-1$ belongs to B'. If the two intervals are in contact instead, either $i \in B'$ and $i+1 \in A'$, or $j \in A'$ and $j+1 \in B'$. In both cases, the decomposition follows immediately from Eq. (3.3.43). Eq. (3.3.52) implies that denominators due to the motion of particles in subset A' and B' factorize when summed over all possible ways in which particles are moved, i.e. that

$$\sum_{P' \in S(N_{A'}+N_{B'})} \prod_{i=1}^{N_{A'}+N_{B'}} \frac{1}{\sum_{j=1}^{i} \Delta V^{\text{exact}}_{P(j),P}} = \frac{1}{\Delta E_{A'}} \frac{1}{\Delta E_{B'}}, \tag{3.3.53}$$

where the index i runs labels all particles belonging to A' and B'. This factorization follows from the fact that, due to Eq. (3.3.52), particles in A' can be seen as non interacting with particles

in B'. Consequently, one is computing via locator expansion the amplitude for moving two sets of particles which do not interact with each other: this is just the product of the amplitudes for moving the two sets separately.

With this factorization property at disposal, it is possible to prove that t_{eff} vanishes for $\vartheta_i^{\pm} = \vartheta_j^{\pm} = 0$. Let us call S_A the sum over all permutations of the N_A particles in subsystem A, multiplied by their respective amplitudes:

$$S_A \equiv \sum_{P' \in S(N_A)} \prod_{i=1}^{N_A} \frac{t}{\sum_{j=1}^{i} \Delta V^{\text{exact}}_{P(j),P}}, \tag{3.3.54}$$

and let us define analogously the sum S_B for subsystem B. The last denominator of all terms appearing in S_A is $1/\Delta E_{ij}$, while the last denominator of all terms in S_B is $1/\Delta E_{ji} = -1/\Delta E_{ij}$. If the products in Eq. (3.3.38) ran on all N particles, one would find $t_{\text{eff}} = S_A S_B$. Since only $N-1$ particles are moved, however, the sum splits into two terms: in the first one, all particles in A are moved, and one in B is not, and vice versa for the second one. This gives the result

$$t_{\text{eff}} = S_A S_B \Delta E_{ji} + \Delta E_{ij} S_A S_B = 0, \tag{3.3.55}$$

which concludes the proof.

The exponential suppression of the effective hopping due to interference has been derived under the assumption that each particle interacts only with its two neighboring ones, as described by the effective Hamiltonian (3.2.2). One may wonder whether it is possible to extend this result to one dimensional Hamiltonians with usual power law interactions, in which the presence of a particle does not screen all the successive ones. Such an extension, if possible, is not straightforward: one may try to attach a "flag" ϑ_k at each interval k, which multiplies all $O(a)$ corrections to interaction terms crossing that interval, and set $\vartheta_i = \vartheta_j = 0$ for two intervals $i \neq j$, as done above. Then, a factorization relation analogous to Eq. (3.3.53) would follow, and one may conclude that t_{eff} vanishes in this case, too. The problem is that, without screening, expanding in these ϑ's does not allow to infer the scaling with ρ, since now the coefficient c_i would have a non-trivial structure. Therefore, this remains an interesting open problem.

3.3.5.1 Estimation of the transition point

The predicted scaling of t_{eff} with ρ has been verified numerically, by studying the scaling of the exact expression (3.3.38) with the density for small N. In Fig. 3.3.4 the ratio $t_{\text{eff}}^{\text{exact}}/t_{\text{eff}}^{(1)}$ is plotted, logarithmically averaged over non-resonant configurations, with an exponential distribution of intervals of mean ρ^{-1}. The numerical data are indeed consistent with Eq. 3.3.51, with $\tilde{c}_2 \approx 4$.

The above estimates are qualitatively good only for very small t. One may nevertheless use them to estimate the hopping t_c at which typical random states delocalize, by requiring that the

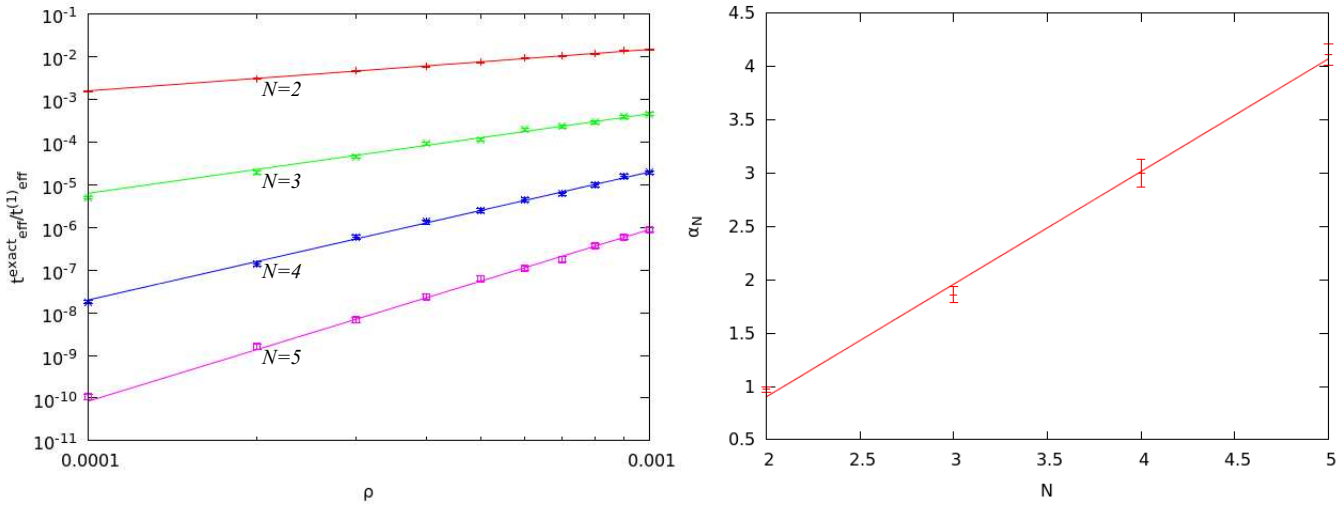

Figure 3.3.4: *Right:* Logarithmically averaged ratio between the exact hopping $t_{\text{eff}}^{\text{exact}}$ and the naive estimate $t_{\text{eff}}^{(1)}$, as a function of density ρ, for different numbers of particles. The ratio was found to scale as ρ^{α_N}. *Left:* A plot of the fitted α_N against N confirms that $\alpha_N = N - 1$ (solid line).

coefficient of N on the right-hand side of Eq. (3.3.51) vanishes. More precisely, one expects

$$\frac{t_c}{U} \lesssim \rho^{-1} \exp\left[\left\langle \ln\left(\frac{\Delta E^{(1)}}{U}\right)\right\rangle\right], \tag{3.3.56}$$

to be an upper bound, since locally resonating structures proliferate with increasing t and change the scaling of the effective hopping with density. For the power-law interactions $v(l) = l^{-\beta}$ considered here, one finds $t_c \sim U\rho^{\beta}$ to be of order of the typical inter-particle interaction. Due to the many-body interference effect discussed above, this is larger by a factor $\rho^{-1} \sim l_{\text{typ}}$ than the naive expectation that t_c should be of the order of typical inter-particle *forces* between particles, as would be predicted by using $t_{(1)}$ for this estimate.

To estimate the value of t_c at the moderate density $\rho = 1/3$ and $\beta = 2$, we have fitted the size dependence of the numerically evaluated t_{eff} as $t_{\text{eff}} \propto (t/t_c)^N$ where $N = \rho L$. This yields

$$t_c(\rho = 1/3) \approx 0.2U. \tag{3.3.57}$$

This is consistent with numerical results found by other authors. [92]

3.3.5.2 Effect of anomalously short intervals and local resonances

The calculation I have just performed relies on two assumptions, namely that all interparticle intervals l_i are of the typical order $O(\rho^{-1})$, and that there are no resonant pairs. Obviously, in a random initial condition, neither of these approximations strictly holds, so it is necessary to investigate at least qualitatively what happens when these effects are correctly taken into account. Let us first see how the presence of anomalously short intervals modifies this picture: if, for example,

$l_j \approx O(1)$, then the corresponding factor ${}^{v''(l_j)}/_{(v'(l_j))^2}$ will be $O(1)$ too, instead of $O\left(\rho^{-\beta}\right)$ as the typical one. Since the probability of finding such a short interval is $O(\rho)$, one expects the scaling of the effective hopping to become

$$t_{\text{eff}} \sim \rho^{-\beta(N-1)(1-O(\rho))}. \tag{3.3.58}$$

At low density, this effect is subdominant with respect to the modifications due to resonances. Indeed, when a resonant pair $(l, l+1)$ is present, there is one less denominator contributing to t_{eff}, which manifests itself in a missing factor of $O\left(\rho^{-\beta}\right)$, just like it happens with anomalously short intervals. However, as computed in Subsec. 3.3.4, the density of such resonant pairs scales as $\sqrt{\rho}$, which dominates over the $O(\rho)$ density of short intervals, for $\rho \ll 1$. One can again apply the arguments of Subsec. 3.3.4 to get convinced that the correct scaling is

$$t_{\text{eff}} \sim \rho^{-\beta(N-1)\frac{\alpha}{2}}, \tag{3.3.59}$$

where the exponent α is the same as in Eq. (3.3.37).

3.4 Melting at low temperature

My perturbative analysis of quantum glasses is adapted to essentially random initial configurations, in which the particle positions are uncorrelated. This is certainly a reasonable assumption for high energy densities in the initial state. However, if the system is prepared in an equilibrium configuration at very low temperature (e.g., by weakly coupling the system to a bath for some time, and then switching the coupling off), one expects the positions of particles to become rather homogeneous and correlated, in order to minimize energy. In particular, the inter-particle intervals become far from exponentially distributed, as assumed in Eq. (3.2.6). Under such circumstances, the probability of finding configurations that resonate at low order in perturbation theory (like the ones of Fig. 3.2.2) increases significantly, since thermal disorder gets weaker. One thus expects that already lower values of t will suffice to induce delocalization and restore ergodicity in the dynamics starting from such initial conditions.

Stated differently, one expects that at fixed hopping t, a *decrease* of the temperature in the initial state renders the dynamics eventually ergodic, even at the perturbative level. As a consequence, the role of temperature is opposite to that in disorder-dominated localization, where high temperature enhances the phase space for scattering, and therefore leads to delocalization. This is one of the most striking differences between disorder- and interaction-induced MBL.

The most important consequence of this fact is that, at the perturbative level, in translation invariant models, low energy states are delocalized at all values of t, since there is a large density of *exact* resonances (i.e. hybridizations of states with exactly zero energy difference). This contrasts

with disorder induced MBL on a lattice, where localization of the whole spectrum is possible at small enough hopping amplitude. As already discussed in Chapter 2, this implies that genuine translation invariant MBL is not possible in the thermodynamic limit. Quantum glasses should be rather thought of as Griffiths systems, in which rare ergodic regions reinstate very weak transport, either by acting as carriers of energy and particles, or as mobile baths that thermalize the rest of the system, and allow for relaxation properties and thus transport. To be more precise, a modified version of the Bose-Hubbard model, in which particles are not conserved, has been rigorously proven to be *"asymptotically localized"* at high temperature, i.e. that its conductivity is non-perturbatively small in the hopping [43]. An analogous behavior is expected to hold for other quantum glasses, too.

A tentative phase diagram for quantum glasses (and, more generally, for quantum disordered systems) is shown in Fig. 3.4.1, as a function of disorder strength W, interaction U and quasi-temperature T. In the U/W plane, a real transition line is present, corresponding to the infinite temperature transition. On the other hand, no genuine transition is possible as a function of temperature, so the phase boundaries (dotted lines) must be interpreted as sharp crossovers.

3.5 Experimental realizations of quantum glasses

All the phenomenology described in this Chapter can be observed experimentally, with the exception of the diverging susceptibility to infinitesimal disorder, which is nevertheless useful from the theoretical and numerical point of view. The simplest experimental realization are strongly interacting cold atomic gases in quasi one dimensional optical lattices [100, 101]. While the calculations of this Chapter assumed periodic boundary conditions, the essence of interaction-induced localization will also be present in dense but randomly distributed cold atoms in a confining trap, which prevents the escape of particles at the boundaries. In this situation, the center of mass of an atomic cloud is predicted to respond to a tilt of the trap exponentially weakly in the number of particles, as the response is governed by the exponentially small t_{eff} discussed in Subsec. 3.3.5.

3.5.0.3 Experimental realization of the two-component quantum glass

The two-particle model (3.2.1) could be realized using highly anisotropic spin ladders. A possible implementation is shown in Fig. 3.5.1, where two unit cells are shown pictorially. The black dots represent $1/2$ spins, while the bonds represent the different kinds of interactions among the spins. In particular, the red lines represent an antiferromagnetic Heisenberg interaction, with coupling $K > 0$; the blue lines represent an antiferromagnetic Ising interaction, with coupling constant $h < K$; the black lines represent a Heisenberg interaction with coupling $\lambda < K$, and similarly for the green lines, with coupling $t \ll \lambda^2 h^2/K^3$. In the last two cases, the interaction can be both ferromagnetic or antiferromagnetic, without qualitatively modifying the physical properties I am

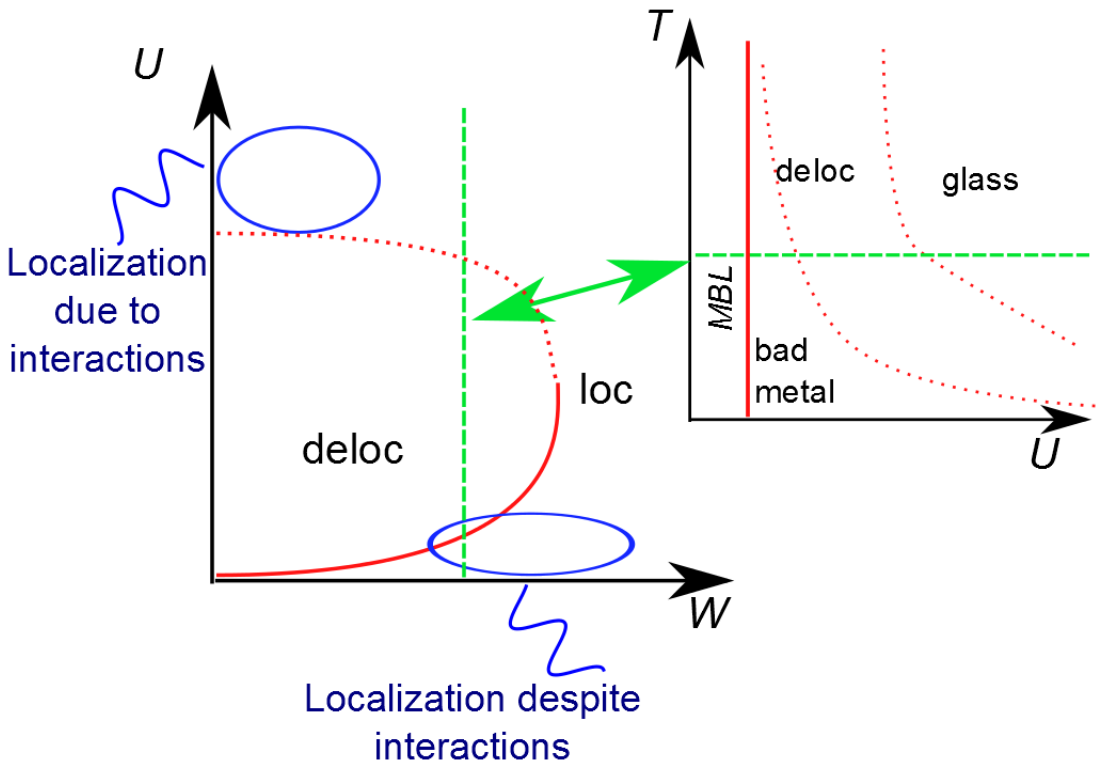

Figure 3.4.1: *Left:* Phase diagram at fixed strength of quantum fluctuations (hopping t) and energy density or (quasi-)temperature $T \geq 0$, for one dimensional models in which commuting interaction (U) and disorder (W) terms define a classical potential. Both ingredients lead to a rough energy landscape which suppresses quantum tunneling and transport. *Right:* The role of temperature differs crucially in the limits of disorder- and interaction-induced localization: from the point of view of perturbation theory, for weak interactions the lower part of the spectrum is localized, whereas highly excited states are ergodic. The reverse happens when the interactions dominate. In the thermodynamic limit, the transition gets smoothed in a crossover, and no localized phase is present: one finds rather a "bad-metal" (disorder-dominated) or "glass" (interaction dominated) behavior. The dashed lines correspond to a cut at constant quantum fluctuations, disorder, and energy density. They suggest a reentrant localization in the many-body spectrum as interaction is increased, as seen numerically in Ref. [46] and experimentally in Ref. [99].

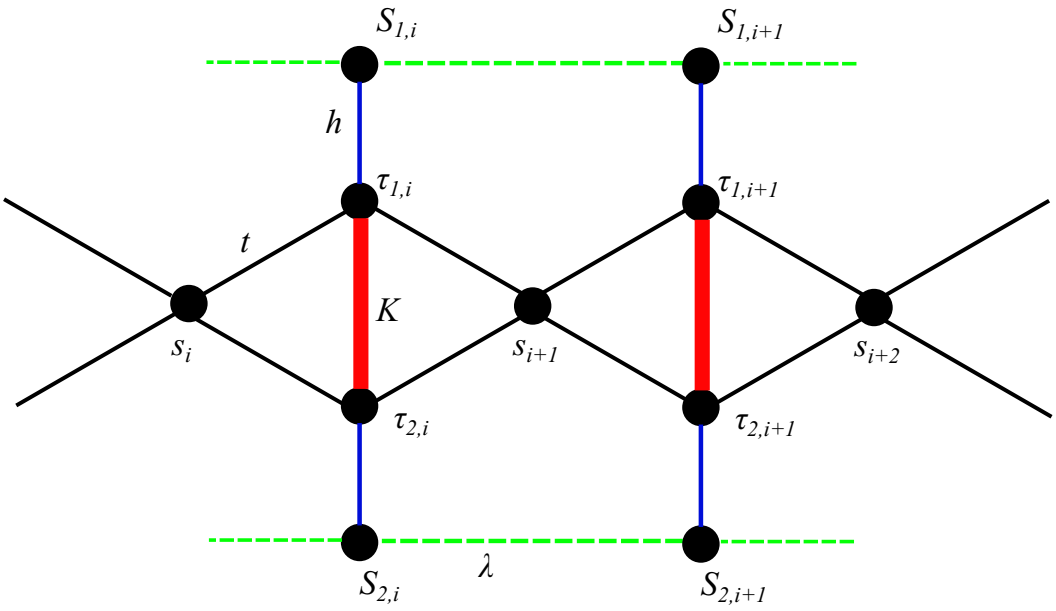

Figure 3.5.1: The spin ladder Hamiltonian (3.5.1). The pairs of τ spins are coupled by a strong antiferromagnetic interaction (red link) and are assumed to be in their local ground state. If the two corresponding S spins are aligned, the τ spins form a barrier which decouples the two neighboring s spins. Conversely, if they are anti-aligned, the τs mediate an interaction among the s spins. This model mimics Eq. (3.2.1), with the S spins taking the role of barriers, and the s ones acting as fast particles.

interested in. The explicit form of the Hamiltonian is the following:

$$\begin{aligned} H &= \sum_i \left[K\left(\vec{\tau}_{1,i}\cdot\vec{\tau}_{2,i}\right) + h\left(S^z_{1,i}\tau^z_{1,i} + S^z_{2,i}\tau^z_{2,i}\right) + \lambda\left(\vec{s}_i\cdot\vec{\tau}_{1,i} + \vec{s}_i\cdot\vec{\tau}_{2,i} + \vec{s}_{i+1}\cdot\vec{\tau}_{1,i} + \vec{s}_{i+1}\cdot\vec{\tau}_{2,i}\right), \right. \\ &- \left. t\left(\vec{S}_{1,i}\cdot\vec{S}_{1,i+1} + \vec{S}_{2,i}\cdot\vec{S}_{2,i+1}\right)\right], \end{aligned} \tag{3.5.1}$$

where S, s, τ are all spin $1/2$ operators.

The idea behind this Hamiltonian is the following: since the coupling between the τ spins is stronger than any other one, each pair of τ's can be roughly thought of as decoupled from the rest of the system. In this case, its ground state is a singlet. Now let us turn on the couplings h and λ: if $S_{1,i}$and $S_{2,i}$ are parallel to each other, the singlet is unperturbed, and the interaction between s spins vanishes, as can be checked using perturbation theory in t. Conversely, if $S_{1,i}$ and $S_{2,i}$ are anti-parallel, the ground state of spins $\tau_{1,i}$ and $\tau_{2,i}$ becomes polarized and acquires a component on the triplet state: in this situation, the s spins interact with an effective coupling $J_{\text{eff}} = {}^{4t^2h^2}/_{3K^3}$. Therefore a pair of aligned spins $S_{1,i}$and $S_{2,i}$ is equivalent to the presence of a barrier on site i, while the spins s take the role of fast particles. Obviously, the coupling t allows for barriers to hop.

One can then work at second order in perturbation theory to construct the following effective

Hamiltonian:

$$\begin{aligned} H_{\text{eff}} &= -J_{\text{eff}} \sum_i \left(s_i^+ s_{i+1}^- + s_i^- s_{i+1}^+ + 2 s_i^z s_{i+1}^z \right) \left(\frac{1 - S_{1,i}^z S_{2,i}^z}{2} \right) + t \sum_i \left(\vec{S}_{1,i} \cdot \vec{S}_{1,i+1} + \vec{S}_{2,i} \cdot \vec{S}_{2,i+1} \right) \\ &+ \mu_{\text{eff}} \sum_i \left(S_{1,i}^z S_{2,i}^z \right), \end{aligned} \tag{3.5.2}$$

which is very similar to Eq. (3.2.1). The main important difference is that the number of barriers is not conserved. However, the coupling $\mu_{\text{eff}} \equiv {}^{h^2}/_{2K}$ acts like a chemical potential for the barriers, which ensures that their number is conserved on average upon time evolution. One could try to probe the localization properties of this model via hole burning techniques, namely by removing a narrow spectral line in the absorption spectrum of the sample, using a laser. In the presence of localization, the resulting dip in the spectrum is expected to persist for very long times. [102]

Chapter 4

Absence of many-body mobility edges

The famous Mott argument, presented in Subsec. 2.2.1, states the impossibility of localized and delocalized eigenstates coexisting at the same energy in non-interacting systems [13]. As a consequence, if both localized and delocalized states are present in the spectrum, they necessarily must be separated by a sharp mobility edge. For a long time, the extension of this argument to many-body systems has been an important open issue. Analytical results obtained by means of perturbation theory [22, 23] suggested that the situation should be qualitatively analogous to the non-interacting one: ergodic states at high energy density and localized states at low energy. They should be separated by a many-body mobility edge (note that, for translation invariant quantum glasses, the role of temperature is inverted, as discussed in Sec. 3.4). From the numerical point of view, the situation is however not clear: various authors have reported the existence of mobility edges [44, 45, 46, 47], while others have failed to observe them, either being able to detect an infinite temperature transition only [48, 49], or, in contrast, finding coexistence of ergodic and non-ergodic states at all energy densities. [62]

In this Chapter, a many-body extension of the Mott argument is given. It states that, in the thermodynamic limit, in systems with local Hamiltonians coexistence of ergodic and non-ergodic eigenstates is not possible. The core of the argument consists in showing that ergodicity and transport do not require the whole system being excited with an energy density ε above the (putative) mobility a ε_c. In contrast, it is enough that a few large, yet finite regions are excited above ε_c. Such regions, which I call *"bubbles"*, will then be able to move resonantly through the system, and act as mobile baths that thermalize the rest of the system [41]. The reason why this effect is not seen in current simulations is that its observation would require system sizes larger than the ones within reach of exact diagonalization. The presence of mobility edges reported so far has hence to be interpreted as a finite size effect.

The remainder of this Chapter is organized as follows. In Sec. 4.1, a simple two-particle model of assisted hopping is presented, which illustrates several important features that this problem has in common with the rare events that induce delocalization in many-body systems and wash out

finite mobility edges whenever there is a ergodic state at some finite temperature. In Sec. 4.2, the main argument is presented, with an analysis that shows its robustness against many effects that might hinder the restoration of ergodicity. In Sec. 4.3, a numerical analysis of finite size effects in small one dimensional disordered systems is provided, showing that the available system sizes are too small to truly host ergodic bubbles. Finally, in Sec. 4.4, the consequences of these arguments for disorder-free quantum glasses are discussed, and I argue that in any realistic experiment glasses will appear as truly MBL, due to the very low probability of a bubble to be present in the initial condition.

4.1 Assisted hopping model

Consider particles on a hypercubic lattice of linear size L, hopping with amplitude t_1 and subject to a disorder potential ϵ_x, i.i.d. uniformly in $[-W, W]$. A particle on site x interacts with others by inducing assisted hopping of strength t_2 along the diagonals of plaquettes containing x (e.g. via lattice distortion)

$$H = -t_1 \sum_{\langle x,y \rangle} (c_x^\dagger c_y + \text{h.c.}) + \sum_x \epsilon_x n_x - t_2 \sum_x \sum_{s,s'=\pm} \sum_{1 \le \alpha < \beta \le d} n_x (c^\dagger_{x+s\vec{e}_\alpha} c_{x+s'\vec{e}_\beta} + \text{h.c.}), \qquad (4.1.1)$$

where $\vec{e}_{1,..,d}$ are lattice unit vectors. Parameters $t_1 \ll W$ are considered, for which the single particle problem is localized in the whole spectrum. For $t_2 \gg W$, the two-particle problem has several interesting features. In dimensions $d > 2$, the assisted hopping term induces a delocalization of close pairs which will move together diffusively as a composite light particle and overcome Anderson localization. This effect is closely related to the interaction-induced increase of the localization length in sufficiently weakly localized systems [103, 104]. A single particle analogue of the phenomenon is the solvable case of two coupled Bethe lattices [105]. The delocalization in (4.1.1) seems natural, since all configurations of two particles at distance one are strongly resonant with each other. They thus form a percolating, delocalized resonant subgraph in configuration space, which supports delocalized wavefunctions with inverse participation ratios that vanish as the inverse volume. This type of effect is confirmed numerically in Refs. [106, 107]. In a system of only two particles the eigenstates come in two kinds: the overwhelming number of states is strongly concentrated on a configuration with two distant, immobile particles. Only a vanishing fraction of order $[\log(L)]^d / L$ of all two-particle states are delocalized as dynamically bound, mobile pairs. In this example localized and delocalized states coexist at the same energy. This is possible because the matrix elements that couple the two kinds of states through a random perturbation of the Hamiltonian are typically exponentially small in the system size and thus negligible as compared to the relevant level spacings.

Let us now discuss how a finite density of particles modifies the situation. In the thermodynamic

limit, there is a finite density of close pairs in typical configurations. These pairs diffuse through the sample. Initially well isolated and localized particles scatter inelastically off these pairs and thus move as well, leading to complete delocalization. Even in exponentially rare configurations where initially all particles are far from each other, particles eventually tunnel together and decay into the continuum of diffusive pair states. Thus no localized eigenstate is expected to survive at finite density.

4.1.1 Numerical analysis of an assisted hopping Hamiltonian

In this Subsection I start by studying numerically an assisted hopping model very similar to Eq. (4.1.1), in order to show that delocalization on a resonant subgraph remains robust to adding additional terms that connect that subgraph to localized states. Coexistence of localized and delocalized states is thus found in this context, corresponding to a failure of Mott's argument, which is, however, a particularity of the zero density limit of the considered model, and is not expected to survive at finite density.

In order to reach in the numerics the largest possible system sizes, I consider a Hamiltonian in $d = 2$ with spin-orbit coupling, which gives rise to weak anti-localization and thus allows for a genuine delocalized phase. To the best of my knowledge, this is the smallest system where delocalization can be expected, and is thus best suited for a numerical study. Here, "smallest" means that the dimension of the Hilbert space grows at the slowest possible rate with growing linear size L.

Let H be the Hamiltonian of two indistinguishable hard-core bosons (with positions $q_{1,2}$) having a single spin $1/2$ degree of freedom, s, attached to them. The results would not be qualitatively altered if the particles were taken as fermions. Periodic boundary conditions are imposed. The full Hamiltonian is

$$H = H_0 + h_1 H_1 + h_2 H_2, \tag{4.1.2}$$

where H_0 is the uniformly distributed on-site potential

$$H_0 = \sum_q \epsilon_q a_q^+ a_q, \quad -W \leq \epsilon_q \leq W. \tag{4.1.3}$$

H_1 is the single-particle hopping Hamiltonian

$$H_1 = \sum_{q \sim q'} (a_q^+ a_{q'} + a_q a_{q'}^+), \tag{4.1.4}$$

($q \sim q'$ denoting nearest neighbors) and H_2 is the assisted hopping, including a spin-orbit interaction. H_2 is described by its matrix elements. Let

$$\mathcal{S} = \{q_1 = (x_1, y_1),\, q_2 = (x_2, y_2) \,:\, q_1 \neq q_2, \max\left[|x_1 - x_2|, |y_1 - y_2|\right] \leq 1\} \tag{4.1.5}$$

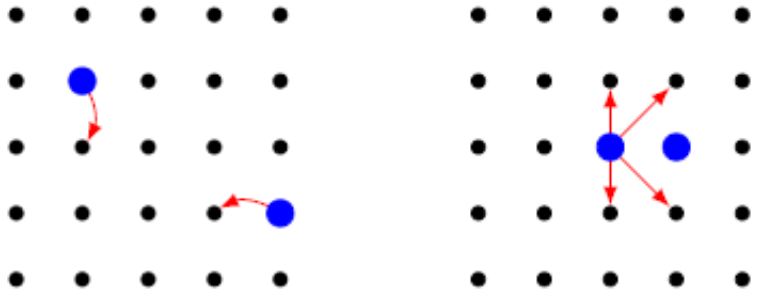

Figure 4.1.1: Hopping processes present in the Hamiltonian (4.1.2). On the left panel, the standard single-particle hopping is depicted. On the right panel, the assisted hopping processes for the left particle, allowed by the presence of the right particle, are shown. Such assisted processes are responsible for delocalization of pairs of particles, whereas isolated particles are Anderson localized.

be the set of pairs of spatially neighboring points. One then defines $\langle q_1', q_2', s'|H_2|q_1, q_2, s\rangle$ to be

$$\mathbb{I}_{\mathcal{S}}(q_1', q_2')\mathbb{I}_{\mathcal{S}}(q_1, q_2)\,\langle q_1', q_2', s'|H_{\rm SO}|q_1, q_2, s\rangle, \tag{4.1.6}$$

where the characteristic functions $\mathbb{I}_{\mathcal{S}}$ ensure that the initial and final pair configuration belong to $\mathcal{S}$. Further, $H_{\rm SO} \equiv H^1_{\rm SO} + H^2_{\rm SO}$ with

$$H^1_{\rm SO} \equiv -i\left[\sigma^{(x)}T_{y_1} - \sigma^{(y)}T_{x_1}\right] - i\left[\frac{(\sigma^{(x)} - \sigma^{(y)})}{2}T_{x_1}T_{y_1} - \frac{(\sigma^{(x)} + \sigma^{(y)})}{2}T_{x_1}T^{\dagger}_{y_1}\right] + \text{h.c.} \tag{4.1.7}$$

Here $\sigma^{(x,y)}$ are Pauli matrices acting on the spin degrees of freedom, while the translation operators are defined by $T_{x_1}\big|(x_1, y_1), (x_2, y_2), s\big\rangle = \big|(x_1{+}1, y_1), (x_2, y_2), s\big\rangle$ and similarly for T_{y_1}. $H^2_{\rm SO}$ is defined analogously for particle 2.

The Hamiltonian $H^1_{\rm SO}$ is a lattice version of the Rashba Hamiltonian $\sigma^{(x)}p_{y_1} - \sigma^{(y)}p_{x_1}$ [108], and is shown pictorially in Fig. 4.1.1. It should be noticed that restricting the definition of $H^1_{\rm SO}$ to the first term $-i\{\sigma^{(x)}T_{y_1} - \sigma^{(y)}T_{x_1}\}$ would lead to a degeneracy due to the lattice structure. This would prevent H from being a generic GSE Hamiltonian for any value of h_2.

The aim of the simulations is to show that delocalized and localized states coexist in this model. First I look at the model for $h_1 = 0$, where this statement is trivial, since the delocalized subspace $\mathcal{H}_{\mathcal{S}}$, spanned by all the classical states in $\mathcal{S}$ (see Eq. (4.1.5)), each coming with spin up/down, is decoupled from all the localized configurations. Then, a finite h_2 is turned on, and it is shown that delocalization is not destroyed by coupling to the localized subspace. In all simulations, $L = 9$ and $W = 1$ are taken. The analysis is divided into two parts. First $h_1 = 0$ and $h_2 > 0$ are taken. This choice corresponds to considering assisted hopping only. Since the majority of states (all configurations outside $\mathcal{S}$) are now trivially localized, the results are restricted to the subspace $\mathcal{H}_{\mathcal{S}}$. The aim is to find a value of h_2 such that $H_0 + h_2H_2$ can be considered a "typical" GSE matrix with truly delocalized eigenstates. For this, the parameter r defined in Subsec. 2.3.2, is evaluated

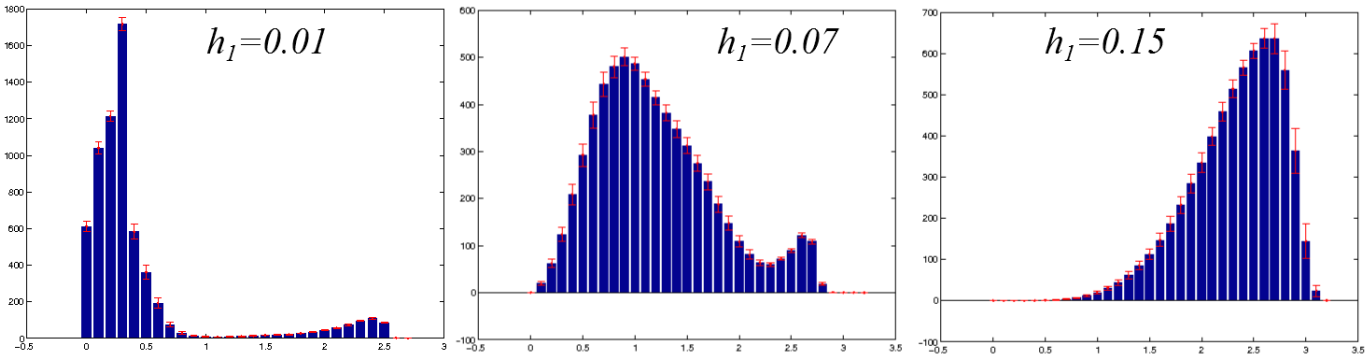

Figure 4.1.2: Statistics for the logIPR's of all eigenstates of H for $h_2 = 0.7$ and different values of h_1. From left to right: at $h_1 = 0.01$ the large majority of the spectrum is localized, but some delocalized states are still present, despite the non-zero coupling to the localized subspace. For $h_1 = 0.07$ the two peaks are still visible, but they are much wider. Finally, for $h_1 = 0.15$ the spectrum is almost entirely delocalized. Averages are taken over 500 realizations of the disorder.

numerically, and averaged over the whole spectrum. For $h_2 = 0.7$, one finds $r = 0.64 \pm 0.05$, which is intermediate between $r_{\rm GUE} \simeq 0.60$ and $r_{\rm GSE} \simeq 0.67$. This discrepancy presumably arises due to the contributions from the more localized edges of the spectrum.

To characterize (de)localization one uses the logarithm of the inverse participation ratio,

$$\text{logIPR}(\psi) \equiv -\log_{10}\Big(\sum_{\eta} |\langle\psi|\eta\rangle|^4\Big), \tag{4.1.8}$$

where the sum over η runs over the classical particle configurations. Note that $\dim(\mathcal{H}_{\mathcal{S}}) = 648$, and thus $\text{logIPR}(\psi) \sim 2.5$ for a fully delocalized state ψ, while $\text{logIPR}(\psi) \ll 1$ for a localized state. From the point of view of the parameter r, $h_2 = 0.7$ is rather optimal: the spectrum is mostly delocalized, but the Hamiltonian is still genuinely GSE. Indeed, when h_2 becomes significantly larger than 0.7, the localized tails of the spectrum are further suppressed, but the value of r starts bending down as an effect of approaching the integrable limit $h_2 \to \infty$.

Let us now fix $h_2 = 0.7$, but vary $h_1 > 0$, and determine numerically the statistics for the logIPR's of the eigenstates ψ of H. The results are shown in Fig. 4.1.2. One can clearly see that, even for non vanishing h_2, delocalized states are still present, as shown by the left and middle panel. In particular, for $h_1 = 0.07$ (middle) one can see delocalized states (inside the subspace $\mathcal{H}_{\mathcal{S}}$) coexisting with a majority of localized states. Obviously a relatively large h_1 leads to delocalization of almost all states, with logIPR's that start approaching the value $\log_{10}[\dim(\mathcal{H}) = 6480] \sim 3.5$ of fully delocalized wavefunctions, cf. the right panel. A comparison of histograms at the same values of h_1, but with $h_2 = 0$ (not shown) revealed that the histograms are significantly shifted to larger logIPR in the presence of the delocalized channel of mobile pairs.

4.2 Delocalization by rare ergodic regions in many-body systems

The argument of Basko et al. [23] for a localization transition as a function of temperature, i.e., a many-body mobility edge, builds on the idea that conduction can set in only if the energy density exceeds a critical level essentially everywhere in the sample. This neglects the possibility that rare *local* fluctuations away from the average energy density could lead to a breakdown of perturbation theory and induce delocalization. Indeed, I argue that delocalization occurs as soon as finite, but mobile excitations exist, even if they are very rare. These constitute the analogues of the diffusive pairs above. Examples of such excitations are large, albeit finite regions which are hotter than their environment and thus internally ergodic. It is important to stress that the bubble excitations considered here are thermal, and not tied to local, anomalous realizations of the disorder. Here the strategy of Ref. [24] to show the existence of an MBL phase, as shown in Subsec. 2.3.1, would fail. Indeed, it requires that the location of all possible resonant spots can be determined *independently* of the state of the system. Hereby I assume that interactions are local, so that the internal ergodicity is only a function of the energy contained in that region.

Let us assume that at some temperature there are conduction and ergodicity. I believe that, in the thermodynamic limit, the presence of finite conduction implies ergodicity, too. This follows by disregarding the exotic scenario of non-ergodic, but delocalized many-body systems, where transport is confined to a fractal support in real space. Indeed, in large enough systems, delocalized modes supported on a finite fraction of space will serve as a bath, which is expected to thermalize any finite set of degrees of freedom in finite times. In typical states and in any given place such ergodic regions occur with finite probability as spontaneous fluctuations of energy density, without being tied to a particular disorder realization. Thus, there exists a (possibly very low) finite density of ergodic spots. Below it will be argued that these excitations are mobile and delocalize the whole system, akin to the diffusing pairs above. From this reasoning it follows that finite conduction at some temperature implies finite conduction at any temperature in thermodynamic systems with local interactions. As a consequence, systems in the continuum should exhibit finite transport at any $T > 0$, as they always possess ergodic states at high enough energy (see also the discussion in Ref. [109]).

To argue for the mobility of the hot bubble excitations one proceeds in two steps: first it is shown that there exists a resonant, delocalized subset of bubble configurations. In a second step I argue that delocalization remains robust when processes are taken into account that lead away from the resonant subgraph. Since the argument is quite lengthy, I shall first describe heuristically its main points. A detailed and formal presentation will be provided later on.

I consider a quantum lattice system with local interactions and a bounded energy density, possessing a putative many-body mobility edge at energy density ϵ_c, such that states below (above) ϵ_c are localized (ergodic). For simplicity, the model is assumed to be one-dimensional. Now consider

a rare hot bubble of a super-critical energy density at some $\epsilon_2 > \epsilon_c$, surrounded by "cold" regions of energy density $\epsilon_1 < \epsilon_c$. If this energy fluctuation is large enough (much larger than a correlation length $\xi(\epsilon_2)$) and decoupled from its surrounding, it is internally ergodic by assumption.

I argue that this state can hybridize with a translate of the bubble by some length $\ell_0 > \max[\xi(\epsilon_1), \xi(\epsilon_2)]$ when the coupling between the hot region and its surrounding is switched on. It suffices to show that extending (or shortening) the hot region by a length ℓ_0 (by heating up or cooling down the relevant region) can occur as a resonant transition. For the latter it suffices to show that changing the energy in the boundary region by a finite amount is a resonant process. Let $H_1 = gO_h \otimes O_c$ be the interaction term coupling a hot (h) and a cold (c) region of size ℓ_0 across their common boundary. Let Ψ, Ψ' be eigenstates in the hot region and η, η' eigenstates in the cold region. For any hot eigenstate Ψ in a sufficiently large bubble one can find (many) Ψ' such that

$$\frac{|\langle \Psi\eta | H_1 | \Psi'\eta' \rangle|}{|E_\eta + E_\Psi - E_{\eta'} - E_{\Psi'}|} \gg 1, \tag{4.2.1}$$

because on the one hand, by ETH $|\langle \Psi | O_h | \Psi' \rangle| \sim d_h^{-\frac{1}{2}}$, where d_h is the dimension of an appropriate micro-canonical ensemble for the hot bubble at the energy density set by Ψ, while the matrix element $|\langle \eta | O_c | \eta' \rangle| \sim O(1)$ is finite and independent of d_h. On the other hand, one can pick Ψ' such that $|E(\eta) - E(\eta') + E(\Psi) - E(\Psi')| \leq Y/d_h$, where Y is the energy width of the ensemble. The ratio in Eq. (4.2.1) thus scales as $\sim d_h^{1/2}$ and grows exponentially with the length of the bubble. It may thus become much larger than unity, indicating a resonant process. This is not surprising: it merely expresses that a sufficiently large ergodic bubble acts as a bath for small systems coupled to it. It follows that configurations with hot bubbles in different positions hybridize with each other.

This way, bubbles are capable of transporting energy or any other conserved quantity at any distance in the system. Additionally, bubbles modify the environment they pass through, since in general $\eta' \neq \eta$ in Eq. (4.2.1) above: it follows that, given enough time, any part of the system can explore all its possible configurations, and therefore gets thermalized. Ergodicity is thus restored everywhere in the system.

4.2.1 Formal presentation of the argument for delocalization

Now let us be more precise. I consider a quantum lattice model with local interactions, having a putative many-body mobility edge. For concreteness, the model is assumed to be one-dimensional, and the states below energy density ϵ_c are assumed to be (putatively) localized, whereas those above ϵ_c are ergodic. The energy density of the bottom of the spectrum is chosen as a reference and set to zero. A maximal energy density $\epsilon_m > \epsilon_c$ is also imposed, reflecting the fact that the Hilbert space is locally finite.

For this argument it is important to have states at disposal that are clearly ergodic or localized in

a given finite volume and therefore I introduce, somewhat arbitrarily, a window of energy densities $\epsilon_{c1} < \epsilon_c < \epsilon_{c2}$ that are too close to critical to be clearly enough of localized or delocalized nature, respectively. Let $\ell(\epsilon)$ be the localization length, diverging as $\epsilon \nearrow \epsilon_c$. Lengths are expressed in units of the lattice spacing a, and energy densities ϵ as energy per site. I will now coarse-grain the model and group ℓ_0 adjacent sites into "units". The length ℓ_0 is chosen such that it is both larger than the localization length $\ell(\epsilon_{c1})$, and large enough so that the interaction energy between two neighboring units is small compared to $\ell_0\epsilon_{c1}$, the maximal energy in a localized unit. The second constraint ensures that the interaction of a low energy unit ($\epsilon < \epsilon_{c1}$) with its surroundings does not trivially suffice to render the unit ergodic, and, similarly, that the interaction of a high-energy unit with its surroundings does not trivially suffice to localize that unit. This will be satisfied by the choice of a large enough ℓ_0, since the interactions are local.

The coarse-graining into units provides a useful starting point, from which to proceed with perturbation theory. Within each unit, the eigenstates are classified in three kinds, cold (below ϵ_{c_1}), hot (above ϵ_{c2}) or intermediate (between ϵ_{c1} and ϵ_{c2}). If one considers the Hamiltonian without the interaction between units, then obviously the eigenstates are products of unit eigenstates. Let us focus on eigenstates at very low energy density $\epsilon \ll \epsilon_{c1}$. Then, typically, non-cold units appear only with a density ν that tends to 0 as $\epsilon/\epsilon_{c1} \to 0$. Chains of labeled units such as *ccciccchhhiiccc* now serve as "mesostates", with $c/i/h$ standing for cold/intermediate/hot. The model can now be rewritten as

$$H = H_0 + H_1, \tag{4.2.2}$$

where

$$H_0 \equiv \sum_x H_0(x), \quad H_1 \equiv \sum_x H_1(x, x+1). \tag{4.2.3}$$

In the above, x label the units, $H_0(x)$ acts on the Hilbert space $\mathcal{H}(x)$ at unit x only, and H_1 describes the coupling between neighboring units. Mesostates are eigenstates of the term H_0. One now considers switching on the coupling terms and evaluate their effect on the unperturbed eigenstates of H_0. This procedure is similar to the one followed in Subsec. 2.3.1. First I add the interaction terms between cold units (see below for what is meant precisely). Since it was assumed that $\ell(\epsilon_{c1}) < \ell_0$, this will not have much effect on the localized eigenstates, which thus remain close to products. Note that by doing this, from the point of view of a typical state at energy density ϵ, one has already added most of the interaction terms. What remains is a small fraction $\sim 2\nu$ (which is controlled by the overall energy density) of all interaction terms. The interaction terms between hot units are now added. By assumption, sufficiently long stretches of such units $\ldots hhhh \ldots$ (which I call *"bubbles"*) are ergodic and I will assume that the resulting hot eigenstates in those bubbles satisfy ETH. The situation at this moment is hence that the Hilbert space has been partitioned into a big direct sum, and the Hamiltonian H_0 is block diagonal, with the blocks labeled by mesostates. Let P_x^r be the projector that restricts the value of $H_0(x)$ so that unit x is

of type $r = h, i, c$. With this notation the interaction terms that have already been added are

$$P_x^{r'_x} P_{x+1}^{r'_{x+1}} H_1(x, x+1) P_x^{r_x} P_{x+1}^{r_{x+1}}, \tag{4.2.4}$$

for $(r_x, r_{x+1}) = (r'_x, r'_{x+1}) = (c, c)$, and for $(r_x, r_{x+1}) = (r'_x, r'_{x+1}) = (h, h)$. Some terms are obviously very small (because the interaction is local in energy) and seem irrelevant, namely those corresponding to, $(r_x, r_{x+1}) = (c, c), (r'_x, r'_{x+1}) = (h, h)$ and with primes and no primes reversed. The main terms that I will be focusing from now on are those that allow bubbles to spread and move. Those are terms with

$$r_x = r'_x = h, \qquad \text{and arbitrary } r_{x+1}, r'_{x+1}, \tag{4.2.5}$$

and with x and $x+1$ reversed. They will be the focus of the following Subsection.

4.2.1.1 Resonant delocalization of bubbles

Let us now consider states of the following form (bubble in a cold environment):

$$cccccccc\underbrace{hh\ldots hh}_{n \text{ units}}cccccccc, \tag{4.2.6}$$

where n is sufficiently large so that the eigenstates in the bubble satisfy ETH. I now argue that this state hybridizes with translates of the bubble when some of the missing coupling terms are added. In particular, one wants to admix the mesostates (with x, y labeling units)

$$\ldots \underset{x}{cc}chhhh\underset{y}{ccc}\ldots \leftrightarrow \ldots \underset{x}{cccc}hhhh\underset{y}{cc}\ldots \tag{4.2.7}$$

in which the bubble has been translated by one unit. More precisely, I mean that most microstates (i.e., eigenstates of the Hamiltonian considered up to now) corresponding to the left mesostate can hybridize with a lot of microstates corresponding to the right mesostate. This in turn strongly suggests that one should expect all eigenstates to delocalize completely over these two mesostates. To obtain this, I have included the relevant coupling terms, of the form of Eq. (4.2.4), corresponding to two bonds $(x, x+1)$ and $(y-1, y)$. This hybridization process can be broken down into elementary steps, that is, transitions at first order of perturbation theory. First, by energy exchange with the hot region, the cold (c) unit at y is heated until it becomes intermediate (i) and finally hot (h). Second, the h unit at x is cooled down until it becomes c, via intermediate stages of i. Microscopically, let us consider a state Φ corresponding to the mesostate *ccchhhhccc* and such that $H_0(y)$ is not far below ϵ_{c1}. I will argue that Φ hybridizes with a lot of states Φ' corresponding to the mesostate *ccchhhhicc* where $r'(y) = i$. If instead $H_0(y)$ is far below ϵ_{c1}, then it hybridizes with a lot of states Ψ' which still corresponds to $r'(y) = c$ (*ccchhhhccc*), but now with $H_0(y)$ a

bit closer to ϵ_{c1}. (A direct step to an intermediate state might instead require adding too much energy in one transition. Therefore the process are split into several small heating steps to make sure the argument remains valid also if the interactions are assumed to be strictly local in energy.) Finally, I need to increase the energy stepwise from i to h at unit y. The argument for all these transitions is essentially the same and for the sake of simplicity, I stick to $r(y) = r'(y) = c$. The next subsection shows the flexibility of the argument.

Obviously, it suffices to take eigenstates in Φ, Φ' in the region $[x, y]$ because of the essential product structure (exact at the left edge, approximate at the right edge around y, because the coupling between cold regions has already been included). They are of the form

$$\Phi = \Psi \otimes \eta, \qquad \Phi' = \Psi' \otimes \eta', \tag{4.2.8}$$

where η, η' are the unperturbed eigenstates at unit y, while Ψ, Ψ' are hot bubble states in the region $[x, y-1]$ consisting of $n = y - x$ units. Consider Ψ' such that its energy (evaluated with H_0) is within a range $W \sim \epsilon_m$ of the energy of Ψ. The space spanned by such states has dimension $d_h \approx \exp[s\ell_0 n]$ which grows exponentially in n, s being the corresponding entropy density. Write $H_1(y-1, y) = gO_h \otimes O_c$, the first factor acting on $y-1$, the second on y. From ETH it then follows that

$$|\langle \Psi | O_h | \Psi' \rangle| \sim 1/\sqrt{d_h}. \tag{4.2.9}$$

In other words, the (non-eigenstate) vector $O_h |\Psi\rangle$ is essentially a random amplitude superposition of eigenstates Ψ'. If one now takes $\Delta E \equiv E_\eta - E_{\eta'}$ sufficiently small, i.e. not exceeding Y, then $\langle \eta | O_c | \eta' \rangle \sim 1$. In fact, assuring the non-vanishing of $\langle \eta | O_c | \eta' \rangle$ is the main reason to choose Y sufficiently small. One can then find many Ψ' (in fact, $\sim \sqrt{d_h}$ of them) such that

$$\frac{|\langle \Psi\eta | H_1 | \Psi'\eta' \rangle|}{|\Delta E + E_\Psi - E_{\Psi'}|} \gg 1, \tag{4.2.10}$$

because the energy spacings are of order Y/d_h and $\langle \Psi\eta | H_1 | \Psi'\eta' \rangle \sim g/\sqrt{d_h}$. Hence the ratio in Eq. (4.2.1) is huge since d_h grows exponentially in n.

The outcome of the above calculation should not come as a surprise: it merely expresses that an ergodic bubble can act as a bath for a small system (here unit y) that is coupled to it. Upon repeating the same calculation a few times, one easily convinces oneself that states with the bubble in different positions hybridize with each other.

4.2.1.2 Spatial range of direct hybridizations

In the above derivation, I focused on hybridizations that result in the translation of a bubble by one unit. One might worry that this is too negligible a translation if the bubble is very large, $n \gg 1$. However, here I show that direct hybridizations can take place at distances which are a

finite fraction of the bubble length.

As already pointed out, in the above derivation, I was careful to pick states η, η' whose energy difference was small enough so that $\langle\eta| O_c |\eta'\rangle \sim 1$. This is, however, not crucial, and if $r'(y) = i, h$ it can not be assured anyhow. The matrix element $\langle\eta| O_c |\eta'\rangle$ will typically decay exponentially in the energy difference $E_\eta - E_{\eta'}$. Hence, it can be as small as $e^{-\ell_0 \epsilon_m}$, but obviously this number decreases with ℓ_0, not with n, so this is not relevant for our argument. To determine at what distance direct hybridizations are possible, I proceed as follows. Instead of making the transition $\eta \to \eta'$ at unit y, I now make a transition $\underline{\eta} \to \underline{\eta'}$ in a stretch of ℓ units starting at y. By the structure of localized states, it is known that

$$\left|\langle\underline{\eta}| O_c |\underline{\eta'}\rangle\right| \sim (g/\epsilon_m)^{\ell\ell_0}. \tag{4.2.11}$$

The transition is possible as long as this small number is larger than $\sqrt{1/d_h}$, so that one finds

$$\ell \sim \frac{s}{2\log(\epsilon_m/g)} n. \tag{4.2.12}$$

This shows us that the bubble hybridizes with translates by a finite fraction of its size. However, this fraction becomes parametrically small as the coupling becomes weak, $g/\epsilon_m \to 0$.

4.2.2 Discussion of potential caveats

One may now ask whether some processes that have not been taken into account in the previous analysis could impede the hybridization of bubbles. The first objection that can be raised is that hot bubbles should not survive dynamically, but should rather spread, dilute their energy and eventually localize, so that they could not evolve back to their original hot configuration. Though such a spreading is indeed entropically favored in real time dynamics, that argument is fallacious. At a fundamental level, Hamiltonian dynamics is micro-reversible. If a given transition is possible, then its reverse is as well. By invariance of the Gibbs ensemble, one can definitely rule out that initially present bubbles typically completely disappear with time for most initial configurations. Looking at it from a different perspective, there are eigenstates that have a significant overlap with bubble configurations and they assure that there is a finite, albeit small, probability per unit volume to observe bubbles at all times.

Though I show that entropic effects alone do not suffice to make bubbles disappear, it still remains to check that their mobility is not suppressed when all the diluted states of a bubble are taken into account, as a result of quantum mechanical effects. This is done in the following Subsections, which show that the delocalization of bubbles is robust against the coupling to states in which their energy is dissolved in their surrounding. This way a resonant subgraph is constructed, and it is assumed that this essentially implies delocalization. While I believe that in the present context this conclusion is correct, the reader needs to be cautioned nevertheless that this condition

is not always sufficient, like in single-particle localization in weak disorder in low dimension, or in hopping problems without potential disorder on structurally disordered lattices close to classical percolation. However, in these cases localization is restored by specific mechanisms, which are not present in our many-body case: the proliferating amplitude of return to the origin in $d \leq 2$ [14], and the generation of random self-energies from the structural disorder along barely percolating paths [110, 111]. Non-ergodic behavior is also known to occur in many-body systems due to orthogonality catastrophes, like in spin-boson systems at $T = 0$ and related spin problems at finite T [112], but such scenarios seem not to apply in our case. Finally, rare regions with anomalously strong disorder, which render transport in $d = 1$ subdiffusive [113], do not prevent delocalization by bubbles either, as I shall explain below.

4.2.2.1 Robustness of hybridizations

I have not yet added all coupling terms from H_1. In particular, I have neglected transitions of the form

$$\begin{array}{ccc} ccchhhhccc & \leftrightarrow & cccchhhhcc \\ \updownarrow & & \updownarrow \\ \ldots \leftrightarrow \ldots cciiiiiiiicc & & cccciiiiiic \ldots \leftrightarrow \ldots, \end{array} \quad , \tag{4.2.13}$$

where the states on the lower line represent a multitude of mesostates. Let us assume that they themselves do not communicate with each other. This simplifying assumption favors maximally the possibility that the coupling to such states could localize the bubble and thus invalidate the preliminary conclusion above. I now consider the two subspaces, each of dimension d_h, that correspond to the mesostates on the upper line, the eigenstates of which are hybridized by the perturbation H_1. Let us refer to them as left and right subspaces. I then couple each of them to a space of dimension $d'_h \gg d_h$ and ask whether the perturbation H_1 is still able to induce hybridization between left and right subspaces. Concretely, the subspace $\mathbb{C}^{d_h}$ is now embedded in the space $\mathbb{C}^{d_h} \oplus \mathbb{C}^{d'_h}$ of dimension $D_h \equiv d'_h + d_h$, and O_h becomes $O_h \oplus 0$. I focus on the transitions between the ergodic states Ψ, Ψ', and just consider the operator O_h which acts on the hot bubble. Let us assume that after diagonalizing within the larger spaces of dimension D_h, the eigenstates $\widetilde{\Psi}, \widetilde{\Psi}'$ are completely ergodic and well captured by random matrix theory. In practice, this defines the relevant space to which the bubble subspace should be extended, and its dimension D_h. One now has to discuss how the ratio

$$\frac{\left|\left\langle \widetilde{\Psi} \right| O_h \left| \widetilde{\Psi}' \right\rangle\right|}{\left|\Delta E + E_{\widetilde{\Psi}} - E_{\widetilde{\Psi}'}\right|} \tag{4.2.14}$$

differs from the original ratio

$$\frac{\left|\langle \Psi | O_h | \Psi' \rangle\right|}{\left|\Delta E + E_{\Psi} - E_{\Psi'}\right|} \sim \frac{\sqrt{d_h}}{W} \tag{4.2.15}$$

with given $|\Delta E| \leq Y$. One finds a suppression of the numerator because now

$$\left|\left\langle \widetilde{\Psi}\right| O_h \left|\widetilde{\Psi}'\right\rangle\right| \sim \frac{\sqrt{d_h}}{D_h}. \tag{4.2.16}$$

Indeed, the simplest way to derive this is by remarking that

$$\sum_{\widetilde{\Psi},\widetilde{\Psi}'} \left|\left\langle \widetilde{\Psi}\right| O_h \left|\widetilde{\Psi}'\right\rangle\right|^2 = \mathrm{Tr}(O_h^\dagger O_h) \sim d_h, \tag{4.2.17}$$

as O_h acts only in the original subspace (with dimension d_h) and it is zero on the attached space with dimension d'_h. On the other hand, the energy spacing $|\Delta E + E_\Psi - E_{\Psi'}|$ can now be made as small as $\widetilde{Y}/D_h$, where $\widetilde{Y}$ is the width in energy of all states that significantly couple to the original bubble states. It follows that the ratio of Eq. (4.2.1) is reduced by a factor $Y/\widetilde{Y}$. If this effect rendered the ratio of Eq. (4.2.1) smaller than 1, the eigenstates would likely not hybridize across the subspaces, i.e. one would find *localization induced by coupling to further degrees of freedom*. However, the maximal conceivable value of $\widetilde{Y}$ is of order $\epsilon_m \ell_h$, with ℓ_h the length of the region to which the energy spreads. Energy conservation and localization below ϵ_c lead to the upper bound $\ell_h(\epsilon_c - \epsilon) \leq n(\epsilon_m - \epsilon)$ (recall that $\epsilon < \epsilon_c$ is the typical energy density in our system). This yields $\widetilde{Y}/Y \lesssim n$, which is insufficient for localization, since the ratio in Eq. (4.2.1) is exponentially large in n. Thus, the hybridization of bubble states survives, despite their spreading to entropically more favorable states. This contrasts with particle problems where the coupling to extra degrees of freedom was found to induce localization under certain circumstances [114, 115]. In those cases, there is no exponentially large factor that offsets the effect of an increased bandwidth $\widetilde{Y}$, which renders coupling-induced localization possible.

4.2.2.2 Dynamic retardation

Even though the inclusion of the states on the lower line of Eq. (4.2.13) cannot prevent hybridization, it does of course increase the *timescale* necessary for transitions between the two bubble positions. The transition rates can be estimated from a simple Fermi Golden Rule calculation as

$$\tau_{\mathrm{bef}}^{-1} \sim \frac{|\langle \Psi\eta|\, H_1\, |\Psi'\eta'\rangle|^2}{|\Delta E + E_\Psi - E_{\Psi'}|}, \tau_{\mathrm{aft}}^{-1} \sim \frac{\left|\left\langle \widetilde{\Psi}\eta\right| H_1 \left|\widetilde{\Psi}'\eta'\right\rangle\right|^2}{\left|\Delta E + E_{\widetilde{\Psi}'} - E_{\widetilde{\Psi}}\right|}, \tag{4.2.18}$$

before and after including the extra states, respectively. The first rate is of order g^2/Y, while the second is of order $(d_h/D_h)g^2/\widetilde{Y}$. Hence, by adding the new states, one has increased the timescale by order D_h/d_h (keeping only terms exponential in n). This is very intuitive: transitions are now only possible from a fraction d_h/D_h of all states, and accordingly it takes longer until a transition will be attempted. Alternatively, one can view this as follows: for a large bubble close to criticality (with structure *cciiiiiiiiicc*) the "active" configurations of the type *cccchhhhcccc*

manifest themselves as large deviations, which occur with exponential rarity. Yet, as shown above, they do lead to hybridization of eigenstates, and hence to delocalization.

4.2.2.3 Harmlessness of rare, strongly disordered regions

So far I have tacitly assumed that the existence of a global thermal phase at some energy density implies that any large enough finite region has ergodic states at that energy density. However, due to rare fluctuations of the disorder, it can happen that rare, large regions still have all their states localized as long as they are disconnected from the rest of the system. One may think that especially in $d = 1$ such regions could block global transport and thus localize the system at low temperature. Even though this effect further increases the time scale necessary for thermalization, it can be argued that it does not prevent it.

As a preliminary, I consider a fully localized system of length L_0 in contact with an ergodic system of length L_1. By an analogous argument as used above for resonant delocalization, one sees that for L_0/L_1 smaller than some number (depending on the localization length and the entropy density of the ergodic system, see e.g. Eq. (4.2.12)), the coupled system will be ergodic: all formerly localized states can hybridize with each other.

Now to the main argument. Let us consider ergodic bubbles of some large size ℓ and let $\delta \equiv \delta(\ell)$ be the typical distance between rare regions of exceptional disorder that could block such bubbles, by not allowing an adjacent bubble to heat up this region to ergodic states (of type h), and thus hampering the translation of the bubble. By the above preliminary remark, such blocking regions have a length $\sim \ell$ and since they are rare regions (large deviations), the typical distance between them is $\delta(\ell) \sim e^{c\ell}$ for some $c > 0$. Now consider a bubble between two blocking regions. Its presence renders the *whole region* between them ergodic. Hence, the blocking regions are in fact next to an ergodic bath of length $\delta(\ell)$, which is exponentially large in ℓ. Accordingly, its level spacing is double-exponentially small. Thus, tunneling under the barrier of thickness $\sim \ell$, which is only exponentially small in ℓ, will easily hybridize the ergodic regions on either side and ensure transport.

4.2.2.4 Bubbles and weak localization in low dimensions

As explained in Subsec. 2.2.2, in dimension $d \leq 2$, non-interacting particles are weakly localized by any non-vanishing disorder strength. Since bubbles resemble a particle-like excitation, one should discuss whether they undergo a similar weak localization in low dimensions.

Indeed, at zero temperature, the answer is expected to be positive. However, since I consider a finite energy density, it would be incorrect to picture the bubble as moving in a low-dimensional fixed disorder potential. As the bubble moves, it can excite or relax degrees of freedom. Thus the Hilbert space locally resembles a tree, rather than a low-dimensional lattice (the number of relevant configurations that can be reached as the bubble moves grows exponentially, rather

than polynomially with the traveled distance), and thus weak localization effects should become irrelevant.

More concretely, let ℓ be the localization length of the bubble motion at zero temperature, i.e. in the ground state (fixed environment). Obviously, ℓ increases with the bubble size since larger bubbles have more internal states (cfr. the increase of single particle localization length with the number of channels in $d = 1$ [14]); for large bubbles ℓ will be due to weak-localization effects. Now consider finite energy density, and $d = 1$ for simplicity. Let $s > 0$ be the entropy density in the cold background. Then the condition $s\ell \gg 1$ is sufficient to ensure that inelastic scatterings of the bubble occur before the weak localization manifests itself, rendering them irrelevant for large enough bubbles. Note, however, that this condition places an additional lower bound on the size of mobile bubbles in low dimensions.

4.3 Lack of ergodicity in small weakly disordered 1d interacting systems

The theoretical arguments explained in this Chapter contradict recent numerical data in favor of mobility edges [44, 45, 46, 47]. The inconsistency is, however, only apparent. Indeed, one finds that numerically accessible system sizes are not sufficiently large to host bubbles that are ergodic enough to be mobile. Therefore, delocalization by bubbles could not have been seen in numerics up to now. In other words, the numerical results do not contradict delocalization by rare bubbles, but rather confirm that available sizes are not large enough. To show this fact, the disordered Ising chain with next-to-nearest neighbor interaction considered in Ref. [44] is studied,

$$H = -\sum_{i=1}^{L} \left[(J + \delta J_i)\, \sigma_i^z \sigma_{i+1}^z + J_2 \sigma_i^z \sigma_{i+2}^z + h_z \sigma_i^z + h_x \sigma_i^x \right], \tag{4.3.1}$$

where $\delta J_i \in \left[-\frac{\delta J}{2}, \frac{\delta J}{2}\right]$ are independent random variables, and periodic boundary conditions are taken. Parameters $J = 1$, $J_2 = 0.3$ and $h_x = 0.6$ are chosen as in Ref. [44], but a finite $h_z = 0.1$ is added to remove the Ising symmetry and the associated degeneracies. The phase diagram in Ref. [44] predicts a mobility edge in the thermodynamic limit at disorder strength $\delta J = 3$. To test the ideas of this Chapter, I prepare the system at $\delta J = 3$ in a product state of the form $|\psi(0)\rangle_L = |\phi_c\rangle_{L_c} \otimes |\chi_h\rangle_{L-L_c}$, where $|\phi_c\rangle$ is the ground state of an interval of L_c sites, while $|\chi_h\rangle$ is an eigenstate of the complement close to the middle of the spectrum, which represents a hot bubble. I choose $L - L_c$ as large as possible but such that the resulting global energy density is below the putative mobility edge. I then compute the time-evolving energy density on link $(i, i+1)$,

$$\varepsilon_i(t) \equiv -(J + \delta J_i) \langle \psi(t) | \sigma_i^z \sigma_{i+1}^z | \psi(t) \rangle . \tag{4.3.2}$$

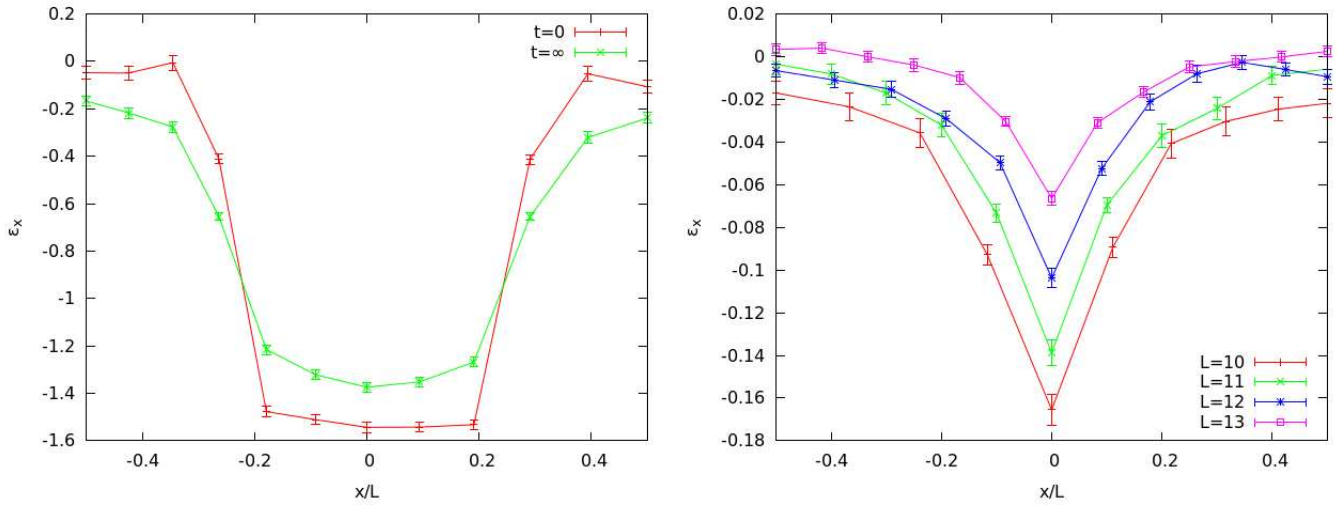

Figure 4.3.1: *Left:* Disorder averaged energy per link ε_i at $t = 0$ (red) and averaged over time (green) for $L = 12$. Initially a cold region of length $L_c = L/2$ is prepared. The disorder strength is $\delta J = 3J$. *Right:* Same protocol, but for $\delta J = J$ and very short cold intervals ($L_c = 2$), at various L. The memory effects diminish with increasing L, but the hot region fails to thermalize the system well, even at the largest sizes. Results were averaged over 5000 disorder realizations.

The theory of mobile bubbles would predict that the $\varepsilon_i(t)$ profile becomes approximately flat as $t \to \infty$. Via exact diagonalization, its time average has been evaluated, but almost no energy spreading from the initial state is observed cf. Fig. 4.3.1 (left). One may wonder that this observation implies that hot bubbles are unable to spread, and thus that it falsifies the argument for delocalization, but this conclusion is wrong. Even for tiny cold regions ($L_c = 2$) and bubbles of almost the system size, still only a very small fraction of the bubble energy spreads to the cold region at $L = 12$ (not shown). However, since the global energy density is by far supercritical, in the thermodynamic limit the energy profile has to obviously thermalize and become flat. Therefore, this data shows unambiguously that at the available system sizes the hot region is still unable to act as a bath.

To document this further, I calculated the inverse participation ratio (IPR) of an eigenstate $|\alpha\rangle$ of the full system, acted upon by a local unitary operator such as σ_1^z, in a basis of eigenstates $|\beta\rangle$:

$$\mathrm{IPR}_\alpha \equiv \sum_\beta |\langle\beta| \sigma_1^z |\alpha\rangle|^4 . \tag{4.3.3}$$

At strong disorder, eigenstates are nearly eigenstates of σ_i^z as well, and thus $\mathrm{IPR}_\alpha \approx O(1)$, whereas deep in the delocalized phase, one expects eigenstate thermalization and behavior akin to random matrix theory, $|\langle\beta| \sigma_1^z |\alpha\rangle| \propto \exp[-sL/2]$, leading to a typical value $\mathrm{IPR}_\alpha \sim \exp[-sL]$, with a narrow distribution. The results shown in Fig. 4.3.2 confirm the absence of a truly ergodic phase at $L = 12$ and $\delta J = 3$, in accordance with results of [44]. In fact, the distribution of IPR's at these parameters looks more characteristic of localization. Nevertheless a slight, but clear tendency

towards enhanced delocalization with increasing size is seen. This hints that in the thermodynamic limit the system will become ergodic, in agreement with the finite size extrapolations in [44].

To chart the lack of ergodicity at small sizes, I also look at $\delta J = 1$, where Ref. [44] suggests that most eigenstates are delocalized, even at $L = 12$. Nevertheless, here, too, strong deviations from fully ergodic behavior are found, using the same two protocols as above. Even in the extreme case of $L_c = 2$ in Fig. 4.3.1 (right), despite some energy transfer, the hot and cold regions are still clearly distinguishable. This behavior can not obviously take place in the thermodynamic limit: this shows that the reachable system sizes are too far from the thermodynamic limit to allow for a trustworthy extrapolation. To quantify this effect, I consider the time average of the energy imbalance between hot and cold regions, $\Delta\varepsilon \equiv (L-3)^{-1}\sum_{i\notin\{c,c\pm1\}}(\varepsilon_i - \varepsilon_c)$, where c denotes the single link fully in the cold region. The imbalance decays exponentially with system size, $\Delta\varepsilon \sim \exp(-L/\xi)$ where ξ increases with disorder strength, as shown in Fig. 4.3.3. For $\delta J/J$ in the range $[1, 1.5]$ I estimate $\xi \approx O(10)$, which sets a characteristic scale required to observe genuine ergodic behavior. This suggests strongly that at reachable sizes the hot bubble is far from being ergodic. Also Fig. 4.3.2 illustrates that $\delta J = 1, L = 12$ is far from the thermodynamic limit: the distribution of $\ln(\mathrm{IPR}_\alpha)$ is much wider (as compared to the mean) than in a clearly ergodic sample.

As a conclusion, the numerical analysis provided in this Section clearly shows that the available system sizes are too small for ETH to be safely applied. Therefore, they are outside the range of applicability of the bubble argument, which crucially relies on ETH, and no numerical data present in the literature at the moment can be used to disprove it.

4.4 Bubbles in quantum glasses

The bubble argument of Sec. 4.2 can be straightforwardly extended to the case of quantum glasses, by simply reversing the role of cold and hot regions, since in absence of quenched disorder localization is favored at high temperature. Indeed, this is the context in which the first version of the argument was formulated [39, 40]. In the thermodynamic limit, one can thus conclude that no real localization can be present in absence of disorder, since for any finite hopping t the lowest part of the spectrum is ergodic, and can thus be used to form a bubble. From the conceptual point of view, this strongly contrasts with disorder induced MBL, where a fully localized phase is truly present in the thermodynamic limit, at least in lattice models.

However, this difference gets blurred for systems which are relevant for the experimental point of view, because the bubble argument assumes both the system size and the time for which it is observed to be infinite. Of course, neither of these assumptions hold in realistic setups. From the numerical point of view, the limitations of the exact diagonalization methods have been pointed out in Sec. 4.3. For what regards experiments, it is very difficult to estimate how long it would take for an inhomogeneous initial condition to relax due to bubbles, since one has to take care

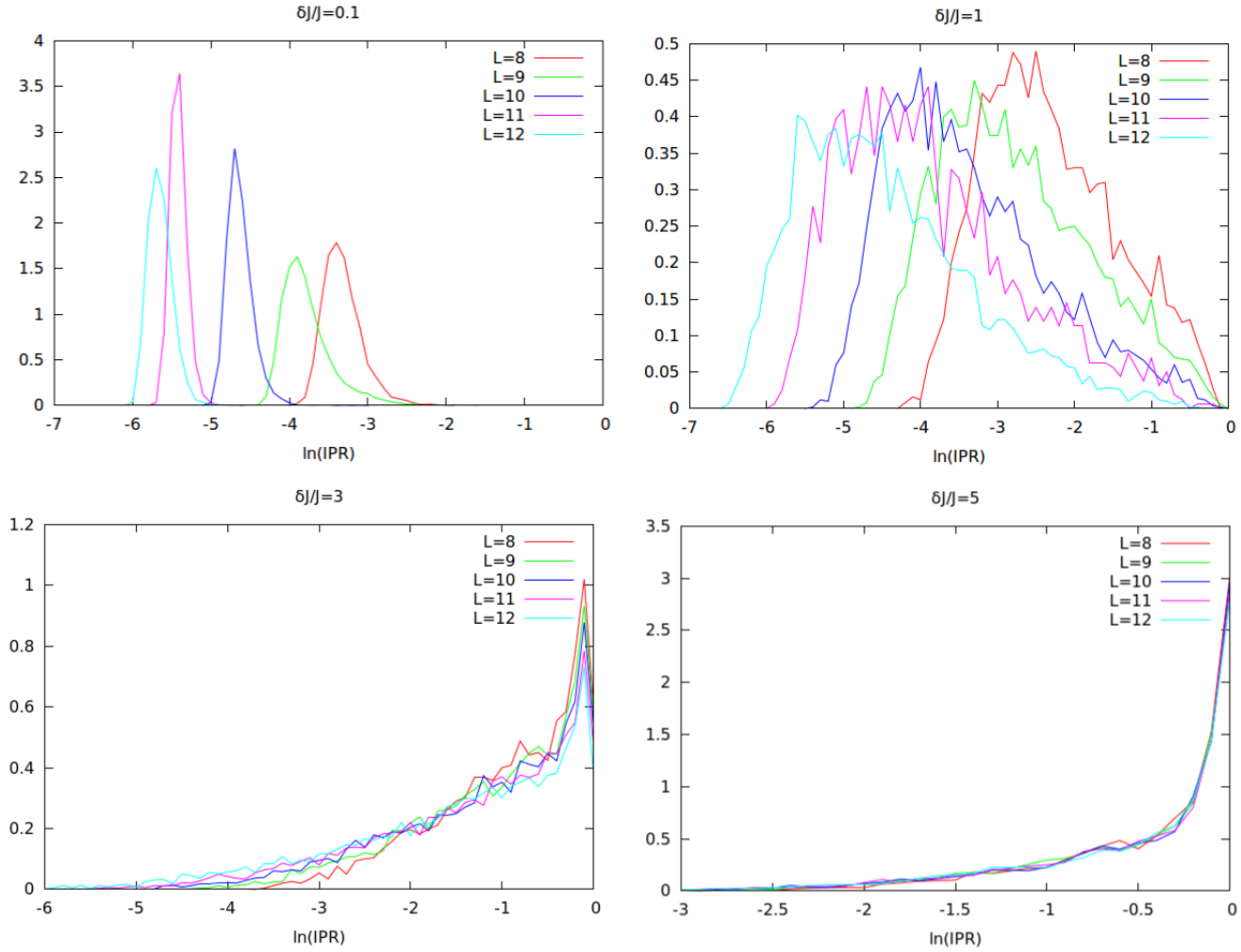

Figure 4.3.2: Distribution of ln(IPR) associated with matrix elements of σ_1^z evaluated on eigenstates randomly picked from the middle of the spectrum, for $\delta J/J = 0.1, 1, 3, 5$. In the ergodic phase, the typical IPR is exponentially small in the size L. In the localized phase, the distribution is size independent. At $\delta J = J$ and the considered L, the distribution is very wide as compared to the typical IPR: the plots at $\delta J = J$ and $\delta J = 0.1J$ are plotted with the same range on the horizontal axis, to better underline the difference. $\delta J = 3J$ is nearly critical: the 'localized' peak at IPR $= O(1)$ slowly decreases with increasing L.

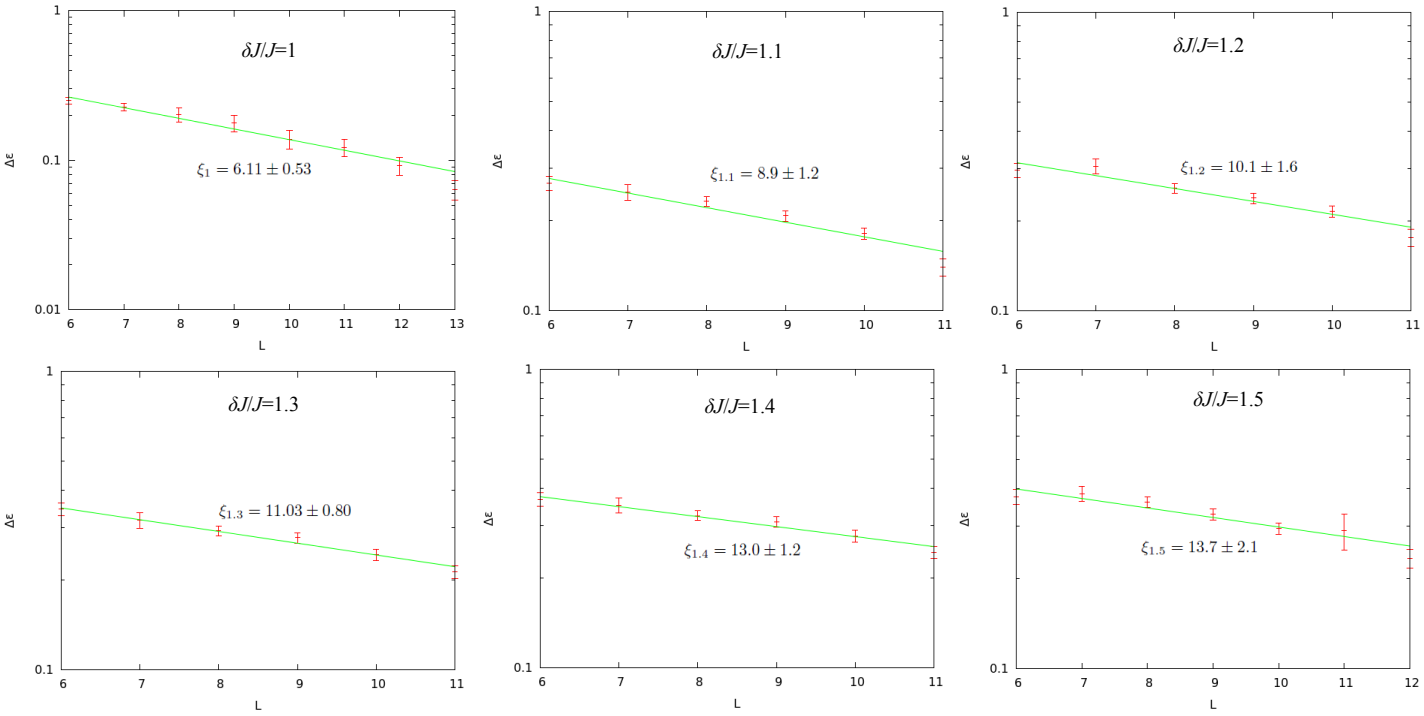

Figure 4.3.3: Energy imbalance $\Delta\varepsilon$ as a function of system size, for disorder strengths $J \leq \delta J \leq 1.5J$. The imbalance decays exponentially in system size, but is still non-negligible for the reachable values of L.

of all caveats explained in Sec. 4.2 to obtain a realistic estimation. However, it is rather easy to estimate the density of bubbles present in a random initial condition, and this calculation is shown here for the effective Hamiltonian (3.2.2).

Let us consider an initial random state which includes an ergodic bubble where the local energy density is below the critical threshold for bulk localization (see Fig. 3.4.1). The global density of particles ρ is assumed to be small, and t sufficiently smaller than the delocalization threshold $t_c(\rho)$, as estimated in Eq. (3.3.56) for states with roughly homogeneous density distributions. Recalling that the critical hopping scales as $t_c \propto \rho^{\beta}$, the density ρ_B in the ergodic bubble should be smaller than

$$\frac{\rho_B}{\rho} \lesssim \left(\frac{t}{t_c}\right)^{\frac{1}{\beta}}. \tag{4.4.1}$$

Denoting by L_B the number of sites in the bubble, the dimension of the Hilbert space $\mathcal{H}_B$ of internal states with $\rho_B L_B$ particles is

$$\dim(\mathcal{H}_B) = \binom{L_B}{\rho_B L_B} \approx \exp\left[\rho_B\left(1 - \ln\rho_B\right) L_B\right] \equiv \kappa^{L_B}, \qquad \rho_B \ll 1. \tag{4.4.2}$$

Since $\rho_B < \rho$ is assumed to be very small, κ is very close to 1, such that the phase space of such bubbles grows slowly with their size. Consequently, very large regions are necessary to obtain

small enough level spacings that might potentially induce delocalization of the bubble.

The minimal size L_B is estimated from the hybridization between an initial bubble state ψ_i and a final state ψ_f in which the bubble has moved by one site. Delocalization may potentially occur if the admixture of ψ_f to ψ_i is large in second order in perturbation theory, i.e., if

$$\sum_{\psi_B} \frac{\langle\psi_f| O |\psi_B\rangle \langle\psi_B| O |\psi_i\rangle}{(E_i - E_B)(E_i - E_f)} \gtrsim 1, \tag{4.4.3}$$

where $|\psi_B\rangle$ runs over the intermediate states, and $t \times O$ is the part of the hopping Hamiltonian that couples the bubble to the surrounding degrees of freedom. This is follows immediately from Eq. (4.2.1). Applying the estimates of Sec. (4.2), matrix elements with a generic local operator scale as

$$\langle\phi| O |\chi\rangle \sim \frac{1}{\sqrt{\dim(\mathcal{H}_B)}} \sim \kappa^{-\frac{L_B}{2}}, \tag{4.4.4}$$

where ϕ, χ label generic internal eigenstates, while the optimal energy difference scale as

$$\min_{\chi} |E_\chi - E_\phi| \sim \frac{U}{\dim(\mathcal{H}_B)} \sim U\kappa^{-L_B}. \tag{4.4.5}$$

Inserting these estimates into Eq. (4.4.3), a condition on L_B is obtained:

$$L_B \gtrsim \frac{\ln(U/t)}{\ln\kappa} = \frac{1}{\rho_B} \frac{\ln(U/t)}{\ln(1/\rho_B) + 1}. \tag{4.4.6}$$

Note that the required length diverges logarithmically in the limit $t \to 0$, implying that these bubbles are non-perturbative in nature. To make a concrete example, for $\rho = 0.1$ and $t = 0.01$ one finds $\rho_B \lesssim 0.01$ and $L_B \gtrsim 60$: of course, such a bubble length is by far impossible to reproduce in current numerics.

The density n_B of such large bubbles is given by the probability of finding only $\rho_B L_B$ particles in a region of length L_B, while the global density is ρ. For small ρ and t this is given by

$$n_B \approx \binom{L_B}{\rho_B L_B} \rho^{\rho_B L_B} (1-\rho)^{L_B(1-\rho_B)} \approx \exp\left[-L_B\left(\rho - \rho_B - \rho_B \ln\frac{\rho}{\rho_B}\right)\right]. \tag{4.4.7}$$

In the regime $t \ll t_c$ (and thus $\rho_B \ll \rho$) this can be approximated as $n_B \approx \exp(-\rho L_B)$. Using the bound on ρ_B from Eq. (3.3.56) we find an upper bound on the density of ergodic bubbles,

$$n_B \lesssim \exp(-\rho L_B) \lesssim \exp\left\{-2\left(\frac{t_c}{t}\right)^{\frac{1}{\beta}} \frac{\ln(U/t)}{\ln\left[\frac{1}{\rho}\left(\frac{t_c}{t}\right)^{\frac{1}{\beta}}\right] + 1}\right\}. \tag{4.4.8}$$

This is exponentially small and non-perturbative in the limit $t \to 0$. For the value considered

above, one finds $n_B \lesssim \times 10^{-3}$. This shows that, deep in the localized phase, such effects can be safely neglected for realistic system sizes, and the perturbative properties of quantum glasses shown in Chap. 3 can be seen in experiments.

If one needs to further increase the minimal size of bubbles, which is able to restore transport, one may resort to long range interactions. The argument of Sec. 4.2 assumed the interactions to have strictly finite range, but this assumption can be relaxed, taking e.g. a power law interaction $v(r) \propto r^{-\beta}$ (without the screening effect present in the effective model (3.2.2)). For $\beta > 2d$, d being the spatial dimension, a local energy density can be defined, and therefore one is still identify finite regions of space as hot and cold, and then proceed in the same way as with local interactions. This follows from the fact that the internal energy of a bubble grows with its volume L_B^d, while the interaction energy with the surrounding regions scales like its surface L_B^{d-1}. One can then conclude that, despite the presence of long range interactions, the energy density of a very large bubble can not be brought above the putative mobility edge by interactions with its environment, and that it can move through the system and act as a mobile bath. But the minimal required L_B will be much larger than the value estimated in Eq. (4.4.6). Still, in the presence of long range interactions quantum glasses will look localized up to much larger system sizes, even though in the thermodynamic limit they will allow for transport.

Finally, even though the situation looks rather unphysical, one may speculate about what happens with a really infinite range interaction, $\beta < 2d$. In this case, each component of the system interacts with all the others, the interaction energy is super-extensive, and it is not possible to define a local energy density. In this particular setup, the coarse-graining procedure of Sec. 4.2 becomes meaningless, and the concept of a "cold bubble" itself can not be defined. So, in this context, it is possible that a quantum glass would behave like a real MBL system, as postulated in a recent work [116]. A model of this kind would not have a well defined thermodynamic limit, however, so the analysis of its properties looks like a quite academic problem, without much interest for realistic situations.

Chapter 5

Discussion and conclusion

The main focus of this thesis consists in discussing the role played by disorder and temperature in the physics of localization. Disordered closed quantum systems are a very difficult subject to study, since one is restricted to rely on perturbative calculations in the thermodynamic limit and numerical simulations of very small systems. Combined with the fact that such systems often behave in a very counter-intuitive way, it is not surprising that our understanding of this subject is limited, and that it represents a very active matter of debate. In my work, I have analyzed some features of MBL systems, which were previously overlooked in the literature, and shown that they lead to highly non-trivial physical consequences.

While real MBL can happen only in the presence of disorder, I have shown that phenomena strikingly similar to it can take place even in translation invariant models, in the presence of strong interactions. I have found that these "quantum glasses", once prepared in an inhomogeneous initial condition, retain their inhomogeneity for exponentially long times. While local resonances induce fast relaxation processes, just like it happens in the presence of disorder, global homogenization requires much longer time scales to take place. This phenomenon, which can be observed in realistic experimental situations, was not previously noticed because it is a feature of the high temperature part of the spectrum only, while the lowest energy excitations above the ground state are always delocalized and ergodic. The presence of a delocalized part of the spectrum for any value of the parameters of the model is the reason for which, in the thermodynamic limit, ergodicity and transport are restored for quantum glasses, due to the very rare events that are not captured by perturbation theory. For realistic systems that can be realized in experiments, however, the probability of such events is so low that, for all practical purposes, the system will look localized, until its non-ergodicity is removed by the residual coupling to the environment.

In the presence of disorder, MBL is possible in lattice models, as long as *the whole spectrum* is localized. If perturbation theory predicts a putative mobility edge to be present instead, it can be shown that localization is unstable against large the inclusion of large but finite regions, where the energy density is higher than the critical value. Such regions, which I call "bubbles",

which are always present in the thermodynamic limit, can be argued to be able to move through the system and to restore transport and thermalization, under the only assumption that they internally satisfy ETH. Therefore, any system with a putative mobility edge behaves qualitatively like a quantum glass in the thermodynamic limit, in the sense that non-perturbatively slow transport and ergodicity are present. Interestingly, this implies that in the continuum no MBL is possible, and a "quantum glassy" behavior is expected even at very strong disorder. Finally, through a careful numerical study, I have found that systems studied numerically so far are too small to host bubbles which can be described in terms of ETH: therefore, the argument for delocalization by bubbles does not contrast with the numerical data present in the literature.

This work raises many interesting open questions, which still need to be addressed. Among the various ones, an important problem regards the role of dimensionality for quantum glasses: up to now, most of the proposed realizations are strictly one dimensional. In higher dimensions, the analysis is made much more difficult by the fact that it is much more difficult to analytically control the probability of resonances. While I believe that there is no fundamental impossibility of having a quantum glass in higher dimension, it would be important to find a simple model in $d > 1$ where quantum glassiness can be shown. This is especially relevant for experimental realizations. Another important challenge regards the transport due to bubbles in the thermodynamic limit. While I have shown that they induce a finite conductivity in the system, up to now it has not been possible to estimate its value. Being able to compute the dependence of conductivity from temperature would allow to study the crossover from the Griffiths phase at low T to the metal at high T, which would be the first step to characterize the full phase diagram of MBL models.

Bibliography

[1] K. Huang, *Statistical mechanics* (Wiley, New York, 1987).

[2] R. J. Baxter, *Exactly solved models in statistical mechanics* (Academic Press, London, 1982).

[3] M. Takahashi, *Thermodynamics of one-dimensional solvable models* (Cambridge University Press, Cambridge, 1999).

[4] M. Rigol, V. Dunjko, V. Yurovsky and M. Olshanii, Phys. Rev. Lett. **98**, 050405 (2007).

[5] A. C. Cassidy, C. W. Clark and M. Rigol, Phys. Rev. Lett. **106**, 140405 (2011).

[6] J. S. Caux and F. H. L. Essler, Phys. Rev. Lett. **110**, 257203 (2013).

[7] B. Pozsgay, M. Mestyán, M. A. Werner, M. Kormos, G. Zaránd, and G. Takács, Phys. Rev. Lett. **113**, 117203 (2014).

[8] F. H. L. Essler, G. Mussardo and M. Panfil, Phys. Rev. A **91**, 051602 (2015).

[9] J. P. Bouchaud, L. F. Cugliandolo, J. Kurchan and M. Mézard, in *Spin Glasses and Random Fields*, edited by A. P. Young (World Scientific, Singapore, 1998).

[10] L. Berthier and G. Biroli, Rev. Mod. Phys. **83**, 587 (2011).

[11] P. W. Anderson, Phys. Rev. **109**, 1492 (1958).

[12] P. W. Anderson et al.,*50 years of Anderson localization*, edited by E. Abrahams (World Scientific, Singapore, 2010).

[13] N. F. Mott, *Metal-insulator transitions* (Taylor & Francis, London, 1990).

[14] E. Akkermans and G. Montanbaux, *Mesoscopic Physics of Electrons and Photons* (Cambridge University Press, Cambridge, 2007).

[15] Y. Imry, *Introduction to Mesoscopic Physics* (Oxford University, London, 2002).

[16]] A. L. Burin, D. Natelson, D. D. Osheroff, Y. Kagan, in *"Tunneling Systems in Amorphous and Crystalline Solids"* edited by P. Esquinazi (Springer Verlag, Berlin, 1998).

[17] A. L. Burin, Phys. Rev. B **91**, 094202 (2015).

[18] I. Bloch, J. Dalibard and S. Nascimbéne, Nat. Phys. **8**, 267-276 (2012).

[19] W. S. Bakr, J. I. Gillen, A. Peng, S. Fölling and M. Greiner, Nature (London) **462**, 74-77 (2009).

[20] L. Fleishman, D. C. Licciardello and P. W. Anderson, Phys. Rev. Lett. **40**, 1340 (1978). L. Fleishman and P. W. Anderson, Phys. Rev. B **21**, 2366 (1980).

[21] R. Berkovits and B. I. Shklovskii, J. Phys. Condens. Matter **11**, 779 (1999).

[22] I. V. Gornyi, A. D. Mirlin and D. G. Polyakov, Phys. Rev. Lett. **95**, 206603 (2005).

[23] D. M. Basko, I. L. Aleiner and B. L. Altshuler, Ann. Phys. **321**, 1126 (2006).

[24] J. Z. Imbrie, arXiv:1403.7837.

[25] D. A. Huse and R. Nandkishore, Annual Review of Condensed Matter Physics, Vol. **6**: 15-38 (2015).

[26] C. Gogolin, J. Eisert, arXiv:1503.07538.

[27] M. Serbyn, Z. Papić, and D. A. Abanin, Phys. Rev. Lett. **111**, 127201 (2013).

[28] D. A. Huse, R. Nandkishore and V. Oganesyan, Phys. Rev. B **90**, 174202 (2014).

[29] V. Ros, M. Müller and A. Scardicchio, Nucl. Phys. Sect. B **891**, 420 (2015).

[30] D. A. Huse and A. Pal, Phys. Rev. B **82**, 174411 (2010).

[31] G. Biroli, C. Chamon and F. Zamponi, Phys. Rev. B **78**, 224306 (2008).

[32] G. Carleo, M. Tarzia and F. Zamponi, Phys. Rev. Lett. **103**, 215302 (2009).

[33] L. Foini, G. Semerjian and F. Zamponi, Phys. Rev. B **83**, 094513 (2011).

[34] Z. Nussinov, P. Johnson, M. J. Graf and A. V. Balatsky, Phys. Rev. B **87**, 184202 (2014).

[35] Y. Kagan and L. A. Maksimov, ZhETF **87**, 348 (1984) [JETP **60**, 201 (1984)].

[36] A. L. Burin, K. N. Kontor and L. A. Maksimov, Teoret. Mat. Fiz. **85**, 302 (1990) [Theoret. Mat. Phys. **85**, 1223 (1990)].

[37] M. Schiulaz and M. Müller, in *15th International Conference on Transport in Interacting Disordered Systems*, edited by M. Palassini, AIP Conf. Proc. No. **1610**, (AIP, New York, 2014), p. 11.

[38] M. Schiulaz, A. Silva and M. Müller, *Dynamics in many-body localized quantum systems without disorder*, Phys. Rev. B **91**, 184202 (2015).

[39] W. De Roeck and F. Huveneers, Phys. Rev. B 90, 165137 (2014).

[40] W. De Roeck and F. Huveneers, in *From Particle Systems to Partial Differential Equations II*, edited by P. Gonçalves and A. J. Soares, Springer Proceedings in Mathematics and Statistics Vol. 129 (Springer, New York, 2015), pp. 173-192.

[41] W. de Roeck, F. Huveneers, M. Müller and M. Schiulaz, arXiv:1506.01505.

[42] G. Carleo, F. Becca, M. Schiró and M. Fabrizio, Sci. Rep. **2**, 243 (2012).

[43] W. De Roeck and F. Huveneers, Comm. Mat. Phys. **332**, 1017 (2014).

[44] J. A. Kjäll, J. H. Bardarson and F. Pollmann, Phys. Rev. Lett. **113**, 107204 (2014).

[45] D. J. Luitz, N. Laflorencie and F. Alet, Phys. Rev. B **91**, 081103 (2015).

[46] I. Mondragon-Shem, A. Pal, T. L. Hughes and C. R. Laumann, Phys. Rev. B **92**, 064203 (2015).

[47] T. Devakul and R. P. Singh, Phys. Rev. Lett. **115**, 187201 (2015).

[48] G. Carleo, G. Boéris, M. Holzmann and L. Sanchez-Palencia, Phys. Rev. Lett. **111**, 050406 (2013).

[49] B. Tang, D. Iyer and M. Rigol, Phys. Rev. B **91**, 161109(R) (2015).

[50] J. J. Sakurai, *Modern quantum mechanics*, edited by San Fu Tauan (Benjamin/Cummings, Menlo Park, CA 1985).

[51] J. M. Deutsch, Phys. Rev. A **43**, 2046 (1991).

[52] M. Srednicki, Phys. Rev. E **50**, 888 (1994).

[53] H. Tasaki, Phys. Rev. Lett. **80**, 1373 (1998).

[54] M. Rigol, V. Dunjko and M. Olshanii, Nature (London) **452**, 854 (2008).

[55] M. Rigol, M. Srednicki, Phys. Rev. Lett. **108**, 11 (2012).

[56] G. Biroli, C. Kollath and A. M. Läuchli, Phys. Rev. Lett. **105**, 250401 (2010).

[57] M. L. Mehta, *Random matrices* (Elsevier, Amsterdam, 2004).

[58] A. Einstein, Annalen der Physik **17**, 549 (1905).

[59] N. W. Ashcroft and N. D. Mermin, *Solid State Physics* (Saunders College, Philadelphia, 1976).

[60] E. Abrahams, P. W. Anderson, D. C. Licciardello and T. V. Ramakrishnan, Phys. Rev. Lett. **42**, 673 (1979).

[61] S. Sachdev, Quantum phase transitions (Cambridge University Press, Cambridge, 2011).

[62] B. Bauer and C. Nayak, J. Stat. Mech.: Theory Exp. (2013) P09005.

[63] H. Kim and D. A. Huse, Phys. Rev. Lett. **111**, 127205 (2013).

[64] W. W. Ho and D. A. Abanin, arXiv:150803784.

[65] E. H. Lieb and D. Robinson, Comm. Math. Phys. **28**, 251 (1972).

[66] M. Znidaric, T. Prosen and P. Prelovsek, Phys. Rev. B **77**, 064426 (2008).

[67] J. H. Bardarson, F. Pollmann and J. E. Moore, Phys. Rev. Lett. **109**, 017202 (2012).

[68] P. Jacquod and D. L. Shepelyansky, Phys. Rev. Lett. **70**, 1837 (1997).

[69] V. Oganesyan and D. A. Huse, Phys. Rev. B **75**, 155111 (2007).

[70] F. Haake, *Quantum signatures of chaos*, Springer Series in Synergetics (Springer, Berlin, Heidelberg, 2010).

[71] V. Khemani, F. Pollmann and S. L. Sondhi, arXiv:1509.00483.

[72] X. Yu, D. Pekker and B. K. Clark, arXiv:1509.01244.

[73] B. L. Altshuler, Y. Gefen, A. Kamenev and L. S. Levitov, Phys. Rev. Lett. **78**, 2803 (1997).

[74] J. W. Essam, Rep. Prog. Phys. **43**, 833 (1980).

[75] K. Malarz, Phys. Rev. E **91**, 043301 (2015).

[76] C. A. Angell, Science **267**, 1924 (1995).

[77] L. C. E. Struik, *Physical aging in amorphous polymers and other materials* (Elsevier, Amsterdam, 1978).

[78] A. W. Kauzmann, Chem. Rev. **43**, 219 (1948).

[79] L. M. Martinez and C. A. Angell, Nature **410**, 663 (2001).

[80] P. G. Debenedetti and F. H. Stillinger, Nature **410**, 259 (2001).

[81] M. Goldstein, J. Chem. Phys. **51**, 3728 (1969).

[82] J. P. Garrahan and D. Chandler, Proc. Natl. Acad. Sci. USA **100**, 9710 (2003).

[83] J. M. Hickey, S. Genway and J. P. Garrahan, arXiv1405.5780.

[84] M. van Horssen, E. Levi and J. P. Garrahan, Phys. Rev. B **91**, 184202 (2015).

[85] D. Chandler and J. P. Garrahan, Ann. Rev. Phys. Chem. **61**, 191 (2010).

[86] W. Kob and H. C. Andersen, Phys. Rev. E **48**, 4364 (1993).

[87] F. Ritort and P. Sollich, Adv. Phys. **52**, 219 (2003).

[88] G. H. Fredrickson and H. C. Andersen, Phys. Rev. Lett. **53**, 1244 (1984).

[89] C. Toninelli, M. Wyart, L. Berthier, G. Biroli and J. P. Bouchaud, Phys. Rev. E **61**, 041505 (2005).

[90] C. Toninelli, G. Biroli and D. S. Fisher, Phys. Rev. Lett. 96, 035702 (2006).

[91] J. P. Garrahan, J. Phys. Condens. Matter **14**, 1571 (2002).

[92] Z. Papić, E. M. Stoudenmire and D. A. Abanin, Annals of Physics **362**, 714 (2015).

[93] N. Y. Yao, C. R. Laumann, J. I. Cirac, M. D. Lukin and J. E. Moore, arXiv:1410.7407.

[94] I. H. Kim and J. Haah, arXiv:1505.01480.

[95] T. Grover and M. P. A. Fisher, J. Stat. Mech.: Theory Exp. (2014) P10010.

[96] C. Chamon, Phys. Rev. Lett. **94**, 040402 (2005). C. Castelnuovo and C. Chamon, Phil. Mag. **92**, 304 (2011).

[97] G. Biroli and M. Mézard, Phys. Rev. Lett. **88**, 025501 (2001).

[98] C. Gruber and D. Ültschi, in *Encyclopedia of Mathematical Physics*, edited by J. P. Françoise, G. L. Naber and T. S. Tsun (Elsevier, 2006), pp. 283-291.

[99] M. Schreiber, S. S. Hodgman, P. Bordia, H. P. Lüschen, M. H. Fischer, R. Vosk, E. Altman, U. Schneider and I. Bloch, Science **349**, 842 (2015).

[100] U. Gavish and Y. Castin, Phys. Rev. Lett. 95, 020401 (2005).

[101] B. Gadway, D. Pertot, R. Reimann and D. Schneble, Phys. Rev. Lett. 105, 045303 (2010).

[102] S. Gosh, R. Parthasarathy, T. F. Rosenbaum and G. Aeppli, Science **296**, 2195 (2002). S. Gosh, T. F. Rosenbaum and G. Aeppli, Phys. Rev. Lett. **101**, 157205 (2008).

[103] D. L. Shepelyansky, Phys. Rev. Lett. **73**, 2607 (1994).

[104] Y. Imry, Europhys. Lett. **30**, 405 (1995).

[105] H.-Y. Xie and M. Müller, Phys. Rev. B **87**, 094202(2013).

[106] F. Borgonovi and D. L. Shepelyansky, J. Phys. (France) I **6**, 287 (1996).

[107] Ph. Jacquod, Phys. Status Solidi **205**, 263 (1998).

[108] D. Bercioux and P. Lucignano, Rep. Progr. Phys. **78**, 106001 (2015).

[109] R. Nandkishore, Phys. Rev. B **90**, 184204 (2014).

[110] Y. Shapir, A. Aharony and A. B. Harris, Phys. Rev. Lett. **49**, 486 (1982).

[111] D. E. Logan and P. G. Wolynes, Phys. Rev. B **31**, 2437 (1985).

[112] N. Prokof'ev and P. Stamp, Rep. Prog Phys. **63**, 669 (2000).

[113] K. Agarwal, S. Gopalakrishnan, M. Knap, M. Müller and E. Demler, Phys. Rev. Lett. **114**, 160401 (2015).

[114] H.-Y. Xie and M. Müller, Phys. Rev. B **87**, 094202 (2013).

[115] D. A. Huse, R. Nandkishore, F. Pietracaprina, V. Ros and A. Scardicchio, Phys. Rev. B **92**, 014203 (2015).

[116] L. F. Santos, F. Borgonovi and G. L. Celardo, arXiv:1507.06649.